The Thesis Committee for Yusra Khan Ahmad
Certifies that this is the approved version of the following thesis:

Nanoparticle-Stabilized Oil-in-Water Emulsions for Residual Oil Recovery

APPROVED BY
SUPERVISING COMMITTEE:

Supervisor:

Hugh Daigle

Chun Huh

Nanoparticle-Stabilized Oil-in-Water Emulsions for Residual Oil Recovery

by

Yusra Khan Ahmad, B.S.Ch.E.

Thesis

Presented to the Faculty of the Graduate School of

The University of Texas at Austin

in Partial Fulfillment

of the Requirements

for the Degree of

Master of Science in Engineering

The University of Texas at Austin

August 2015

Dedication

To my mother i.e., my strength

Acknowledgements

I would like to thank my former supervisor, Dr. Steven Bryant, for his undying support and faith in me and the guidance he provided in our time together. I would also like to thank Dr. Chun Huh and Dr. Hugh Daigle for their advice and help throughout my graduate studies.

I would like to especially thank my friend Victor Duribe for the support he provided which encouraged me to put my best foot forward. I would also like to thank Nana Asiamah and Deji Lana for their company throughout my two years; without them the journey would not have been as pleasant. I would like to also thank Scott Gabel for providing the proper framework required for me to build my research on.

Finally, I would like to thank Gary Miscoe for all the help I needed with laboratory equipment and all the sponsors who funded this exciting research.

Abstract

Nanoparticle-Stabilized Oil-in-Water Emulsions for Residual Oil Recovery

Yusra Khan Ahmad, M.S.E

The University of Texas at Austin, 2015

Supervisor: Hugh Daigle

Transport of emulsions through porous media has the ability to play a significant role in many EOR processes. Nanoparticles can act as efficient emulsifying agents, producing emulsions that can improve sweep efficiencies leading to improved oil recoveries. This thesis has explored emulsion stability and flow through porous media whilst also assessing emulsion capabilities in residual oil recovery.

Hydrophilic nanoparticle-stabilized oil-in-water emulsions of two different average droplet sizes were injected into hydrophobic beadpacks of varying bead size diameters. The smaller sized emulsion appeared to be more stable in its properties, more frequently being regenerated in the effluent in comparison to the larger droplet sized emulsion. With a decrease in bead diameter, the smaller droplet sized emulsion could not survive passage with regeneration. Smaller bead pack sizes also did not allow passage of the less stable emulsions with larger droplet sizes. The fastest emulsion regeneration was

seen for emulsions with small droplet sizes through a beadpack of larger sized beads. Through the largest bead sized beadpack, small amounts of the less stable emulsion were seen to be regenerated but much later in the life of the experiment. Higher flow rates were able to regenerate emulsion for smaller droplet sizes but were unable to do so for the less stable larger sized emulsion. Pressure profiles appeared to similar for most runs where approximately the first 0-10 pore volumes show the greatest pressure buildup followed by what appears to be a more stable and slower increase in pressure.

Coreflood experiments were performed to assess residual oil recovery for various oil-in-water emulsions. Higher percentage recoveries were seen to be dependent on a few leading factors. For more viscous, stable emulsions, it appeared that lower flow rates lead to higher percentage recoveries. At lower flow rates, no emulsion would also be produced in the effluent for the duration of the experiment. As pressure profiles were seen to increase throughout the experiment, attempted coalescence and regeneration were likely taking place. However, as regeneration was less successful, complete coalescence might be the reason for increased miscibility in the core, leading to higher recovery potentials.

Encouraging recoveries were seen when a more viscous stable emulsion was used to recover residual oil less viscous than that of the continuous oil in the emulsion. Increasing the slug size of the emulsion injected helped recover more residual oil. Increasing the slug size however is only advantageous up till a limiting value where the injected emulsion slug would produce the same result as injected emulsion continuously through the sandstone core. Where enough emulsion was injected and therefore available inside the core, emulsion regeneration was seen.

Lighter organic phases in emulsion form were used for oil recovery coreflood experiments. Similar to experiments performed with heavier organic phases in emulsion form i.e. mineral oil-in-water emulsion, octane-in-water emulsion was also not

regenerated for low flow rates, completely coalescing inside the sandstone core. For higher flow rates, small amounts of octane emulsion were regenerated. In this case, similar to that of the mineral oil emulsion, increasing the flow rate seemed to have a negative effect on the percentage oil recovery.

Surfactant stabilized octane-in-water emulsions showed the highest amount of percentage residual oil recovery. The pressure plot of these emulsions was different to those of nanoparticle stabilized emulsions where although the initial pressure increase matched up with the movement of the oil bank through the core, the latter part of the pressure profile appeared to decrease. This pressure profile was seen in both cases where the octane emulsion was injected into a fully brine saturated core as well as a core at residual oil saturation. It is interesting to note, however that surfactants by themselves are not capable of recovering any residual oil. It is only in emulsion form that this recovery is possible.

Pentane-in-water emulsions were not seen to be stable for days unlike the other emulsions stated above. This was due to partial and continuous evaporation of pentane from the emulsion form at room temperature and pressure. When pressurized to 100 psi, however, the emulsion was seen to be stable for a number of days. All experiments were performed at high flow rates however emulsion was not seen to be regenerated in the effluent. This would suggest a lack of stability of the emulsion. Due to complete coalescence of the emulsion inside the core, miscibility would increase and this might be a reason for the higher percentage recoveries. Pressure profiles seemed to mimic all other oil-in-water emulsion injection experiments to sandstone cores at residual oil saturation.

Table of Contents

List of Tables

List of Figures

Chapter 1

Introduction

Transport of emulsions through porous media has the potential to play a significant role in many EOR processes. When emulsions flow through porous space, they have the tendency to follow the already swept permeable paths. This diverts the already injected water/oil to un-swept pore spaces and can therefore lead to more efficient recovery of residual oil. For the emulsion to be efficient, it must be stable, i.e., one phase be dispersed in another for long periods of time. Oil-in-water as well as water-in-oil emulsions both require a third component, namely an emulsifying agent, which helps assist the stability of the emulsion by reducing the interfacial tension between the oil and water phases. For this purpose, silica nanoparticles are employed. Surface-coated silica nanoparticles can help form emulsions that appear to remain stable for large periods of time without the evidence of any coalescence. These nanoparticle stabilized emulsions act as recovery enhancing agents that enter the reservoir, contact the residual oil present and help recover it. This is done through coalescence and regeneration.

When a nanoparticle stabilized emulsion enters a reservoir, it has the ability to break up into its base components. As the oil in the emulsion is released, the residual oil present in the core can be found, contacted and partially trapped, forming a potential oil bank. When the emulsion regenerates, these oil droplets can be recovered. In this way, nanoparticle stabilized emulsions have a huge potential to help in residual oil recovery. Figure 1 shows a schematic as to the mechanism of coalescence and regeneration as stated above.

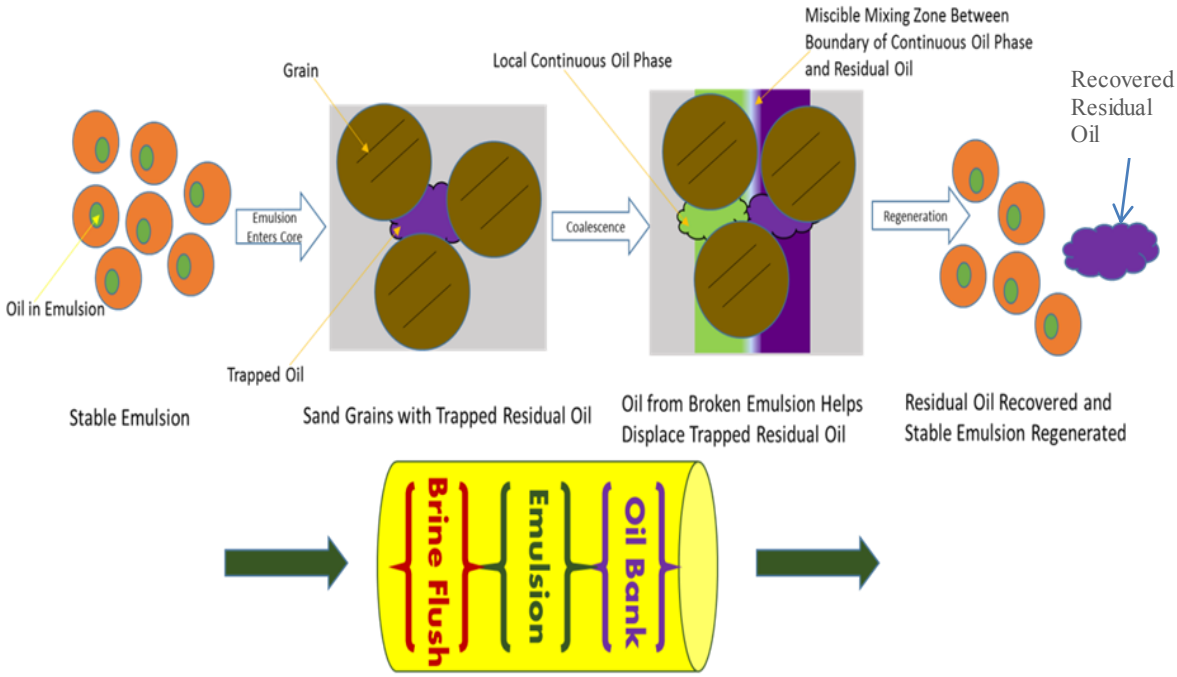

Figure 1.1: Schematic of Mechanism of Residual Oil Recovery.

1.1 THESIS OUTLINE

The work in this thesis investigates the stability, flow and recovery potential of various nanoparticle-stabilized emulsion in porous media. There are five chapters in this thesis. The first chapter is a brief introduction on the appeal and potential of nanoparticle-stabilized emulsions. The second chapter provides a literature review of previous research work that has performed. The third chapter presents experimental work in beadpacks of hydrophobic wettability. The fourth chapter investigates nanoparticle-stabilized emulsion injection experiments through sandstone cores. The fifth and final chapter discusses the conclusions of this research work in detail and presents future research work.

Chapter 2

Literature Review

2.1 NANOPARTICLE-STABILIZED EMULSION STABILITY AND RHEOLOGY

Current conventional emulsions used in the petroleum industry employ surfactants or colloidal particles as emulsifying agents. Recently, researchers have shown an increased attention towards nanoparticle-stabilized emulsions due to their advantages over conventional methods, like increased conformance control and improved sweep efficiencies. Colloidal particles above 100 nm in diameter may be retained in pore throats and lead to filtration which in turn may result in a loss of particles and retention in the rock. Colloidal particles also have a broad size distribution which may hinder the control and design of the desired emulsion. These problems can be alleviated by the incorporation of nanoparticles in the 1-100 nm diameter range. Not only are nanoparticles over a hundred times smaller than colloidal particles, the emulsions they help stabilize have the potential to stay stable through harsh conditions like high temperature, high salinity with little to no retention.

Nanoparticles used in recent experimental work are most commonly known to have a spherical structure with an outer silica coating. The coating extent of the silanol groups determines the wettability of these nanoparticles. Hydrophilic nanoparticles contain over 90% of silanol groups on their surface and have a contact angle $< 90^{o}$ whereas hydrophobic nanoparticles exhibit about 10% of silanol groups on their surface and have a contact angle $> 90^{o}$. Consequently, hydrophilic nanoparticles produce oil-in-water emulsions whereas hydrophobic nanoparticles produce water-in-oil emulsions (Zhang 2010). This can be seen in figure 2.1 One may point out the advantage that

changing the surface coating provides the ability to tailor any given nanoparticle for different applications. An example of this would be ferromagnetic nanoparticles that may be controlled by an external magnetic field to carry out various actions.

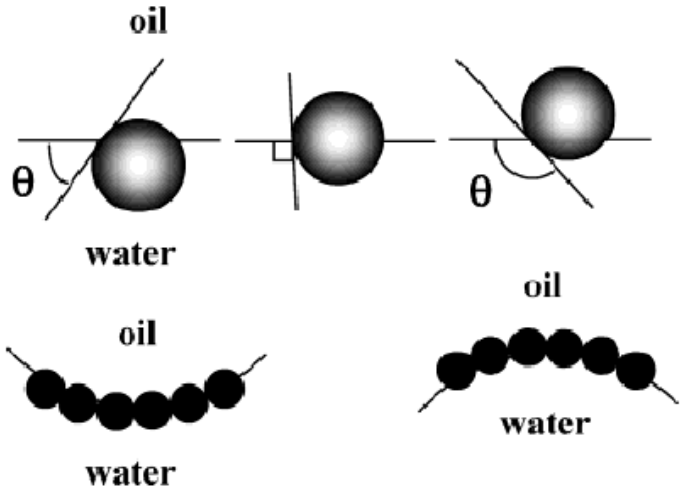

Figure 2.1: Contact Angle for Oil-Water Interface in Relation to Emulsion Structure (Dickson et al. 2004)

Zhang et al. (2010) generated a set of decane-in-water emulsions as well as water-in-decane emulsions, using hydrophilic and hydrophobic nanoparticles respectively, of varying concentrations, salinities and initial volume ratios. The hydrophilic and hydrophobic nanoparticle concentration for generation of decane-in-water and water-in-decane emulsions varied from as low as 0.05 wt% to as high as 5 wt%. Salinity was varied from 0 to 10 wt% and the emulsions were created using a sonification gun. Zhang et al. showed that well over half of the decane had formed emulsion in nearly all the samples, with very little decane left in excess while attempting to generate decane-in-water emulsions. The most stable emulsions were seen to form when the nanoparticle concentration exceeded 0.5 wt% which was shown while creating water-in-decane

emulsions. For both kinds of emulsions, more emulsification was seen with an increase in the nanoparticle concentration, in addition to exhibiting an increase in the dispersed phase volume. All emulsions generated were seen to be stable over a time period of several months. This stability is the main advantage of nanoparticle-stabilized emulsions over surfactant-stabilized emulsions. Surfactants do not have the ability to attach irreversibly to the oil-water interface and form the monolayer that nanoparticles do. In fact, Aveyard et al. (2003) has shown that very little energy is required to detach a surfactant molecule from the oil-water interface, leading to instability in the emulsion structure. Additional problems can be created when surfactant adsorption onto reservoir rocks may create chemical oil recovery problems and surfactant chemical solutions lose their effectiveness over time as they flow through porous media.

Zhang (2010) and Gabel (2014) have observed the rheology of a generated stable nanoparticle-stabilized emulsion in detail. They have determined nanoparticle-stabilized oil-in-water emulsions to be highly shear-thinning power-law fluids. This suggests that as the shear rate applied on the emulsion increases, the viscosity of the emulsion decreases. This shear thinning behavior is similar to other emulsions stabilized using surfactants. The shear stress,τ, of this power-law oil-in-water emulsion can be calculated using:

$$\tau = K\dot{\gamma}^{n}, \qquad \text{(Eq. 1)}$$

where K is the consistency index, $\dot{\gamma}$ is the shear rate and n is the flow behavior index.

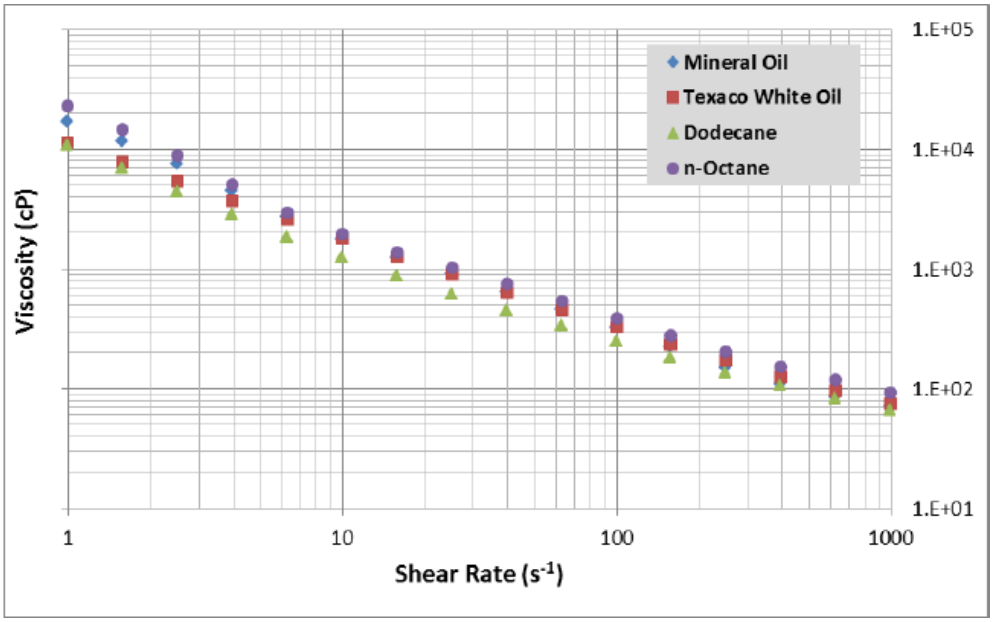

Figure 2.2: Plot of Rheology of Emulsions Generation with Different Oils (Gabel 2014)

Figure 2.2 shows the rheology of various nanoparticle-stabilized emulsion created by varying the hydrocarbon phase. As can be seen, a very strong shear-thinning trend existed for all the generated oil-in-water emulsions (Gabel 2014)

2.2 EMULSION GENERATION BY CO-INJECTION

Zhang et al. (2010) used a closed-batch high shear mixing process or high frequency vibrations in order to generate emulsions. Although this method is reliable and has been used by the majority of previous researchers, the amount of emulsion generated is limited, as are the physical properties. In order to generate large amounts of emulsions that have the potential to be injected at a field scale, Gabel (2014) presented a continuous generation method of co-injection.

Gabel (2014) used various nanoparticles at a 2 wt% concentration with a salinity of 3 wt% NaCl, diluted in de-ionized water. The nanoparticle dispersion was then co-injected with the hydrocarbon phase in a high pressure column filled with beads of

diameter ranging from 180-3000 micron. For the generation of a stable emulsion, a critical shear rate was determined, below which an emulsion would not stay stable over time. Each critical shear rate varied with the glass bead size that was used to fill up the beadpack. For each glass bead size, it was only above this critical shear rate that a stable emulsion was seen to be produced.

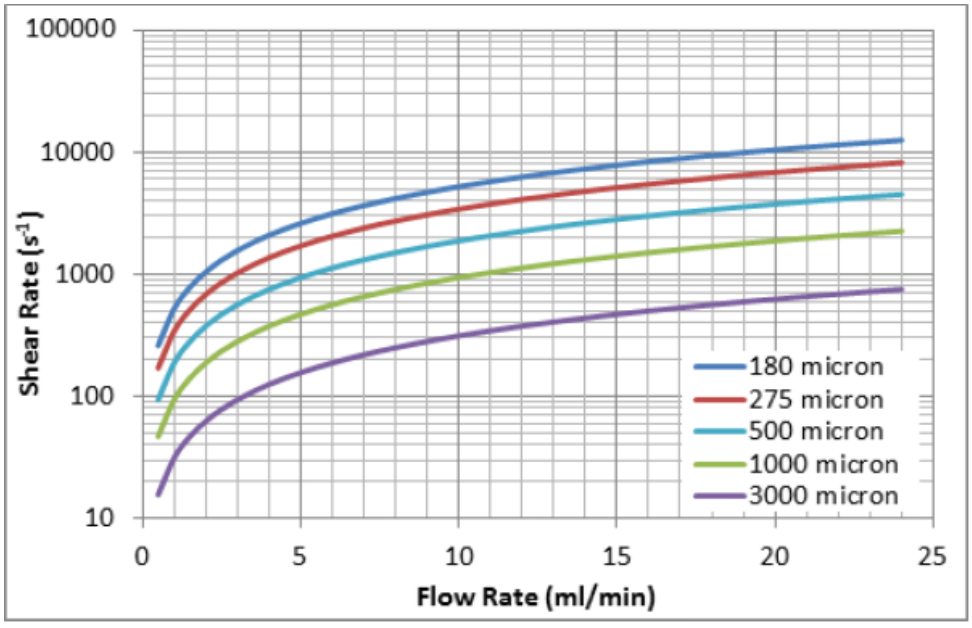

Figure 2.3: Plot of Shear Rate vs. Flow Rate for Different Bead Sizes (Gabel 2014)

As can be seen from Figure 2.3, as the glass bead size increased, the critical shear rate to form a stable emulsion decreased.

2.3 THE DYNAMICS OF COALESCENCE OF EMULSION DROPLETS

The coalescence behavior of emulsion droplets in porous media is important for use in various processes in enhanced oil recovery. In many cases, coalescence is a desirable trait which is highly dependent on the dynamics of the film between the droplets. The capillary number *Ca*, is among the most important determining factors of coalescence, and is defined as the ratio between the viscous forces and the interfacial forces. It is routinely calculated as:

$$Ca = \mu U/\gamma, \qquad \text{(Eq. 2)}$$

where μ is the viscosity, U is the bulk fluid velocity and γ is the interfacial tension.Other important factors include interfacial tension, the viscosity ratio, the droplet-to-pre size ratio, the pore-body-to-throat size ratio and the type of pore geometry.

Yan et al. (2006) provided simulations for the deformation of a pair of droplets with the same radius as they approached a constricted pore throat. At the entrance of the pore throat, as the two droplets collide, coalescence occurs for a lower boundary value of *Ca* with very little deformation. At higher *Ca* values the droplets became more and more elongated with coalescence now occurring at the center of the pore throat with the separation *h* between the droplets at a minimum value. This can be seen in Figure 2.4 A critical capillary number *Cac* was determined where coalescence was seen to occur at the lower boundary but did not occur at the higher boundary.

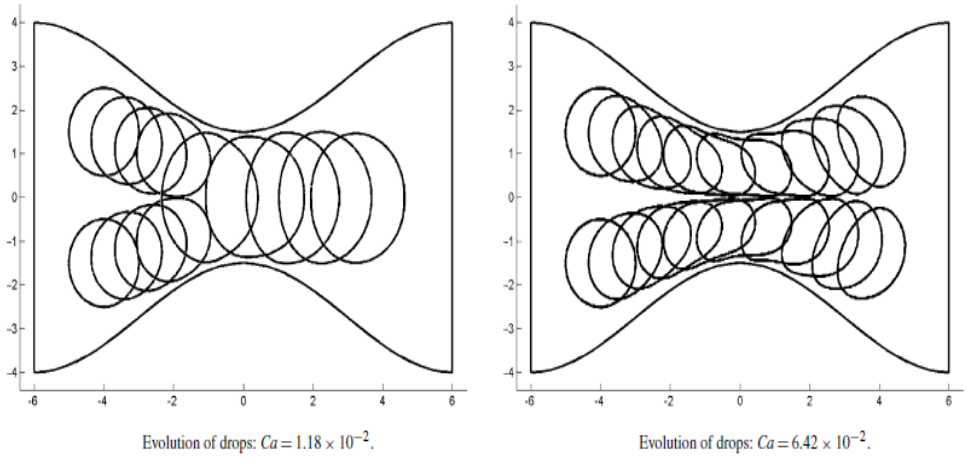

Figure 2.4: Evolution of droplets through a pore throat. Coalescence is favored at low capillary numbers. (Yan et al. 2006)

Gabel (2014) performed various corefloods where a nanoparticle-stabilized emulsion was injected through a sandstone core. The concept of coalescence and regeneration was demonstrated in the effluent collected from the results of the various corefloods. Not only was there a critical shear rate required to maintain a stable emulsion in the core, a high pressure drop was also seen which could be directly associated with the continued coalescence of droplets. In most of the coreflood research work performed by Gabel (2014), the phenomenon of a pressure drop increase across the core was observed and various phases were seen in the effluent i.e., oil from the coalesced emulsion, an aqueous nanoparticle phase from the coalesced emulsion and the regenerated emulsion itself. The regenerated effluent emulsion was seen to have a different droplet size as well as a different viscosity than the injected emulsion for the majority of the cases.

2.4 EMULSION POTENTIAL IN IMPROVED MOBILITY AND CONFORMANCE CONTROL

There has been continued limitation in attempts to improve mobile oil recovery in the petroleum industry. Although fluids like brine and carbon dioxide are common displacement fluids employed, at many instances the viscosity of these fluids are significantly lower than the hydrocarbon that they are trying to displace. Due to this significant difference in viscosity, mobility ratios are unfavorable and when combined with viscous fingering, the result is poor sweep efficiencies. Many reservoirs have heavier resident oils that range from 40 to 5,000 cP in viscosity. Unfavorable mobility ratios would not allow efficient oil recovery economically from simply water-flooding. This is partly due to the tendency of brine to bypass areas of high viscosity oil. For this purpose, emulsions are used to increase water viscosity, decrease mobility ratios and result in a much more efficient oil recovery.

Poor sweep efficiencies are quite commonly seen in crude oil reservoirs that exhibit a high degree of heterogeneity. Brine has shown a preference to flow through the most permeable zones, sometimes completely bypassing the heaviest viscosity portions of the reservoir. These “thief zones” leave a significant amount of high viscosity still in place. Nanoparticle-stabilized emulsions have the ability to potentially plug these high permeability thief zones and in such a way divert flow into the near wellbore region.

2.5 NATURAL GAS LIQUIDS EMULSIONS

Natural gas liquids (NGLs) are short carbon chain alkanes often produced along with crude oil. Ethane, propane, butane, all through heptane are NGLs that are useful in various aspects of the economy. NGLs are not only used in petrochemical plants, but can also be burned for heat as well as be used as automotive fuel. NGLs are very cheap and are often treated as waste products in the oil and gas industry. As NGL field production

increases, the supply picture provides further insight as to the possibilities and potential for NGLs.

Natural gas liquids can be incorporated as the organic phase in oil-in-water emulsions. By incorporating light hydrocarbons in emulsion form, stabilized by nanoparticles, to recover heavier more viscous resident oils, a new practical method can be developed in tertiary recovery.

Chapter 3

Emulsion Flow through Hydrophobic Beadpacks

It is essential to be able to better understand the behavior and mechanisms of flow of nanoparticle-stabilized emulsions to help assist in residual oil recovery. For this purpose, it is necessary to perform characterization studies on the properties of these emulsions. These include rheological studies, particle size analyses, and nuclear magnetic resonance (NMR) techniques. It is equally pertinent to take into account the wettability of the system and how this might influence the flow properties of these nanoparticle-stabilized emulsions. The influence of such experimental conditions can in turn provide better insight on the emulsion system.

For the purposes of our experiments, the nanoparticles that are used exhibit a spherical shape. They are hydrophilic in terms of wettability due to an outside layer of silica coating on their surface. Their particle diameter ranges from 15-25 nm in size. Due to their hydrophilic nature, these nanoparticles generate stable oil-in-water emulsions with the oil being the dispersed phase and the nanoparticle dispersion being the continuous phase.

Gabel (2014) performed experiments using hydrophilic nanoparticles to create oil-in-water emulsions. The behavior of these oil-in-water emulsions has been examined by flowing them through water-wet hydrophilic beadpacks. Various nanoparticle-stabilized oil-in-water emulsions flowed through hydrophilic beadpacks of differing bead diameters and their rheology and stability was analyzed. For each run, a case by case analysis was crucial to help characterize these emulsions. In attempts to theoretically tie all the runs performed together as well as be able to understand the influence of pore wall wettability on emulsion coalescence and regeneration, similar runs were performed in oil-wet hydrophobic beadpacks.

3.1 MATERIALS AND EXPERIMENTAL SET-UP

In this section a discussion will be provided on the materials and methods used to not only generate emulsion, but to allow flow into hydrophobic beadpacks.

3.1.1 Materials Used

Silica nanoparticles were used at having an average diameter in the 15-25 nm range. These surface-coated silica nanoparticles were provided by the manufacturer at a concentration of 20 wt% dispersion in de-ionized water. The nanoparticle dispersion was Nyacol DP9711 and was purchased from Nyacol Nano Technologies. The 20 wt% dispersion was diluted down to 2 wt% in de-ionized water for the purposes of our experiments. Sodium chloride at 3 wt% was used as the salinity of the dispersion. The nanoparticle dispersion had a viscosity of 1.06 cP and a density of 1.03 g/cm$^{3.}$ The sodium chloride was 99% pure and was purchased from Fisher Scientific.

Light mineral oil was the oleic phase used to create the oil-in-water emulsion. This oil was purchased from Fisher Scientific. The light mineral oil had a viscosity of 40 cP and a density of 0.861 g/cm^3. All experiments were performed in varying diameter beadpacks at room temperature.

A high pressure column purchased from HiP (High Pressure Equipment Company) was used as the steel beadpack with diameter 0.44 cm and length 15.24 cm. Mesh pieces were placed in the end caps of the high pressure column in order to keep the contents of the beadpack in place while flow occurred. Spherical glass beads were used to fill this steel beadpack; three different bead size diameters were used: 180 micron, 500 micron, and 1000 micron. As glass beads are inherently hydrophilic, a surface coating must be provided to the beads in order to change the wettability of the beadpack. For this purpose, Gelest Siliclad was used which was purchased from Gelest. The procedure to

alter the wettability of the glass beads, and therefore the beadpack, will be discussed in the next section.

3.1.2 Wettability Alteration of Glass Beads

Gelest Siliclad is a dilute aqueous dispersion of reactive silane and is used for hydrophobic water-dispersible coatings for glass and ceramics. Siliclad is a monomeric octadecylsilane derivative dispersed in tertiary alcohols and diacetone alcohol. It reacts with water to form a silanol-rich prepolymer which further forms chemically bound alkylsilicone to provide water-repellency, lubricity as well as surface resistivity to glass and ceramic surfaces. The wettability alteration process of the glass beads was as follows:

I. Immerse glass beads in 2 wt% sodium hydroxide in order to thoroughly clean the glass surface
II. Thoroughly rinse glass beads using tap water
III. Prepare a 1% solution of Siliclad diluted in in tap water and immerse glass beads in this solution for approximately 10 seconds ensuring that the entire spherical surface has been wetter by the solution via agitation of the solution
IV. Remove the solution gently and rinse glass beads to remove excess Siliclad from the surface
V. Leave beads in a 100 °C oven overnight to help cure the Siliclad.
VI. Pack the glass beads into the steel beadpack

A simple experiment was performed to confirm the hydrophobicity of the glass beads. Hydrophilic and treated hydrophobic glass beads were both dipped in water in a plastic container and their behavior was assessed. The untreated hydrophilic glass beads settled to the bottom of the container when placed in the water whereas the treated hydrophobic glass beads remained at the surface, thereby confirming their water-repellency. This can be seen in Figure 3.1:

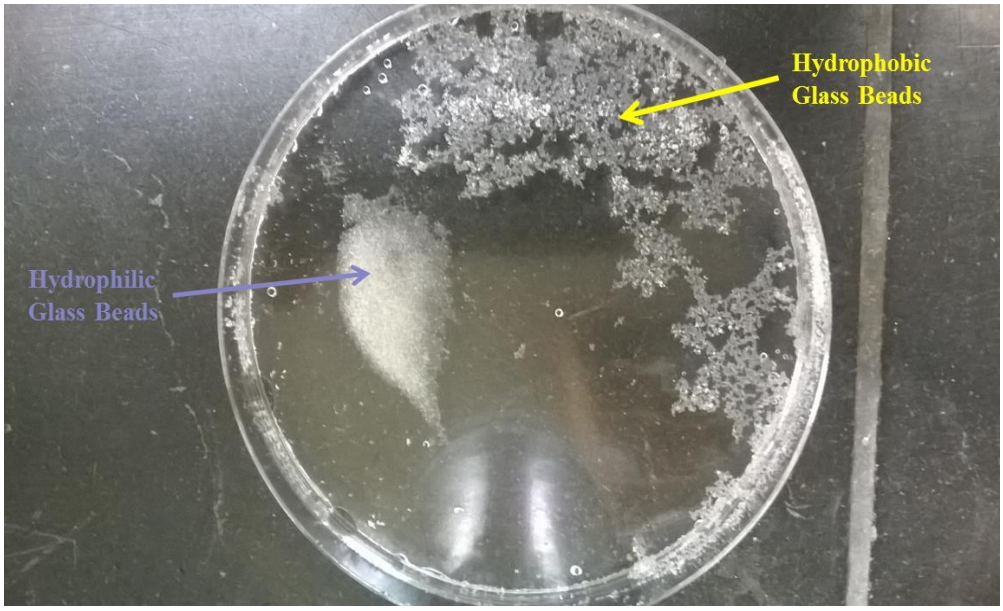

Figure 3.1: Wettability Alteration of Glass Beads

3.1.3 Beadpack Co-Injection Set-Up

In order to generate stable oil-in-water emulsions, a co-injection set-up is used. This set-up is designed to provide simultaneous, continuous flow of the aqueous nanoparticle dispersion and organic light mineral oil through a high pressure column of hydrophilic wettability. The glass beads present in the beadpack provide shearing of the two phases which allows for the creation of the oil-in-water emulsion.

Figure 3.2 shows the schematic of the beadpack co-injection set-up. Two Teledyne ISCO syringe pumps were used with the capacity to pump up to 408 mL/min of fluid at a maximum operating pressure of 2000 psi. Pump (a) as shown contained the light mineral oil organic phase whereas pump (b) provided to water drive to allow flow into (c) the steel accumulator containing a movable piston (to separate phases) having the capacity to carry 400 mL of nanoparticle dispersion into the steel beadpack.

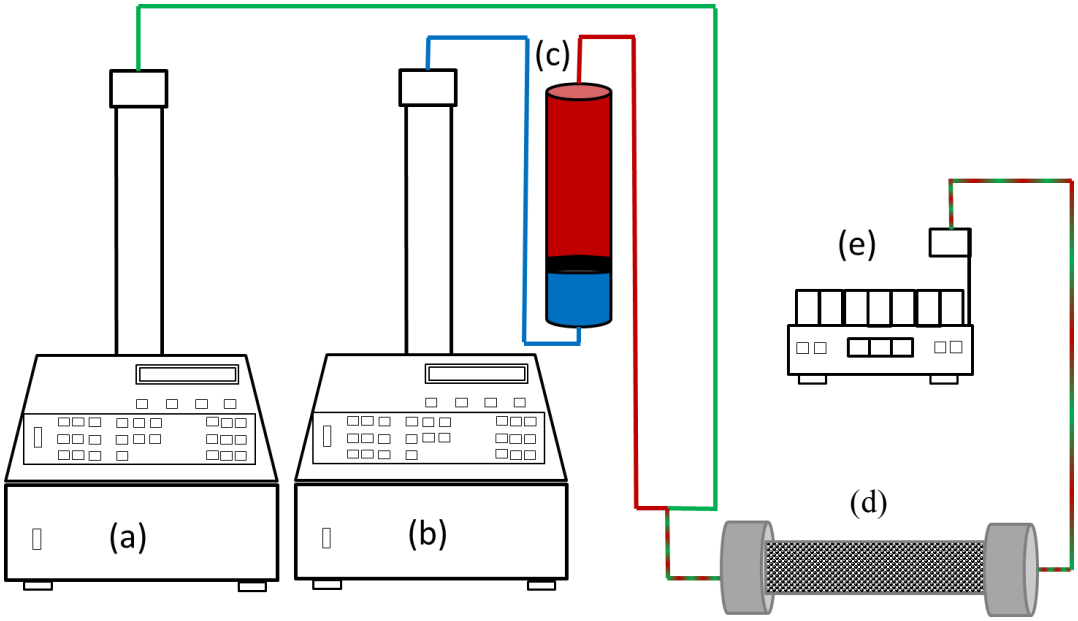

Figure 3.2: Co-Injection Set-Up: (a) Syringe pump for mineral oil, (b) Syringe pump for water drive, (c) Accumulator carrying nanoparticle dispersion, (d) Hydrophilic beadpack, (e) Fraction collector for effluent (Gabel 2014)

The experimental procedure is as follows:

I. Open beadpack using a vise grip and insert mesh into the end caps

II. Attach one end cap back onto the beadpack and position the beadpack vertically to allow filling with hydrophilic glass beads

III. Attach the other end cap to the beadpack

IV. Load pump (a) with light mineral oil and pump (b) with drive brine

V. Load the steel accumulator with nanoparticle dispersion

VI. Connection and flow through various apparatus is provided using steel flow lines rated to a maximum operating pressure of 2000 psi

VII. Co-inject the two fluids through the steel beadpack

VIII. Collect effluent in the fraction collector

3.1.4 Emulsion Flow through Beadpack Set-Up

Emulsion Injected

Two different emulsions were used for injection into the hydrophobic beadpack. The nanoparticles used for the generation of the emulsion were Nyacol DP9711 and were dispersed at 2 wt% in de-ionized water of 3 wt% salinity. The organic phase was light mineral oil. The first emulsion (emulsion 1) was created using a 180 micron hydrophilic beadpack at a 1:1 ratio of nanoparticle dispersion to light mineral oil. The two phases were co-injected at a flow rate of 12 mL/min each (total 24 mL/min) providing a shear rate above the previously determined critical shear rate of between 781 s^{-1} and 1042 s^{-1} by Gabel et al for 180 micron beads. The average droplet size of this emulsion was measured by Gabel et al. to be between 20 and 24 microns. The second emulsion (emulsion 2) was created using a 500 micron hydrophilic beadpack at a 1:1 ratio and the two phases were co-injected at a flow rate of 6 mL/min each (total 12 mL/min), also well above the critical shear rate for this particular sized beadpack, i.e. between 187 s^{-1} and 281 s^{-1} for 500 micron beads. The average droplet size of this emulsion was measured by Gabel et al. to be between 50 and 62 microns. Both emulsions were approximately 66% light mineral oil by volume.

Initial Saturation

All experiments were performed using an initial complete saturation of the beadpack with de-ionized water.

The hydrophobic beadpack injection set-up uses the same beadpack that was previously used for the emulsion generation co-injection set-up. A Teledyne ISCO syringe pump was used to provide the drive brine which was pumped into the steel accumulator. This steel accumulator, as stated above, contains a movable piston which

allows for separation of the drive brine from the emulsion that has been loaded into it previously. As the drive brine is pumped into the steel accumulator, the piston displaces the emulsion which is thereby injected into the hydrophobic beadpack. A differential Rosemount pressure transducer was connected across the beadpack to measure the pressure drop. Effluent from the hydrophobic beadpack was collected in the fraction collector. Figure 3.3 shows this set-up.

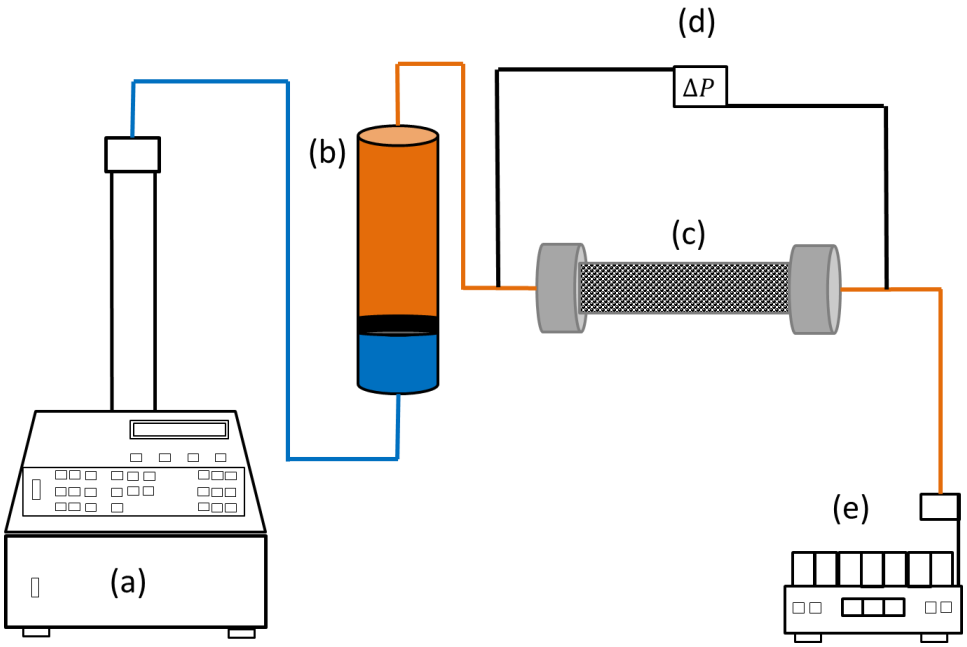

Figure 3.3: Emulsion Flow through Beadpack: (a) Syringe pump providing drive brine, (b) Steel accumulator containing emulsion, (c) Hydrophobic beadpack, (d) Pressure transducer, (e) Fraction collector for effluent (Gabel 2014)

The experimental procedure is as follows:

I. Load syringe pump (a) with de-ionized water used to initially saturate the beadpack

II. Fill the beadpack with hydrophobic glass beads of desired diameter

III. Connect beadpack to the syringe pump and inject saturating fluid through the beadpack

IV. Disconnect beadpack from the syringe pump and empty syringe pump

V. Load syringe pump (a) with drive brine

VI. Connect syringe pump (a) to the steel accumulator (b) which has been previously loaded with emulsion

VII. Attach pressure transducer lines across beadpack and record pressure via the LabVIEW software

VIII. Allow emulsion to flow through beadpack

IX. Collect effluent using the fraction collector

3.2 DATA ANALYSIS

3.2.1 Permeability, Shear Rate, and Apparent Viscosity of the Beadpack

The permeability, *k*, of the hydrophilic as well as hydrophobic beadpack used for the co-injection and emulsion flow experiments was calculated using the following equation:

$$k = \frac{1}{72\tau}\frac{\phi^3 D_p^2}{(1-\phi)^2}, \quad \text{(Eq. 3)}$$

where τ is the tortuosity, ϕ is the porosity, and D_p is bead diameter. A value of 25/12 was used for tortuosity which is the value suggested for randomly packed spheres (Lake 1989). The porosity value was assumed to be 0.36 as per Zhang et al. (2006).

The shear rate, $\dot{\gamma}_{eq}$, in the hydrophilic as well as hydrophobic beadpack was calculated using the following equation (Lake 1989):

$$\dot{\gamma}_{eq} = 4v\left(\frac{\phi}{8k}\right)^{\frac{1}{2}} = \frac{4q}{A\sqrt{8k\phi}}, \quad \text{(Eq. 4)}$$

where $v = q/A/\phi$ is the interstitial velocity (cm/s), q is the volumetric flow rate (cm^3/s), A is the cross-sectional area (cm^2), k is the permeability (cm^2), and ϕ is the porosity. This equation uses the bundle of capillary tubes model to predict rheological properties of non-Newtonian fluids flowing through porous media.

The apparent viscosity, μ_{app}, of the emulsion flowing through the hydrophobic beadpack was calculated from Darcy's law:

$$\mu_{app} = \frac{\mathrm{kA}}{\mathrm{Q}} \frac{(\mathrm{P_i} - \mathrm{P_o})}{\mathrm{L}}, \quad \text{(Eq. 5)}$$

where k is the permeability of the beadpack (cm^2), A is the cross-sectional area of the beadpack (cm^2), P_o and P_i are the outlet and inlet pressure (dyne/cm^2), Q is the volumetric flow rate (cm^3/s), and L is the length of the bead pack (cm).

3.2.2 Emulsion Viscosity

Stable oil-in-water emulsions generated via the co-injection method described above are known to be highly shear thinning power-law fluids (Gabel et al. 2014). This is to say that as the shear rate increases, the emulsion viscosity decreases. The shear stress, τ, of a power law fluid is calculated using the following equation:

$$\tau = K\dot{\gamma}^n, \quad \text{(Eq. 6)}$$

where K is the consistency index, $\dot{\gamma}$ is the shear rate, and n is the flow behavior index.

3.3 Results and Discussion

In this section results from the emulsion injection experiments through a hydrophobic beadpack will be presented and discussed. Photographs will be provided to show the collected effluent which was collected in 15 mL centrifugal test tubes. For all experiments the pore volume of the beadpack was calculated to be approximately 0.85 mL. The beadpack experiments were performed to determine whether emulsion droplets

would survive passage through beadpacks of various size diameters and whether coalescence (and regeneration) would occur.

3.3.1 Emulsion Injection Experiments

Two different emulsions have been used for experimental purposes. These have been outlined in the previous section and will be denoted by their average droplet size i.e. 24 microns and 62 microns. These emulsions were injected into hydrophobic beadpacks of different bead sizes with de-ionized water as the initial saturation. The beadpack used for these experiments has been described in the previous section.

Beadpack Run 1 was performed using the smaller sized emulsion (24 microns in diameter). The emulsion was injected at 0.5 mL/min into a hydrophobic beadpack that had been initially saturated with de-ionized water filled with glass beads of 500 micron diameter. The shear rate for Beadpack Run 1 was 94 s^{-1}. Although the first 8 PV of injected emulsion coalesced, stable emulsion was produced afterwards. Volumes of aqueous phase as well as organic phase were also produced along with the emulsion as can be seen in Figure 3.4

.

			Run 1			
Emulsion Used (Microns)	**Flow Rate (mL/min)**	**Bead Diameter (Microns)**	**Shear Rate (1/s)**	**Initial Saturation**	**PV Injected**	**PV When Emulsion Arrived**
24	0.5	500	94	De-ionized Water	140	8

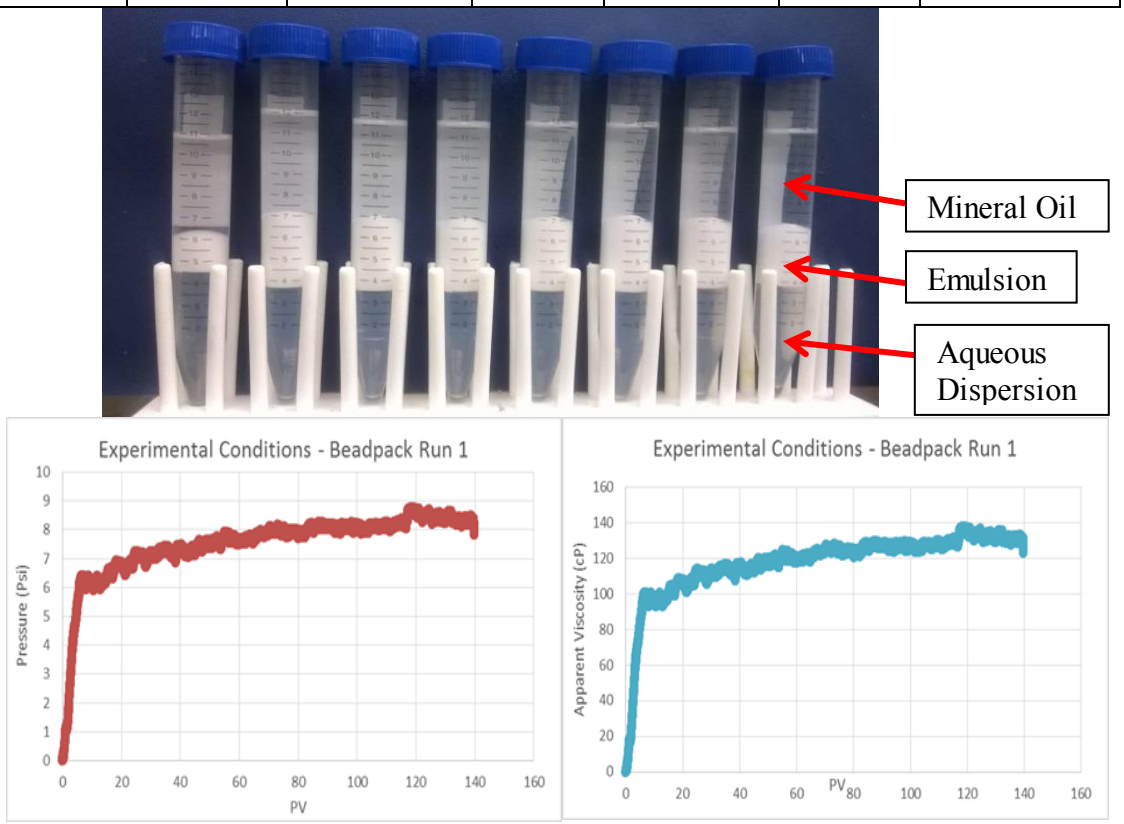

Figure 3.4: Experimental conditions and effluent from Beadpack Run 1. The constituent phases from the broken emulsion were produced along with the regenerated emulsion.

For the same experiment performed in a hydrophilic beadpack by Gabel (2014), much more volume of regenerated emulsion was seen to be collected in the effluent. However, the emulsion started to show regeneration at about the same PV (close to 8 PV). The pressure profile for the hydrophilic beadpack run was not collected. The pressure profile for the hydrophobic Beadpack Run 1 is seen to build up for about the first 0-10 PV after

which it is seen to relatively stabilize. It is within this first 0-10 PV that the effluent is seen to contain coalesced emulsion. Once emulsion is regenerated, pressure starts to stabilize.

In Beadpack Run 2, the larger sized emulsion was injected (62 microns) through a hydrophobic beadpack of size 500 micron diameter with all other conditions identical to that of Beadpack Run 1. No emulsion was collected throughout the entire experiment, i.e. complete coalescence was seen. This would support the hypothesis that smaller droplet sized emulsion are seen to be more stable while flowing through a hydrophobic beadpack. A contrast was seen from the same experiment performed through a hydrophilic beadpack by Gabel (2014) where regenerated emulsion was collected after approximately 45 PV after which all three phases (aqueous, emulsion and organic) were collected in the effluent. The pressure plot shows that pressure is seen to build up in the first 0-10 PV, which is comparable to Beadpack Run 1 and corresponds to coalesced emulsion. However, pressure is again seen to stabilize afterwards even though no regenerated emulsion is ever collected in the effluent. The effluent and the pressure profile for Beadpack Run 2 are shown below:

			Run 2			
Emulsion Used (Microns)	**Flow Rate (mL/min)**	**Bead Diameter (Microns)**	**Shear Rate (1/s)**	**Initial Saturation**	**PV Injected**	**PV When Emulsion Arrived**
62	0.5	500	94	De-ionized Water	140	Never

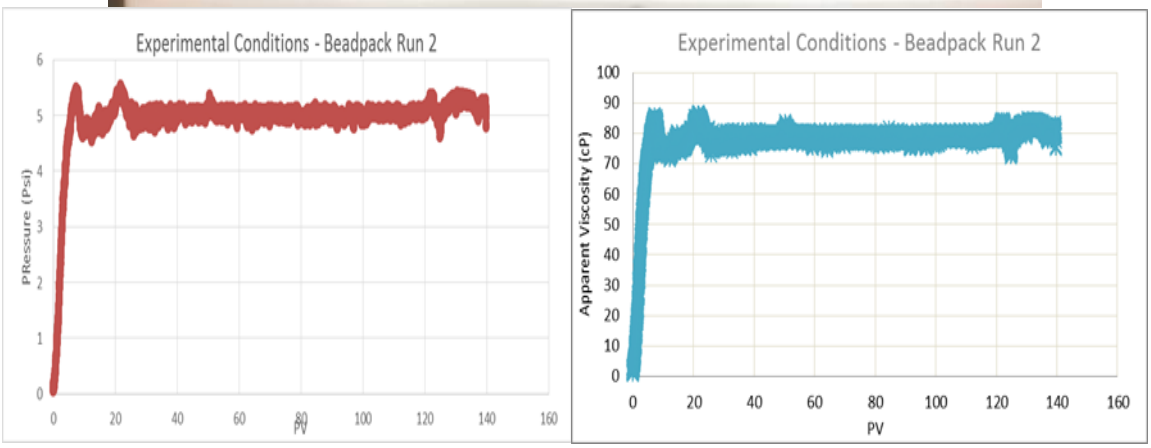

Figure 3.5: Experimental conditions and effluent from Beadpack Run 2. Only the constituent phases from the coalesced emulsion were collected in the effluent. The volume ratio of the effluent is the same as the injected emulsion at approximately 2:1 light mineral oil to aqueous nanoparticle dispersion.

Beadpack Run 3 was performed using the 24 micron emulsion through a 180 micron beadpack with initial saturation of de-ionized water. This experiment was performed at a shear rate much higher than Beadpack Runs 1 and 2 which is a direct result of the glass bead diameter size; the shear rate was calculated to be 260 s^{-1}. As can be seen from the effluent, no emulsion was regenerated. This is in direct contrast with the same experiment performed using a hydrophilic beadpack by Gabel (2014). For the hydrophilic beadpack run, the regenerated emulsion was collected after 13 PV and was continuously produced from there onwards. From this contrast, and that from Beadpack Run 2, it is becoming evident that the wettability of the beadpack has some influence on the stability of the emulsion injected. A pressure profile trend which is similar to that of Beadpack Runs 1 and 2 was observed for Beadpack Run 3. The experimental conditions, effluent and pressure profile for Beadpack Run 3 can be seen in Figure 3.6.

			Run 3			
Emulsion Used (Microns)	**Flow Rate (mL/min)**	**Bead Diameter (Microns)**	**Shear Rate (1/s)**	**Initial Saturation**	**PV Injected**	**PV When Emulsion Arrived**
24	0.5	180	260	De-ionized Water	98	Never

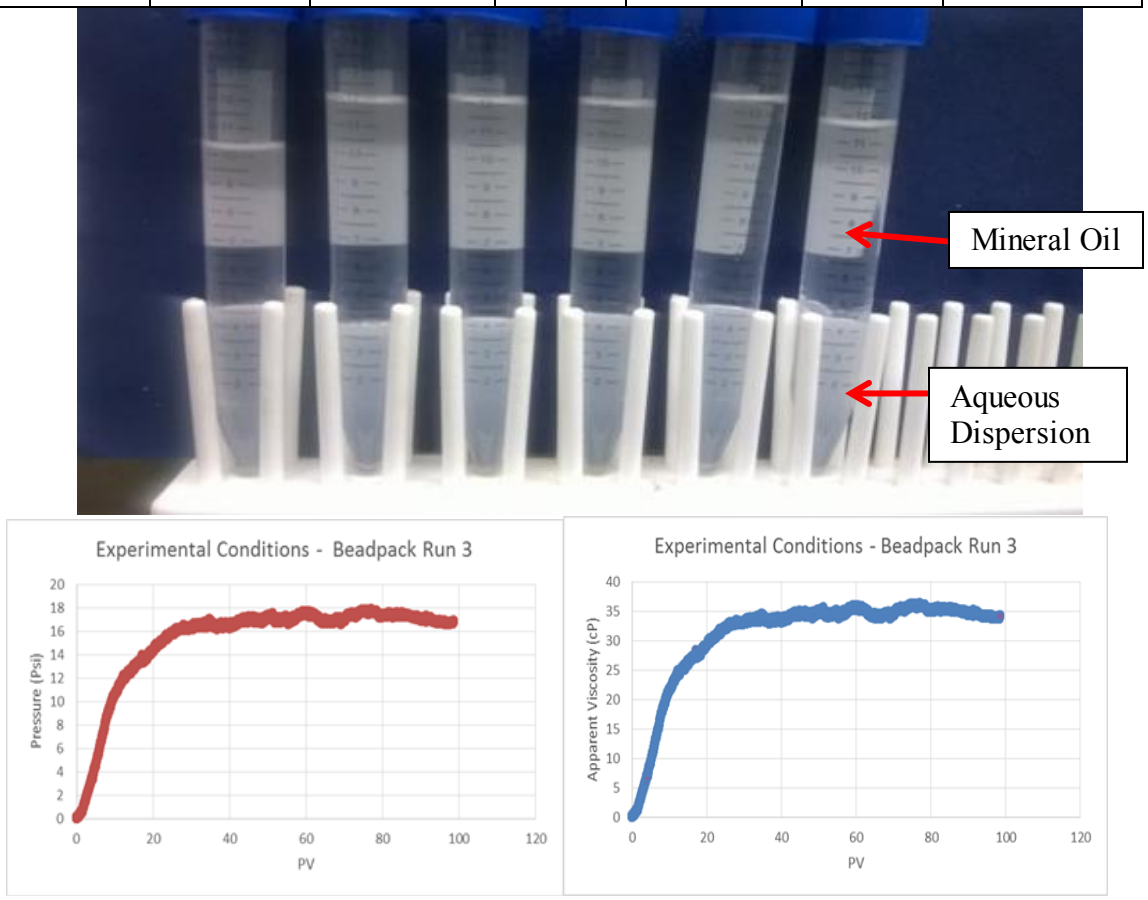

Figure 3.6: Experimental conditions and effluent from Beadpack Run 3. Only the constituent phases from the coalesced emulsion were collected in the effluent. The volume ratio of the effluent is the same as the injected emulsion at approximately 2:1 light mineral oil to aqueous nanoparticle dispersion.

Beadpack Runs 4A and 4B were performed to provide more insight on the comparison between the stability of the smaller to the larger sized emulsion. Emulsion 2, which was 62 microns in diameter, was injected into a hydrophobic beadpack filled with

180 micron glass beads for both runs. The shear rate for both Beadpack Runs 4A and 4B was 260 s^{-1}. As for previous experiments, the initial saturation of the beadpack was done using de-ionized water. The effluent and the pressure profiles showed that regeneration of the injected emulsions never occurred for both cases with a similar build up (for the first 0-10 PV) and stabilization of the pressure.

			Run 4A			
Emulsion Used (Microns)	**Flow Rate (mL/min)**	**Bead Diameter (Microns)**	**Shear Rate (1/s)**	**Initial Saturation**	**PV Injected**	**PV When Emulsion Arrived**
62	0.5	180	260	De-ionized Water	85	Never
			Run 4B			
Emulsion Used (Microns)	**Flow Rate (mL/min)**	**Bead Diameter (Microns)**	**Shear Rate (1/s)**	**Initial Saturation**	**PV Injected**	**PV When Emulsion Arrived**
62	0.5	180	260	De-ionized Water	130	Never

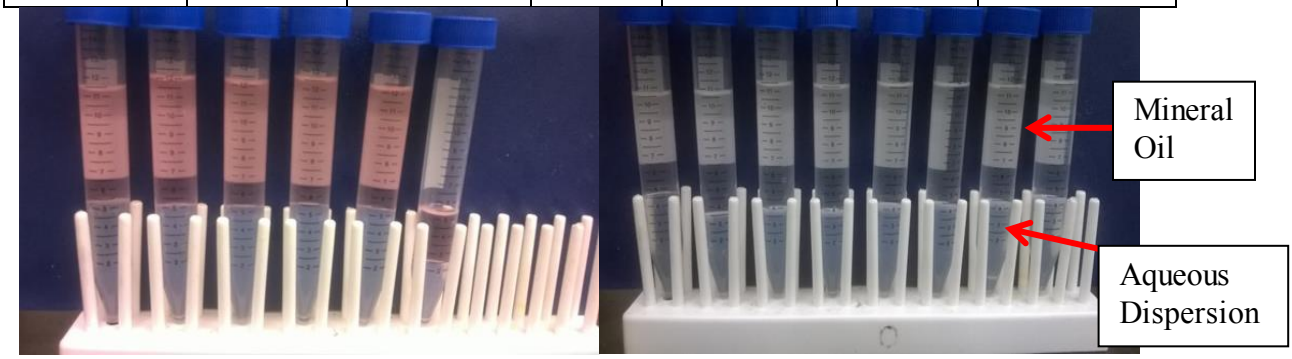

Effluent for Beadpack Run 4A

Effluent for Beadpack Run 4B

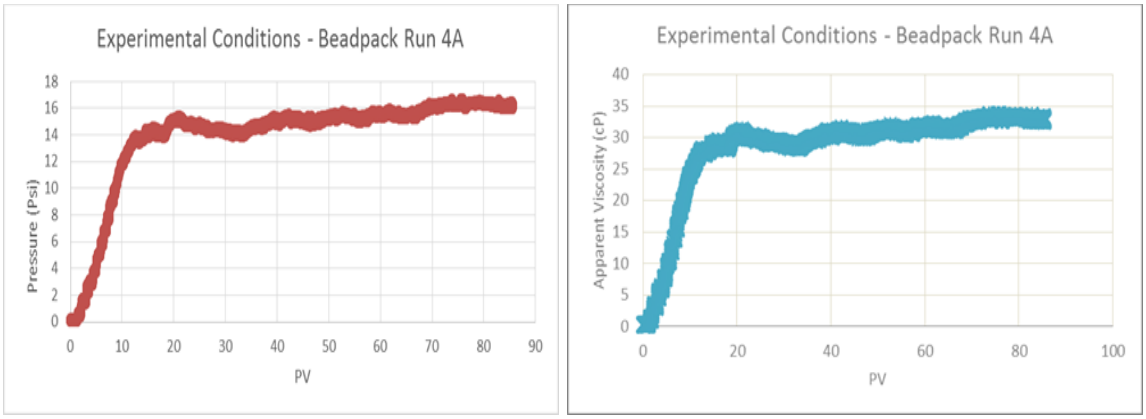

Figure 3.7

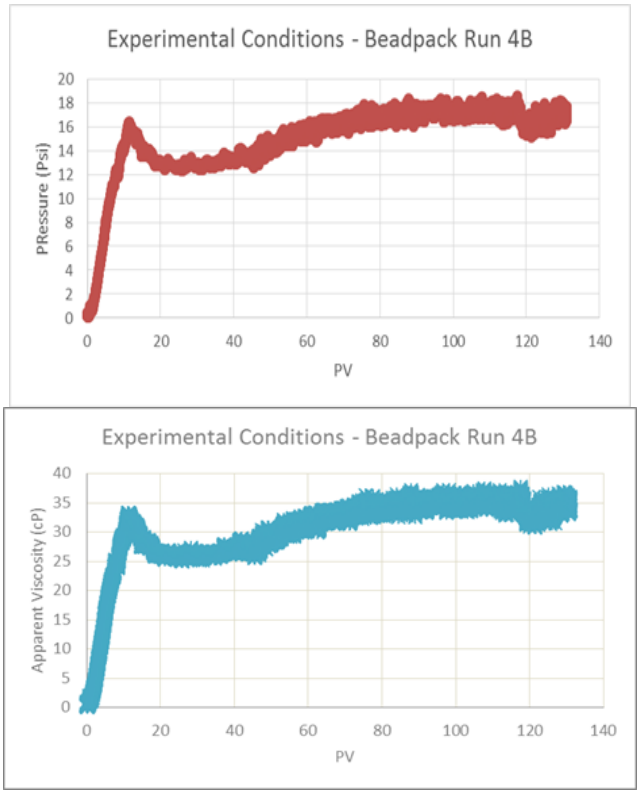

Figure 3.7: Experimental conditions and effluent from Beadpack Runs 4A and 4B. Only the constituent phases from the coalesced emulsion were collected in the effluent. The volume ratio of the effluent is the same as the injected emulsion at approximately 2:1 light mineral oil to aqueous nanoparticle dispersion for both runs.

Beadpack Run 5 was performed using a 24 micron emulsion through a 1000 micron hydrophobic beadpack at a shear rate of 47 s^{-1}. Coalescence and regeneration of the emulsion were both seen to occur. The regenerated emulsion appeared at approximately 5 PV.

			Run 5			
Emulsion Used (Micron)	**Flow Rate (mL/min)**	**Bead Diameter (Micron)**	**Shear Rate (1/s)**	**Initial Saturation**	**PV Injected**	**PV When Emulsion Arrived**
24	0.5	1000	47	De-ionized Water	185	5

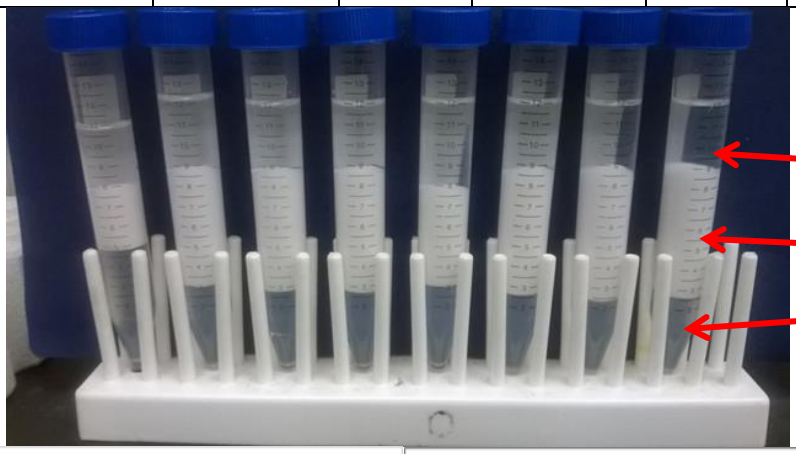

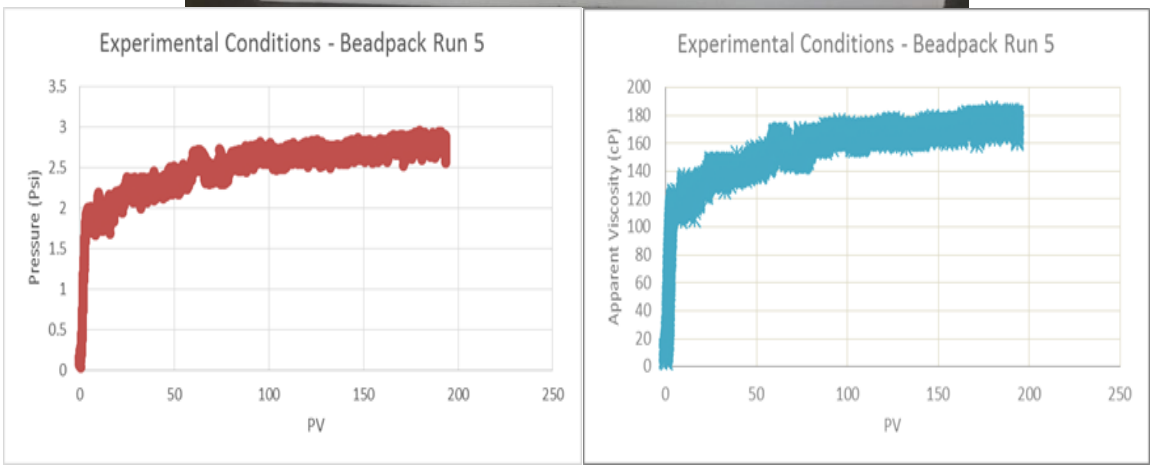

Figure 3.8: Experimental conditions and effluent from Beadpack Run 5. The constituent phases from the broken emulsion were produced along with the regenerated emulsion.

When comparing the hydrophobic Beadpack Run 5 to the hydrophilic run by Gabel (2014), it can be seen that much higher pressure profiles are exhibited for the hydrophilic case. For the hydrophilic beadpack, a periodic pressure profile was observed which fluctuated between 10-45 psi. This was very different from the pressure profile

seen for the hydrophobic Beadpack Run 5 (pressure build up for the first 0-10 PV followed by relatively stable pressure). This observation is will be explored later in this discussion. For Beadpack Run 5, emulsion was regenerated at about 5 PV. A possibility as to why the emulsion was generated was perhaps the combination of the more stable emulsion with a smaller droplet size with the more permeable path provided by the 1000 micron beadpack.

Beadpack Run 6 was performed with conditions identical to Beadpack Run 5 however the emulsion injected was the larger sized 62 micron emulsion. The effluent profile and the pressure drop figures are shown as follows:

			Run 6			
Emulsion Used (Microns)	**Flow Rate (mL/min)**	**Bead Diameter (Microns)**	**Shear Rate (1/s)**	**Initial Saturation**	**PV Injected**	**PV When Emulsion Arrived**
62	0.5	1000	47	De-ionized Water	125	65

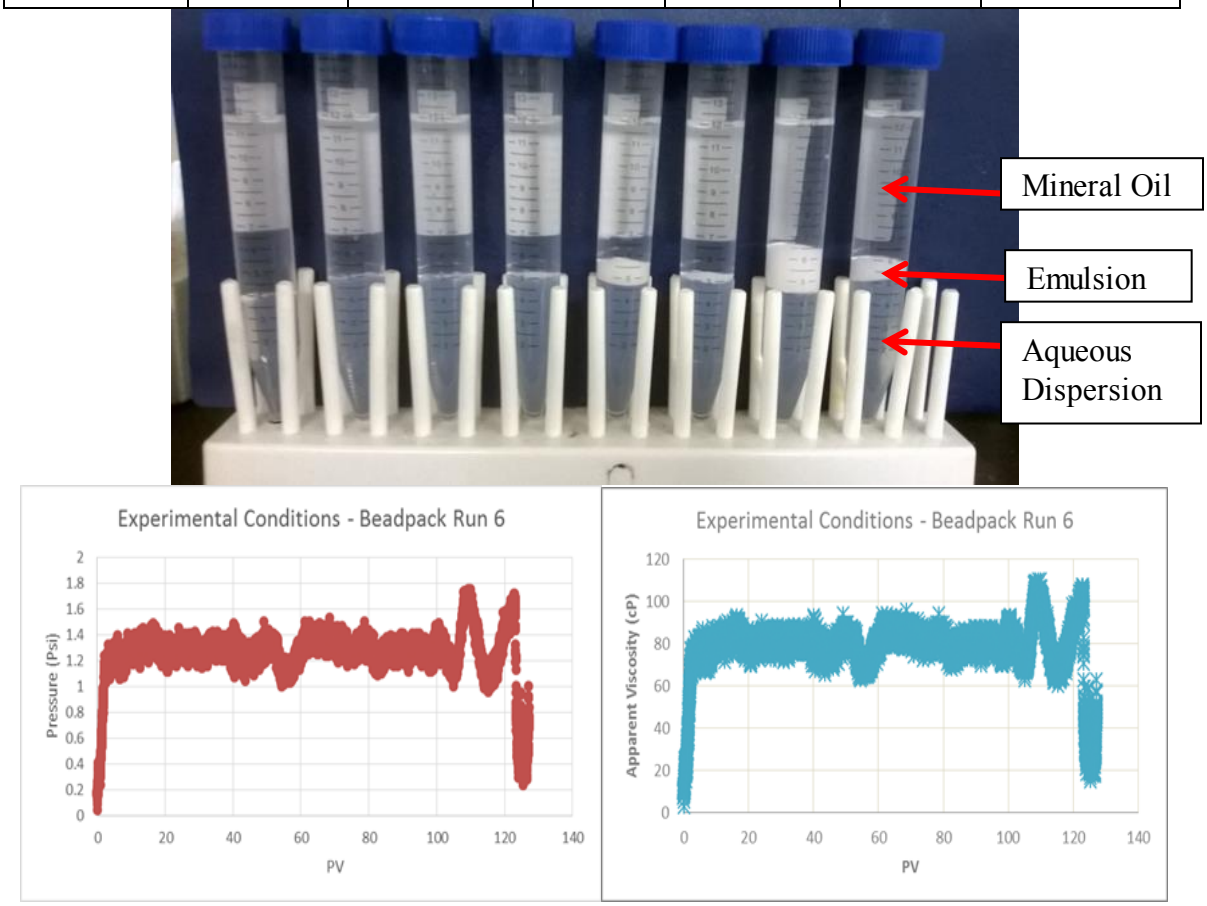

Figure 3.9: Experimental conditions and effluent from Beadpack Run 6. The constituent phases from the broken emulsion were produced along with the regenerated emulsion. Emulsion was seen to be regenerated after 65 PV.

Beadpack Run 6 suggests that the larger sized emulsion was less stable than the 24 micron emulsion. It was regenerated much later in the experiment at about 65 PV. At and after 65 PV, very little regeneration of the emulsion was seen. This would suggest

that both the emulsion droplet size as well as the beadpack permeability affect the coalescence and regeneration of the injected emulsion. The pressure profile for Beadpack Run 6 shows the initial expected pressure build up for 0-10 PV. This is followed by relative stability of the pressure. Close to 65 PV, when some emulsion started to regenerate, slight fluctuations in pressure were observed which continued for the rest of the emulsion injection until the end of the experiment.

Beadpack Runs 1-6 have all been performed below the critical shear rate for their specific beadpack sizes. Beadpack Run 7 was performed well above the critical shear rate for the 500 micron hydrophobic beadpack used at a calculated value of 750 s^{-1}. It was performed using emulsion 1 (24 micron) at an initial saturation of de-ionized water. The flow rate at which the emulsion was injected was 4 mL/min.

Comparing the effluent of Beadpack Run 7 to the case with the hydrophilic beadpack performed by Gabel (2014), hydrophobic Beadpack Run 7 showed much less regeneration of the emulsion. The hydrophilic beadpack experiment had emulsion regeneration at 11 PV whereas that in the hydrophobic beadpack was at 5 PV. Compared to Beadpack Run 1 which had identical conditions but a much smaller shear rate, more emulsion was regenerated for Beadpack Run 7. This suggests that coalescence and regeneration of the emulsion is not only dependent on the emulsion droplet size and permeability of the beadpack, but also on the shear rate. Higher shear rates have the ability to push more emulsion through the beadpack and provide better conditions for the regeneration of the injected emulsion.

			Run 7			
Emulsion Used (Microns)	**Flow Rate (mL/min)**	**Bead Diameter (Microns)**	**Shear Rate (1/s)**	**Initial Saturation**	**PV Injected**	**PV When Emulsion Arrived**
24	4	500	750	De-ionized Water	105	5

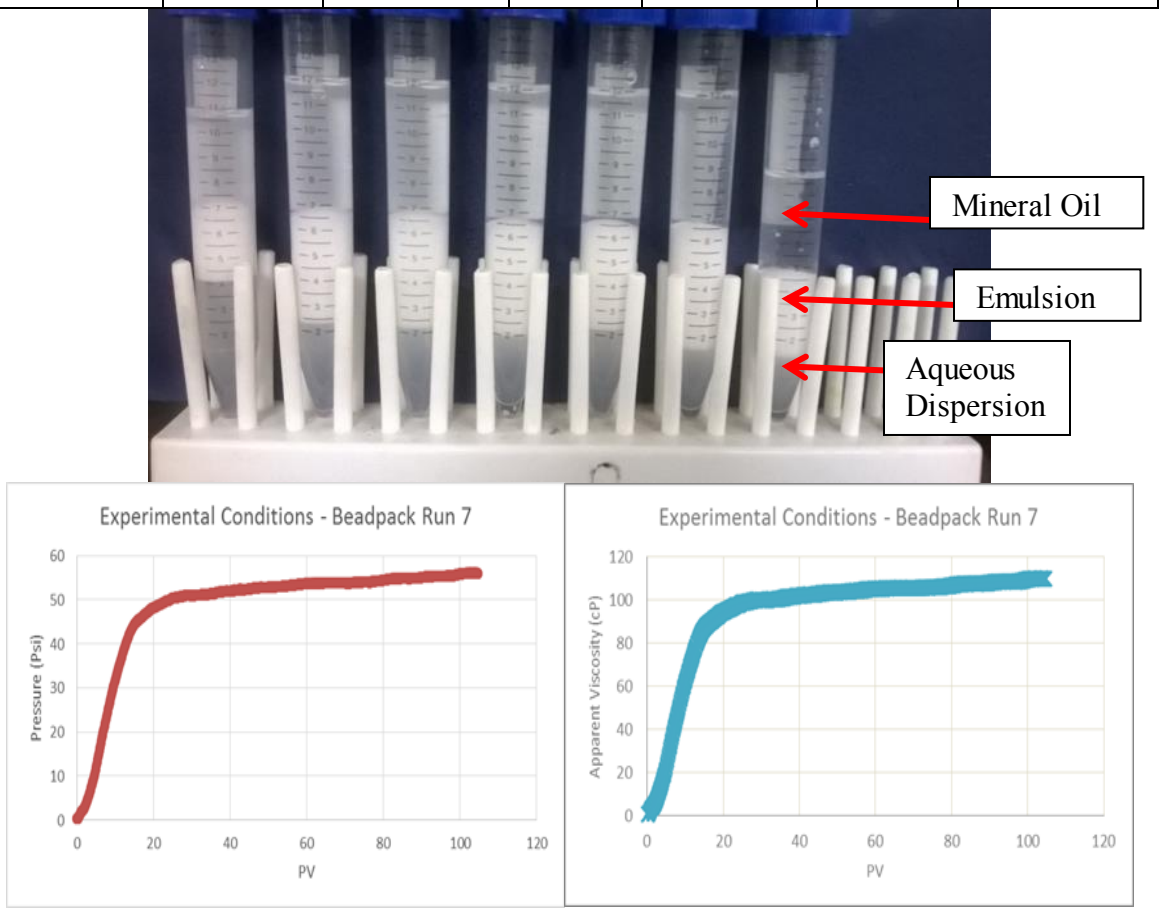

Figure 3.10: Experimental conditions and effluent from Beadpack Run 7. The constituent phases from the broken emulsion were produced along with the regenerated emulsion. Emulsion was seen to be regenerated after 5 PV.

Beadpack Run 8 had identical conditions to Beadpack Run 7 however the injected emulsion was the larger droplet size emulsion (62 micron). The results are as follows:

`			Run 8			
Emulsion Used (Microns)	**Flow Rate (mL/min)**	**Bead Diameter (Microns)**	**Shear Rate (1/s)**	**Initial Saturation**	**PV Injected**	**PV When Emulsion Arrived**
62	4	500	750	De-ionized Water	100	Never

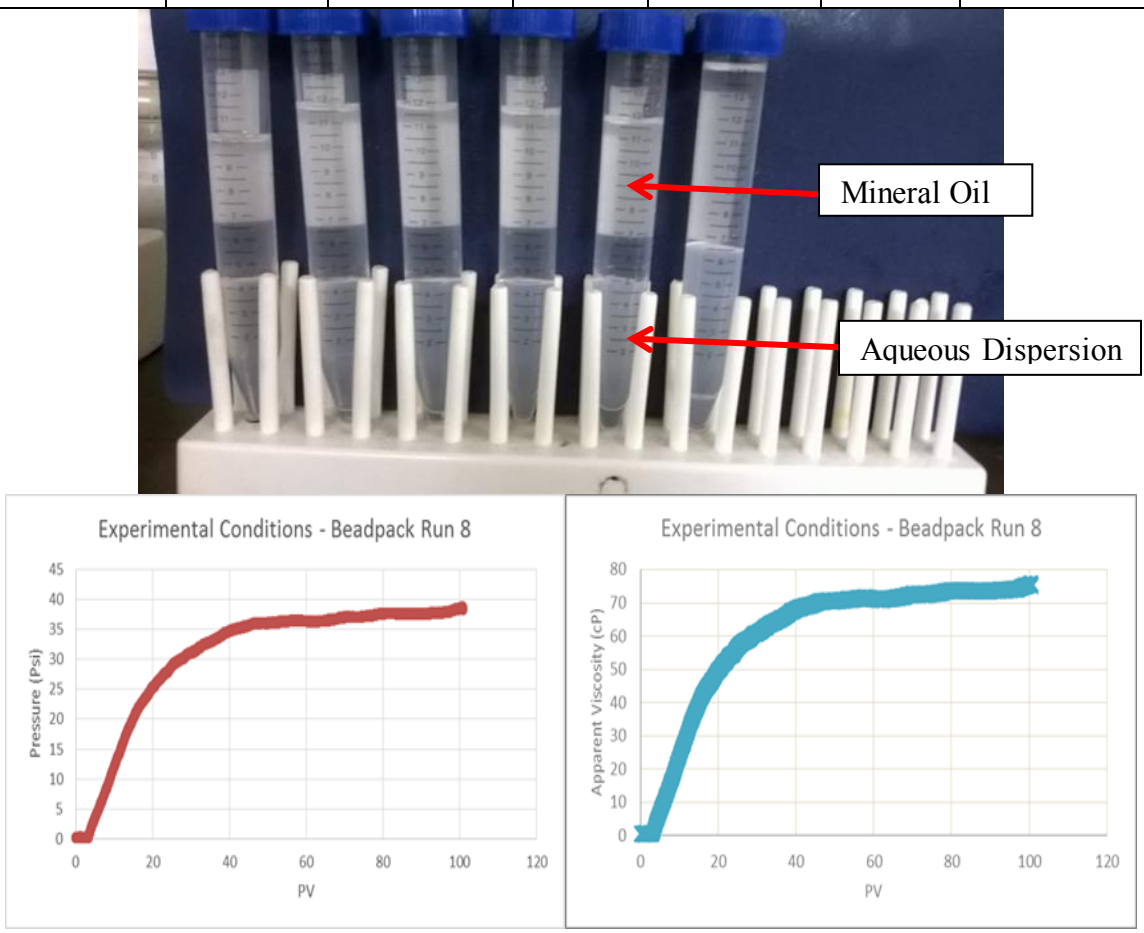

Figure 3.11: Experimental conditions and effluent from Beadpack Run 8. Only the constituent phases from the coalesced emulsion were collected in the effluent. The volume ratio of the effluent is the same as the injected emulsion at approximately 2:1 light mineral oil to aqueous nanoparticle dispersion.

From Beadpack Run 8 it appears that due to the lesser stability of the larger droplet sized emulsion the higher shear rate could still not cause regeneration of the

emulsion. Coalescence of the emulsion was seen throughout the course of the experiment and the pressure profile appeared to follow the predicted build up and stabilizing trend.

Comparing the hydrophilic runs performed by Gabel (2014) and hydrophobic Beadpack Runs 1-8, certain observations were consistent. The hydrophobic beadpack has lesser tendency for the regeneration of the injected emulsion. In general, much less emulsion was regenerated (if any) for most runs compared to the hydrophilic beadpack experiments. The second consistent observation was that the pressures appeared to be much higher for the hydrophilic beadpack experiments by Gabel (2014). A proposed hypothesis is that hydrophobic beadpacks have a tendency to prevent accumulation of the hydrophilic nanoparticles within the beadpack. When the injected emulsion coalesces inside the beadpack, the two phases present are the organic mineral oil and the aqueous nanoparticle dispersion. The hydrophilic nanoparticles would then have a much greater tendency to accumulate near the hydrophilic glass beads when compared to the hydrophobic glass beads. If hydrophilic nanoparticles are present in a hydrophilic beadpack, the tendency for accumulation would be greater, which could possibly result in a clumping of the hydrophilic nanoparticles around the hydrophilic glass beads resulting in an obstruction to flow. Due to this obstruction in flow, pressures in the hydrophilic beadpack would appear to be much higher than those for hydrophobic beadpacks. For the case of the hydrophobic beadpacks, the now hydrophobic glass beads are not the ideal positioning place for the hydrophilic nanoparticles. It is expected that for this case, the organic light mineral oil would be more attracted to the beads and therefore would not allow clumping of the nanoparticles around the hydrophobic glass beads. The nanoparticles would perhaps clump together and flow out of the beadpack rather than get retained. This would therefore prevent an obstruction to flow and pressures would appear to be much lower. To test this hypothesis it is necessary to measure the concentration of

nanoparticles in the effluent aqueous phase. As both emulsions were created using a 2 wt % nanoparticle dispersion, the effluent concentration could possibly provide an indication of either retention of nanoparticles or ease of flow of nanoparticles when compared to this reference point.

3.3.2 Particle Size Analysis of Effluent Nanoparticles

The effluent collected from Beadpack Runs 1-8 all contained an aqueous phase of hydrophilic nanoparticle dispersion. To test the hypothesis that hydrophilic nanoparticles are not accumulated in hydrophobic beadpacks, it is essential to measure the concentration of this effluent aqueous phase. NMR was used to measure the concentration of various dispersions of Nyacol DP9711 silica nanoparticles.

The longitudinal relaxation rate $1/T_1$ is composed of two relaxation mechanisms. T_{1B} is a bulk relaxation mechanism which is a fluid property and is dependent on how the fluid molecules interact with one another. T_{1S} is a surface relaxation mechanism which is dependent on how the fluid molecules interact with the surface of the nanoparticles. $1/T_1$ can be calculated by the sum of the two different relaxation mechanisms:

$$1/T_1 = 1/T_{1B} + 1/T_{1S} , \qquad \text{(Eq. 7)}$$

The bulk relaxation is easily measured from experiments by using a pure fluid in the absence of any nanoparticles. The surface relaxation is dependent on the S, the total nanoparticle surface area, and V, the total fluid volume, and is given below:

$$1/T_{1S} = \rho_1 (S/V) , \qquad \text{(Eq. 8)}$$

where ρ_1 is the longitudinal surface relaxivity constant and S/V is given as:

$$S/V = 6 \chi/d , \qquad \text{(Eq. 9)}$$

where χ is the ratio of volume of nanoparticles to the total fluid volume and d is the nanoparticle diameter.

A calibration curve was prepared using the following concentrations: 0.1 wt %, 0.5 wt %, 1 wt %, 1.5 wt % and 2 wt %. A linear plot was seen and the retention time was seen to be inversely proportional to the concentration. Using this calibration curve as a reference point, the effluent aqueous nanoparticle phase of Beadpack Runs 2, 3, 4A and 4B was taken and measurements were made in order to compare the retention times and therefore decipher the concentration. Higher concentrations of nanoparticles in the aqueous phase would be expected from these runs as our hypothesis suggested ease of flow for hydrophilic nanoparticles through hydrophobic beadpacks. The NMR showed concentrations for runs 2, 3, 4A and 4B to be much higher than expected; all greater than 2 wt %. This plot is shown below:

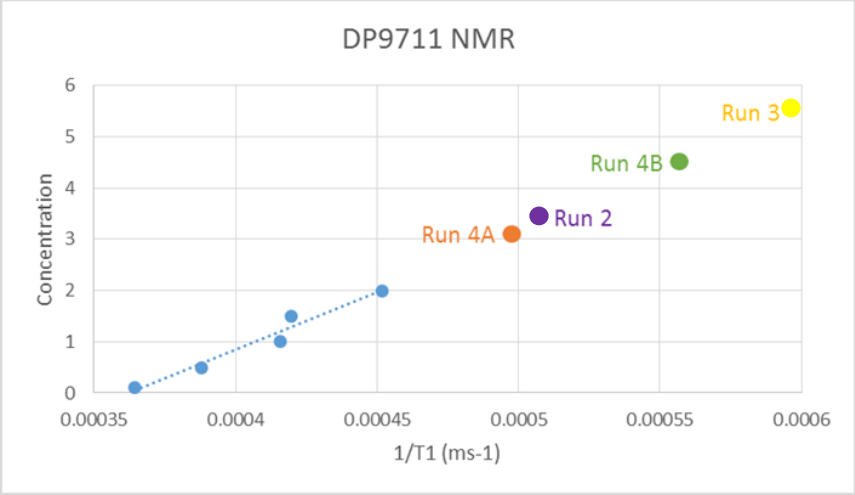

Figure 3.12: NMR Spectroscopy Results for Nyacol DP9711: The calibration curve points are seen in blue whereas the Beadpack Run points are shown in various colors.

As this is quite unrealistic, the possibility of the hydrophilic nanoparticles clumping was explored. If nanoparticles are to clump together in the beadpack and flow out to the effluent in such a state, the particle size for these nanoparticles would not stay in the 15-25 nm range as is the case in the original dispersion. For this purpose, laser particle size analysis was performed on runs 2, 4A and 4B as well as the original 20 wt %

nanoparticle dispersion of Nyacol DP9711. A Beckman Coulter Delsa Nano machine was used to perform these measurements.

For the 20 wt % nanoparticle dispersion, the average particle size was seen to be 23.8 nm with a standard deviation of 8.6. This is considered to be the reference point for all further particle size analysis runs. Figure 3.13 shows the results of this analysis:

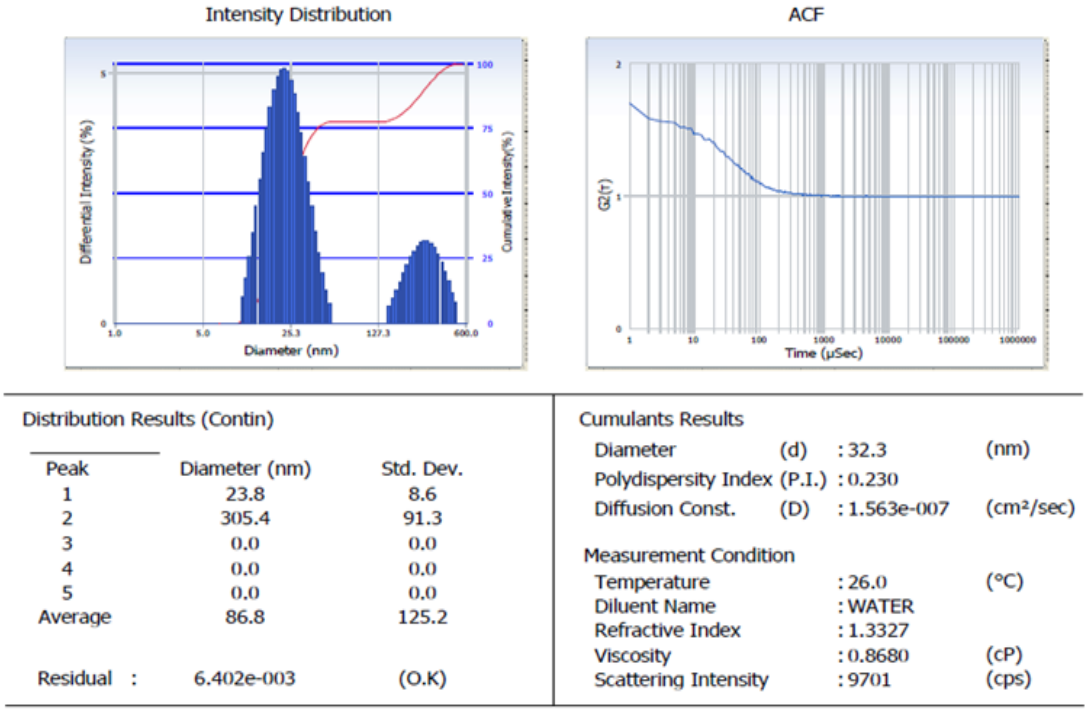

Distribution Results (Contin)

Peak	Diameter (nm)	Std. Dev.
1	23.8	8.6
2	305.4	91.3
3	0.0	0.0
4	0.0	0.0
5	0.0	0.0
Average	86.8	125.2
Residual :	6.402e-003	(O.K)

Cumulants Results

Diameter	(d)	: 32.3	(nm)
Polydispersity Index	(P.I.)	: 0.230	
Diffusion Const.	(D)	: 1.563e-007	(cm²/sec)

Measurement Condition

Temperature	: 26.0	(°C)
Diluent Name	: WATER	
Refractive Index	: 1.3327	
Viscosity	: 0.8680	(cP)
Scattering Intensity	: 9701	(cps)

Figure 3.13: Particle Size Analysis for Nyacol DP9711: Original 20 wt% Dispersion. The average particle size was estimated to be 23.8 nm with a standard deviation of 8.6.

This particle size analysis was then performed for Beadpack Run 2. The average diameter was determined to be 58.2 nm with a standard deviation of 26.5. This large particle size, when compared to the particle size of the original dispersion, strengthens the hypothesis of clumping of hydrophilic nanoparticles in hydrophobic beadpacks to

allow ease of flow (and therefore lower pressures profiles). This can be seen in Figure 3.14:

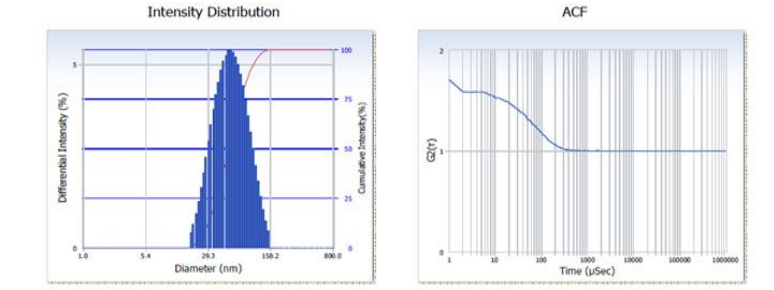

Distribution Results (Contin)

Peak	Diameter (nm)	Std. Dev.
1	58.2	26.5
2	0.0	0.0
3	0.0	0.0
4	0.0	0.0
5	0.0	0.0
Average	58.2	26.5

Residual : 4.405e-003 (O.K)

Cumulants Results

Diameter	(d)	: 48.0	(nm)
Polydispersity Index	(P.I.)	: 0.167	
Diffusion Const.	(D)	: 1.034e-007	(cm²/sec)

Measurement Condition

Temperature	: 25.3	(°C)
Diluent Name	: WATER	
Refractive Index	: 1.3328	
Viscosity	: 0.8818	(cP)
Scattering Intensity	: 10419	(cps)

Figure 3.14: Particle Size Analysis for Nyacol DP9711: Beadpack Run 2. The average particle size was estimated to be 58.2 nm with a standard deviation of 26.5.

Beadpack Runs 4A and 4B also showed much higher particle sizes (56 nm and 64.4 nm respectively) which would be expected from the NMR spectroscopy results and the proposed hypothesis. The results are shown below:

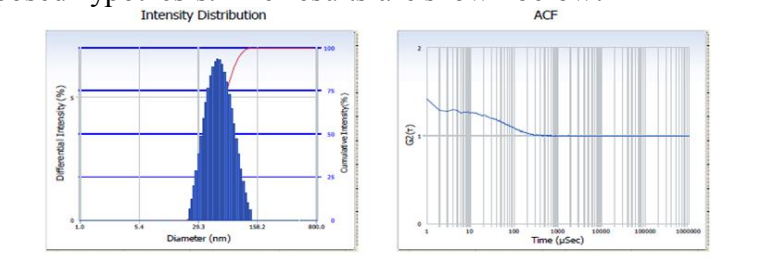

Distribution Results (Contin)

Peak	Diameter (nm)	Std. Dev.
1	56.0	21.4
2	0.0	0.0
3	0.0	0.0
4	0.0	0.0
5	0.0	0.0
Average	56.0	21.4

Residual : 5.571e-003 (O.K)

Cumulants Results

Diameter	(d)	: 49.8	(nm)
Polydispersity Index	(P.I.)	: 0.194	
Diffusion Const.	(D)	: 1.036e-007	(cm²/sec)

Measurement Condition

Temperature	: 26.8	(°C)
Diluent Name	: WATER	
Refractive Index	: 1.3326	
Viscosity	: 0.8526	(cP)
Scattering Intensity	: 9924	(cps)

Figure 3.15: Particle Size Analysis for Nyacol DP9711: Beadpack Run 4A. The average particle size was estimated to be 56.0 nm with a standard deviation of 21.4.

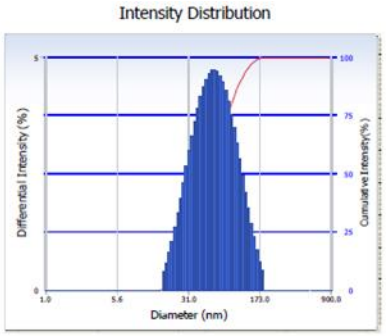

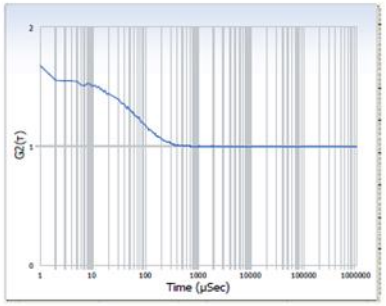

Distribution Results (Contin)

Peak	Diameter (nm)	Std. Dev.
1	64.4	34.0
2	0.0	0.0
3	0.0	0.0
4	0.0	0.0
5	0.0	0.0
Average	64.4	34.0
Residual :	5.821e-003	(O.K)

Cumulants Results

Diameter	(d)	: 50.0	(nm)
Polydispersity Index	(P.I.)	: 0.203	
Diffusion Const.	(D)	: 1.009e-007	(cm²/sec)

Measurement Condition

Temperature	: 26.0	(°C)
Diluent Name	: WATER	
Refractive Index	: 1.3327	
Viscosity	: 0.8680	(cP)
Scattering Intensity	: 10011	(cps)

Figure 3.16: Particle Size Analysis for Nyacol DP9711: Beadpack Run 4B. The average particle size was estimated to be 64.4 nm with a standard deviation of 34.0

Although it was proven that hydrophilic nanoparticles are in fact clumping together, this does not match up with equations 8 and 9. As the equations would suggest, an increase in the nanoparticle diameter would suggest a smaller ratio of nanoparticle surface area to total fluid volume in the dispersion. This would therefore lead to a shorter $1/T_{1S}$ and therefore suggest a lower nanoparticle concentration. This is not the case that we saw in Figure 3.12. The unrealistically high measurements of concentration for hydrophilic nanoparticles in the effluent therefore remained unaccounted for.

3.4 CONCLUSIONS

Various experiments were performed to assess the stability of two emulsions with different droplet sizes in hydrophobic beadpacks of different diameter glass beads. The coalescence and regeneration of the emulsions is dependent on certain experimental factors. The emulsions with the smaller droplet size are seen to be more stable than the

emulsions with larger droplet size. Permeability of the beadpack also influences regeneration of the emulsion; the more permeable the beadpack, the more regeneration of the injected emulsion. Higher shear rates also help regenerate more emulsion.

In comparison to the hydrophilic beadpack experiments by Gabel (2014), hydrophobic beadpacks show a lesser tendency to allow the regeneration of the emulsion. In addition, pressures are much lower for hydrophobic beadpacks than hydrophilic beadpacks. This could be explained by the possibility of the accumulation of hydrophilic nanoparticles in hydrophilic beadpacks and much less retention of hydrophilic nanoparticles in the hydrophobic beadpacks. The particle size analysis provides some support for this hypothesis however the NMR results for effluent concentration remained inconclusive.

Chapter 4

Coreflood Experiments through Boise Sandstones

Although flow through beadpacks provides essential information on emulsion characteristics, it is essential to also perform coreflood experiments in order to solidify hypotheses posed for observations seen in these beadpack experiments. Boise sandstone cores are primarily used for the coreflood experiments as their properties seem to align well with the practical application of nanoparticle-stabilized emulsions projected in the field. Many, but not all, corefloods were performed to assess residual oil recovery after the core had initially been waterflooded and was at residual oil saturation. All coreflood experiments were performed at room temperature with an outlet pressure of 0 psig.

4.1 MATERIALS USED

Sandstone Core

The majority of the experiments were performed using Boise sandstone cores. Boise sandstones are readily available, have low clay content, are relatively low in heterogeneity and have reasonable permeabilities where emulsion flow is a viable, practical application. All Boise sandstone cores used were 30.48 cm in length and 2.54 cm in diameter. Typical pore volumes were in the 40-45 mL range with porosities seen in the 0.25-0.30 range.

Nanoparticle Stabilized Emulsions

Various emulsions were used for injection into Boise sandstone cores under different experimental conditions. All emulsions injected were generated by co-injection

through a beadpack filled with 180 micron glass beads. All emulsions injected were stabilized using Nyacol DP9711 nanoparticles dispersed in brine.

Organic and Aqueous Phases

Various internal organic phases were used in the emulsion coreflood experiments. Among the organic phases were Texaco oil, light mineral oil, n-octane and pentane. The physical properties of these oils are outlined below:

Oil	Mineral Oil	Texaco White Oil	n-Octane	Pentane
Viscosity (cP)	41.5	26.6	0.49	0.24

Table 4.1 Bulk viscosity of the oils used to generate emulsions

3 wt% NaCl brine was used as the continuous phase of the emulsions generated. 2 wt% NaCl brine was used to initially saturate the core in order to measure the permeability of the Boise sandstone.

Effluent Test Tubes

Plastic centrifugal tubes were used to collect the effluent generated from the coreflood experiments. Each test tube had the capacity to collect about 15 mL of effluent but in most experiments about 12 mL of effluent was collected per tube. 12 mL amounted to approximately 0.25-0.30 pore volumes depending on the specific Boise sandstone core. A typical sample of coreflood effluent contained an excess organic phase on the top, emulsion, if any, in the middle and the aqueous nanoparticle dispersion at the bottom. All

effluent test tubes were placed in a fraction collector with an appropriate time setting dependent on the injection rate.

Pressure Transducers and Data Acquisition

Three Rosemount differential pressure transducers were used to monitor pressure changes across the core for the entirety of the coreflood experiments. These pressure transducers were of model 3051CD5A22A1A. The differential pressure transducers were connected to a data acquisition card, powered by a power supply unit, which allowed the collection of all pressure points and recorded them into the computer. LabView software was used to display and record the collected pressure data. The pressure data was corrected for any offset from zero pressure drop if seen. Although the Rosemount differential pressure transducers had a maximum working pressure of 2,000 psi, the three transducers were calibrated to a specific pressure range to provide most accuracy within that range.

Summary of Coreflood Experiments in Chapter 4								
Experiment Type	Core	SS	ϕ	k (mD)	Initial Saturation	Injected Fluids	Flow Rate (mL/min)	Percentage Recovery (%)
Mineral Oil Residual Oil Recovery using MO-NP Emulsion	U	Boise	0.29	635	Residual Mineral Oil and Brine	Mineral Oil Emulsion (NP)	0.1	45
Mineral Oil Residual Oil Recovery using MO-NP Emulsion	U	Boise	0.29	635	Residual Mineral Oil and Brine	Mineral Oil Emulsion (NP)	0.5	27
Texaco Oil Residual Oil Recovery using MO-NP Emulsion	U	Boise	0.29	635	Residual Texaco Oil and Brine	Mineral Oil Emulsion (NP)	0.5	74
Texaco Oil Residual Oil Recovery using MO-NP Emulsion 0.33 PV Slug	W	Boise	0.27	855	Residual Texaco Oil and Brine	Mineral Oil Emulsion (NP) and Brine	0.5	19
Texaco Oil Residual Oil Recovery using MO-NP Emulsion 0.50 PV Slug	W	Boise	0.27	855	Residual Texaco Oil and Brine	Mineral Oil Emulsion (NP) and Brine	0.5	44
Texaco Oil Residual Oil Recovery using MO-NP Emulsion 0.75 PV Slug	W	Boise	0.27	855	Residual Texaco Oil and Brine	Mineral Oil Emulsion (NP) and Brine	0.5	55
Mineral Oil Residual Oil Recovery using O-NP Emulsion 0.75 PV Slug	X	Boise	0.26	1055	Residual Mineral Oil and Brine	Octane Emulsion (NP)	0.1	30
Mineral Oil Residual Oil Recovery using O-NP Emulsion 0.70 PV Slug	X	Boise	0.26	1055	Residual Mineral Oil and Brine	Octane Emulsion (NP)	2	28
Mineral Oil Residual Oil Recovery using O-Igepal Emulsion	Y	Boise	0.27	3750	Residual Mineral Oil and Brine	Octane Emulsion (Surfactant)	0.5	99
Mineral Oil Residual Oil Recovery via Co-Injection of Mineral Oil and Brine	Y	Boise	0.27	3750	Residual Mineral Oil and Brine	Mineral Oil Emulsion (NP) and Brine	4	48
Mineral Oil Residual Oil Recovery via Co-Injection of Mineral Oil and Brine	Z	Boise	0.29	3350	Residual Mineral Oil and Brine	Mineral Oil Emulsion (NP) and Brine	12	58
Octane-Surfactant Emulsion Injection to Brine Saturated Core	Z	Boise	0.29	3350	Brine	Octane Emulsion (Surfactant)	0.5	N/A
Mineral Oil Residual Oil Recovery using Igepal	A	Boise	0.28	4750	Residual Mineral Oil and Brine	Igepal	0.5	0
Mineral Oil Residual Oil Recovery using P-NP Emulsion	E	Boise	0.28	3225	Residual Mineral Oil and Brine	Pentane Emulsion (NP)	4	69
Mineral Oil Residual Oil Recovery using P-NP Emulsion	E	Boise	0.28	3225	Residual Mineral Oil and Brine	Pentane Emulsion (NP)	1	81
Mineral Oil Residual Oil Recovery using P-NP Emulsion 0.50 PV Slug	F	Boise	0.28	1690	Residual Mineral Oil and Brine	Pentane Emulsion (NP) and Brine	4	82
Mineral Oil Residual Oil Recovery using P-NP Emulsion 0.50 PV Slug	F	Boise	0.28	1690	Residual Mineral Oil and Brine	Pentane Emulsion (NP) and Brine	1	57

Table 4.2

Table 4.2: Emulsion coreflood experiments reported in this thesis. All emulsions were generated using 180 micron beadpack. Nyacol DP 9711 nanoparticle dispersion was used to stabilize the nanoparticle-stabilized emulsions. Igepal Co-70 surfactant dispersion was used to stabilize the surfactant-stabilized emulsions.

4.2 COREFLOOD EXPERIMENTAL SETUPS

This section will provide an outline of the experimental setups in detail. The different equipment used for the coreflood experiments will also be discussed. Two different setups were used to inject fluids through the Boise sandstone cores.

4.2.1 Emulsion/Nanoparticle Dispersion Experimental Setup

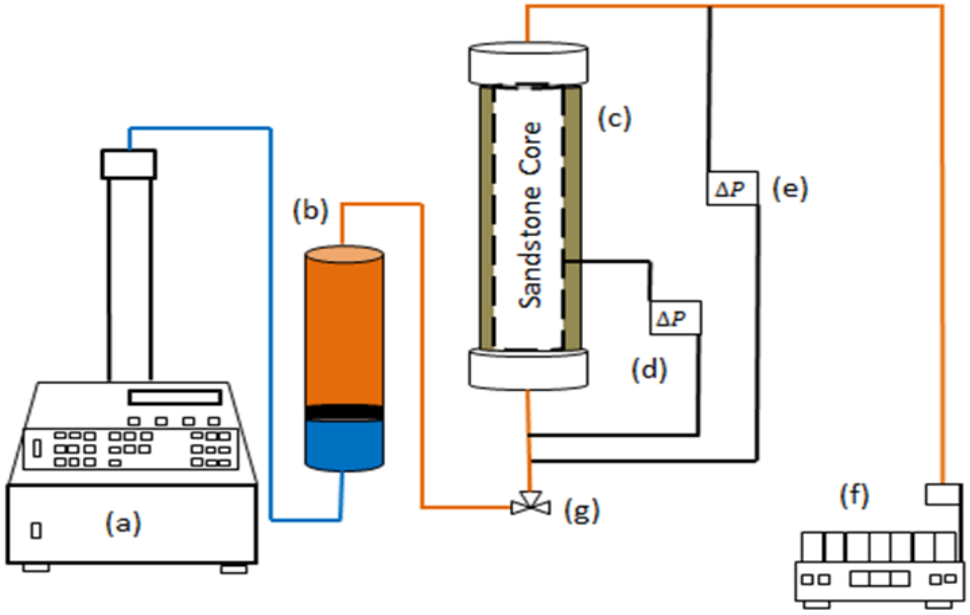

Figure 4.1: Schematic of Emulsion/Nanoparticle Dispersion Setup: (a) ISCO syringe pump, (b) accumulator, (c) core holder, (d & e) differential pressure transducer, (f) fraction collector, and (g) three-way valve (Gabel 2014)

The setup shown in Figure 4.1 was used for the majority of the experiments where emulsion was injected into the core holder containing a Boise sandstone core via the accumulator. This setup is quite similar to the experimental setup described in the previous chapter where emulsion injection experiments were performed in a beadpack. In

the experimental setup shown below, the emulsion is loaded and allowed to settle into its various components inside the accumulator (b). The emulsion held in the accumulator is pumped into the core holder (c) via the syringe pump (a). As the emulsion is transported through the sandstone core, effluent is produced which is collected in the fraction collector (f). Rosemount differential pressure transducers (d & e) are used to measure the pressure drop across the sandstone core. For the majority of the experiments the overall pressure drop was measured, i.e. at the beginning and at the end point of the core. (e) was used to measure the pressure drop across specific desired sections of the core and was not always incorporated.

For permeability measurements of the core, a similar setup was used where the injection fluid was brine. Similar setups were also used to waterflood the core, the only difference being the absence of the accumulator.

Core Holder

A Hassler type core holder was used for all of the experiments performed that are reported in this thesis. This core holder was manufactured by Phoenix Instruments Inc. and is designed to hold cores cut to 2.54 cm in diameter and 30.48 cm length. The confining pressure of the core holder was set to 2000 psi with a working temperature of 156 °C. A Viton sleeve was present inside the core holder for better placement of the core as well as for efficient confining. Confining the sandstone core is important to allow all injected fluids to enter the core rather than flow around it. Metal framing by Unistrut was used to mount the core holder vertically for all experiments performed. The core holder has 5 equally spaced pressure taps to enable the measurement of pressure drop across specific sections of the sandstone core. These taps were not used for the majority of the experiments.

4.2.2 Co-Injection Experimental Setup

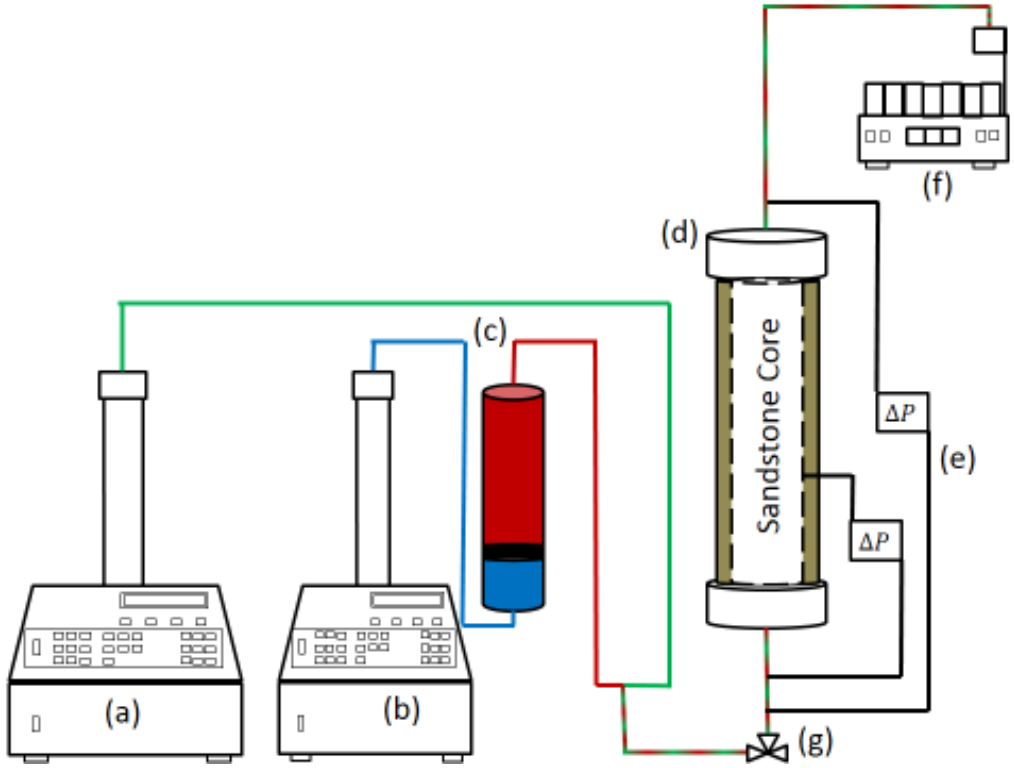

Figure 4.2: Schematic of Co-Injection Setup: (a) ISCO oil syringe pump, (b) ISCO brine syringe pump, (c) accumulator, (d) core holder, (e) differential pressure transducers, (f) fraction collector, and (g) three-way valve (Gabel 2014)

The setup shown in Figure 4.2 was used for all co-injection experiments performed. Normally, aqueous and organic phases were co-injected through the sandstone core and effluent was collected. Brine injection was performed directly from the syringe pump (b) whereas if nanoparticles were injected, this dispersion would be loaded into the accumulator (c) from which it would be pumped into the sandstone core. All organic phases were loaded into syringe pump (a). The two fluids to be injected together were designed to meet at a tee where they would flow together in alternating slugs. Pressure drop across the core was measured similarly through transducers located at (e).

4.3 COREFLOOD PROCEDURE

This section outlines the procedure used for all coreflood experiments performed in detail. This procedure consists of the sandstone core preparation and loading followed by the pressurizing of the core holder and permeability measurements.

4.3.1 Sandstone Core Preparation and Loading

All sandstone cores used for the experiments reported in this thesis were cut from large blocks of Boise sandstone. For the purposes of measuring the pore volume of the Boise sandstone, the dry weight of the core was recorded. Once the dry weight was recorded, the core was placed in a plastic container to be vacuumed overnight using a 1402 Welch Duoseal vacuum pump. After removing any trapped air in the core by vacuuming the core for approximately 24 hours, the dry core was then saturated with brine for approximately 2-3 hours. Finally the wet core was removed from the plastic sealed container and weighed again to get the wet weight of the core. The pore volume of the core was determined by simply subtracting the dry weight of the core from the wet weight of the core divided by the density of brine.

After the wet weight of the sandstone core had been measured, it was loaded into the core holder. Before opening the end caps of the core holder, care was taken to de-pressurize the core holder from the previous experiment. The core holder consisted of two end caps. The top end cap was screwed into place using a steel screw piece whereas the bottom end cap was twisted to fit in place by hand. To place the sandstone core into place, both the end caps were removed. The previously used sandstone core was removed from the core holder using a steel rod which would push the core from the top end, to be collected at the bottom end. Before adding the new core to the core holder, the bottom

end cap piece was flushed with brine to remove any presence of dead volume accumulated from previous experiments. After the bottom end cap was flushed clean, it was twisted by hand and locked into place. The core was then inserted from the top end, gently by hand. Once the core was inserted all the way, the top end cap was secured using the steel-screw piece. The core was then confined to a desired confining pressure. Confining pressure was applied to the core via a hand pump which pumped mechanical pump oil. A pressure gauge was monitored until the desired pressure of approximately 2000 psi was obtained. An Enerpac P-392 hydraulic hand pump was used to pump mechanical pump oil into the annulus of the core holder. This pump had the capacity to pump up to 10,000 psi.

4.3.2 Permeability Measurement

After the sandstone core was placed and confined to 2000 psi in the core holder, it was necessary to measure the permeability of the core before any experiment can be performed. The permeability of the core was measured by injecting brine pumped by the ISCO syringe pump, into which it had been previously loaded. Brine was injected into the bottom of the core until a steady state pressure drop was recorded by the transducer. The pressure drop was measured by the differential pressure transducer and recorded via the LABView software. If there was a small offset in the baseline recorded pressure, this was corrected by recording the pressure at zero flow rate and adjusting all values recorded afterwards.

4.3.3 Saturating the Core with Oil

After the permeability of the core was recorded, the initial saturation of the core was changed, depending on the specific organic phase required to be recovered for any

given experiment. Light mineral oil, Texaco oil, n-octane and pentane were all used to saturate the core for use in different experiments. The desired oil was injected into the core until the effluent showed no sign of recovering any more water, i.e. residual water saturation, Swr. Usually residual water saturation was reached by injection of approximately ten pore volumes of organic phase. Oil was injected from the top of the core, rather than the bottom, to provide a more gravity-stable, uniform displacement of denser brine by less dense organic phase. Because oil was being injected from the top, for this particular step of the experiment, it was essential to reverse the configuration of the differential pressure transducers. If the lines were not reversed, a negative value would be recorded for pressure.

4.3.4 Waterflooding the Core to Reach Residual Oil Saturation

Most experiments in this thesis were performed to assess the percentage of residual oil recovered by injecting a specific nanoparticle-stabilized emulsion. Before this emulsion could be injected into the core, the sandstone core had to be waterflooded to reach residual oil saturation, Sor. For this purpose, brine was injected through the bottom of the core to displace oil. Brine injection was initially performed at a low flow rate (~ 2 mL/min). When no more oil was recovered at this low flow rate, the flow rate was increased to potentially displace small amounts of more oil. The flow rate was incrementally increased until no more oil was displaced by brine. Residual oil saturation was reached when after all incremental flow rates, only brine was collected in the effluent. Typical flow rates for the waterflooding procedure typically began at 4 mL/mim and were incrementally increased to 8 mL/min, and finally 12 mL/min.

4.3.5 Cleaning Procedure for Core Reuse

After most of the corefloods performed were completed, the sandstone core used was cleaned and reused for the subsequent experiment. Isopropyl alcohol (IPA) was flowed through the sandstone core to flush out any residual volumes of oil and brine. Approximately 20 pore volumes of IPA were injected at high flow rates to ensure proper flushing of the core. After the core was flushed with IPA, about 10 pore volumes of brine were injected into the core to saturate the core with brine for subsequent experimentation. As brine was injected into the core, pressure measurements were recorded for permeability calculation. If the calculated permeability of the core matched the initial permeability of the core (upon the first experiment), the core was deemed fit for a subsequent coreflood.

4.4 DATA ANALYSIS

4.4.1 Core Pore Volume

As explained earlier in this chapter, the core was weighed initially before vacuuming to measure the dry weight. After saturating the core with brine, it was weighed again to measure the wet weight of the core. The core pore volume, PV, was calculated using the following equation:

$$PV = \frac{M_{wet} - M_{dry}}{\rho_{brine}}, \qquad \text{(Eq. 10)}$$

where M_{wet} is the mass of the core after brine saturation (g), M_{dry} is the dry mass of the core (g), and ρ_{brine} is the density of the brine (g/mL). The pore volumes of the cores ranged from 40-45 mL for Boise sandstone, corresponding to porosities of approximately between 0.25 and 0.30.

4.4.2 Core Permeability

The permeability, k, of the core is calculated using Darcy's Law:

$$k = \frac{\mu L Q}{A \Delta P}, \quad \text{(Eq. 11)}$$

where A is the cross-sectional area of the core (cm), ΔP is the pressure drop across the core (dynes/cm^2), Q is the volumetric flow rate (cm^3/s), L is the length of the core (cm), and μ is the viscosity of the brine (poise).

The permeability was calculated from the steady state pressure drop value recorded from the LABView software.

4.4.3 Apparent Viscosity

The apparent viscosity of the injected fluid (emulsion or nanoparticle dispersion) while flowing through the Boise sandstone core was also calculated using Darcy's law:

$$\mu_{app} = \frac{-kA}{Q} \frac{(P_o - P_i)}{L}, \quad \text{(Eq. 12)}$$

where k is the permeability of the core (cm^2), A is the cross-sectional area of the core (cm), P_o and P_i are the outlet pressure and inlet pressure (dynes/cm^2), Q is the volumetric flow rate (cm^3/s), and L is the length of the bead core (cm).

4.4.4 Residual Water Saturation and Residual Oil Saturation

The residual water saturation, S_{wr}, was calculated by counting the amount of brine collected in the effluent which was displaced from the core by injection of the desired organic phase. The equation used is as follows:

$$S_{wr} = \frac{PV - displaced\ water\ during\ oil\ injection}{PV}, \quad \text{(Eq. 13)}$$

where PV is pore volume. Figure 4.3 shows a sample effluent collected from mineral oil injection displacing brine to get to residual water saturation. The mineral oil was dyed red to help distinguish it from the brine. The first few pore volumes were collected in 15 mL centrifugal tubes to accurately estimate the volume of brine displaced and collected. When little to no water was observed, the effluent was collected in bulk in a large container:

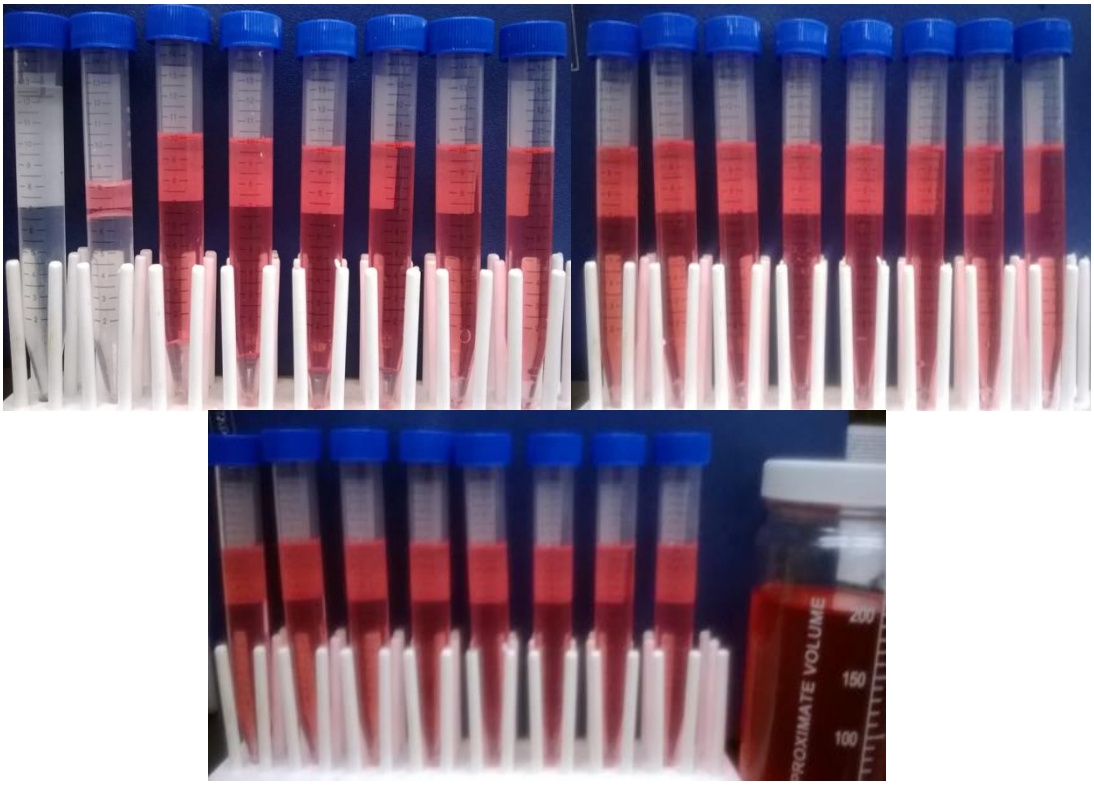

Figure 4.3 Sample effluent of brine displacement by light mineral oil to reach residual water saturation

The residual oil saturation, Sor, was calculated from the amount of organic phase that was collected in the effluent after displacement by brine. It was calculated using the following equation:

$$S_{or} = \frac{PV(1-S_{wr}) - oil\ displaced\ during\ waterflood}{PV}, \qquad \text{(Eq. 14)}$$

where *PV* is pore volume.

Brine was injected into the core at incrementally increasing flow rates until no more oil was recovered in the effluent. The core was then considered to be at residual oil saturation.

The effluent for the entire waterflood was collected in similar 15 mL centrifugal tubes as in the previous step. A sample effluent collected from a waterflooding experiment is shown in Figure 4.4. In Figure 4.4, the light brown color can be identified as Texaco oil which was being displaced by brine. Incremental increase in flow rate shows small amounts of oil displaced at various pore volumes of effluent collected.

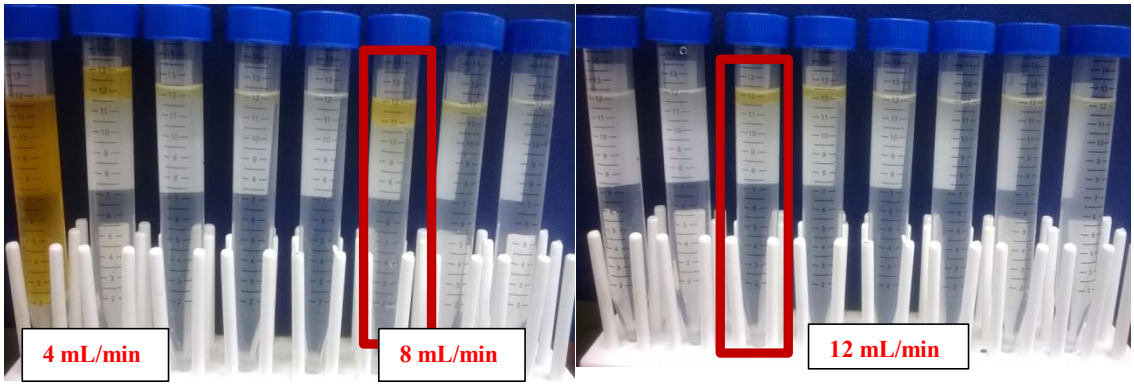

Figure 4.4 Sample effluent of Texaco oil displacement by brine to reach residual oil saturation. The red rectangles around the centrifugal tubes suggest an increase in brine injection flow rate

4.5 RESULTS

4.5.1 Continuous Emulsion Injection

Emulsion was injected through a Boise sandstone core to assess residual oil recovery potential as well as to further investigate emulsion flow and stability while flowing through porous media. In Core U Experiment 1, a mineral oil emulsion was injected into a sandstone core at an initial saturation of brine and residual oil saturation, with the resident oil also being light mineral oil. The mineral oil emulsion was stabilized with Nyacol DP-9711 nanoparticles dispersed to 2 wt% concentration in brine solution. The emulsion generation took place using a beadpack which was filled with glass beads of 180 micron diameter. The flow through the beadpack was performed at a 1:1 phase ratio for a total flow rate of 24 mL/min. The emulsion had a droplet diameter of approximately 24 microns and was approximately 66% mineral oil by volume. The pressure drop was measured across the entirety of the core and was measured using one differential pressure transducer.

Core U – Experiment 1					
k (mD)	ϕ	Pore Volume (mL)	Sor	Flow Rate (mL/min)	Percentage Recovery (%)
635	0.29	42.85	0.30	0.1	45

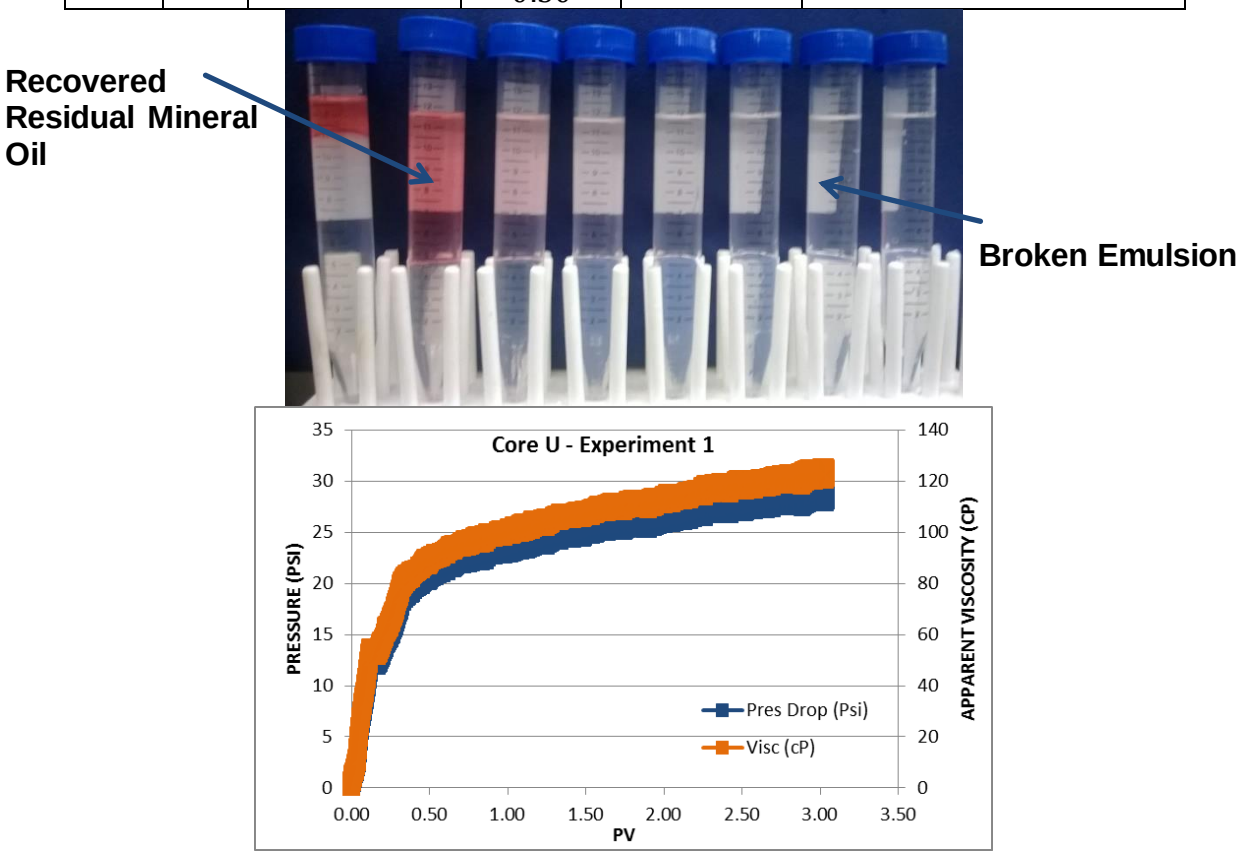

Figure 4.5 Core U Experiment 1: Recovery of light mineral oil (dyed red) by mineral oil emulsion stabilized by Nyacol DP9711 nanoparticles. The mineral oil present in the emulsion was colorless. The amount of recovered oil can therefore be assessed by the lightness of shade of the red dye. Experiment performed at 0.1 mL/min.

Figure 4.5 shows the experimental conditions, effluent of emulsion injection into Core U, pressure drop and apparent viscosity for Experiment 1. The pressure drop recorded by the LABView software was seen to increase throughout the duration of the experiment, with the pressure showing less of an increase after about 1 PV. 1 PV roughly corresponds to when all the mineral oil from the core had been recovered. The steadily

building pressure profile corresponds to the slow progression of the oil bank which is directly related to the coalescence and regeneration hypothesis. No stable emulsion was regenerated from the core throughout the duration of the experiment. It is possible that any regenerated emulsion inside the core was not stable enough to survive passage through the core. The injected mineral oil emulsion was seen to coalesce completely, leading to miscibility with the residual resident mineral oil present in the core. This can be seen from the shade of the dye in the effluent. Test tube 1 shows the darkest red, which would suggest the most amount of mineral oil recovered. The darkness of the red dye seems to diminish with each test tube, suggesting lower amounts of recovered mineral oil.

When the mineral oil was injected, the sandstone core was at an initial saturation of brine and residual oil saturation. The residual oil saturation, Sor, was computed to be 0.30 which at a pore volume of 42.85 mL would suggest 13.0 mL of mineral oil available for recovery. The estimated oil recovery based on the effluent collected was approximately 5.80 mL of mineral oil. This led to a residual oil recovery of about 45%.

Core U – Experiment 2					
k (mD)	ϕ	Pore Volume (mL)	Sor	Flow Rate (mL/min)	Percentage Recovery (%)
635	0.29	42.85	0.34	0.5	27

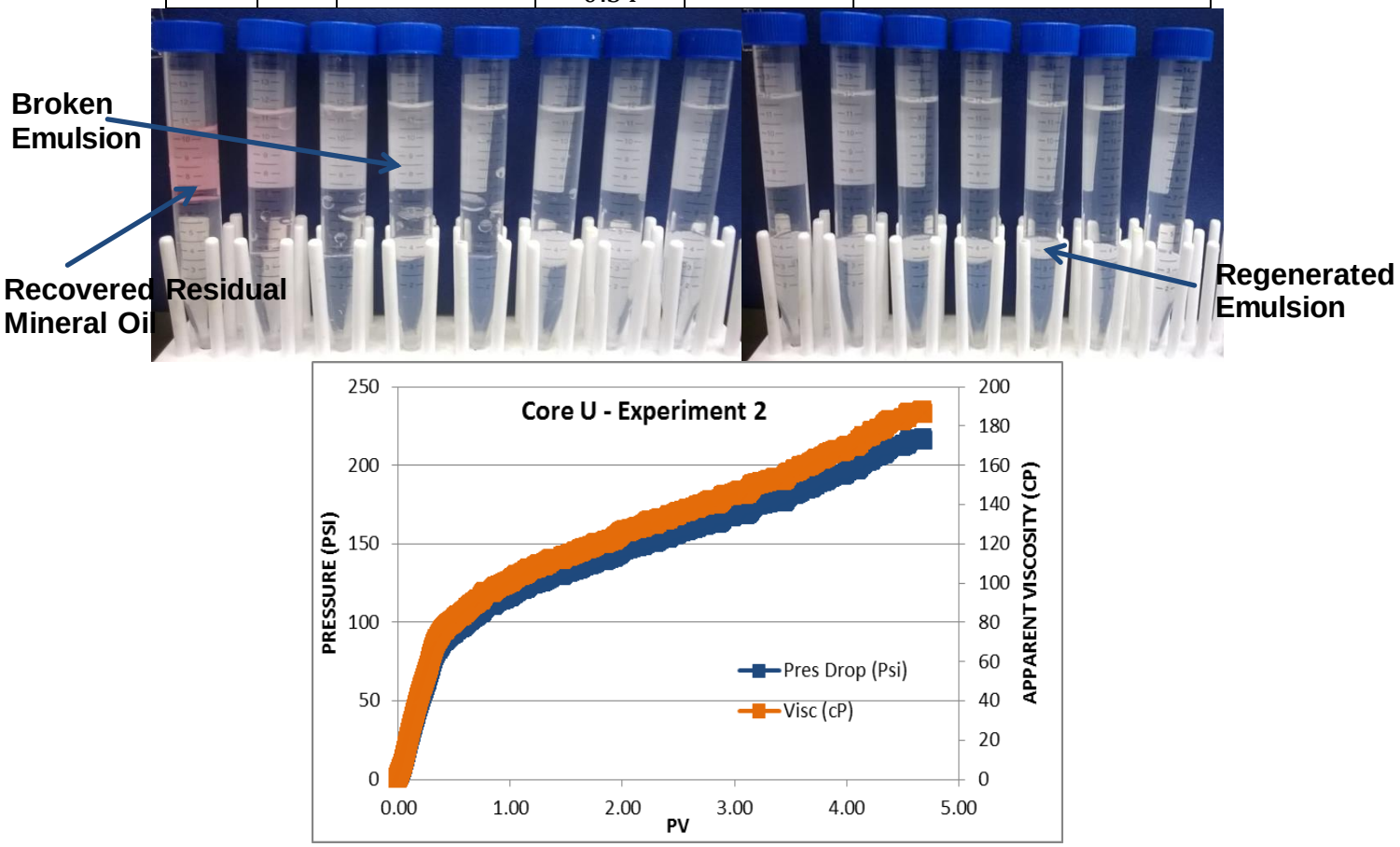

Figure 4.6 Core U Experiment 2: Recovery of light mineral oil (dyed red) by mineral oil emulsion stabilized by Nyacol DP9711 nanoparticles. The mineral oil present in the emulsion was colorless. The amount of recovered oil can therefore be assessed by the lightness of shade of the red dye. Experiment performed at 0.5 mL/min.

Figure 4.6 shows the experimental conditions, effluent of emulsion injection into Core U, pressure drop and apparent viscosity for Experiment 2. The core was flushed with IPA and saturated with brine to prepare the core for Experiment 2. This experiment

had similar conditions to that of Experiment 1 with the exception of the flow rate; a flow rate of 0.5 mL/min was used to assess if a higher shear rate would help assist in the recovery of more residual oil. The pressure drop recorded by the LABView software was seen to increase throughout the duration of the experiment. The steadily building pressure profile corresponds to the slow progression of the oil bank similar to that in Core U Experiment 1. Very little stable emulsion was regenerated from the core throughout the duration of the experiment. The injected mineral oil emulsion was seen to coalesce completely inside the core, leading to miscibility with the residual resident mineral oil present in the core. This can be seen from the shade of the dye in the effluent. Test tube 1 shows the darkest red, which would suggest the most amount of mineral oil recovered.

When the mineral oil was injected, the sandstone core was at an initial saturation of brine and residual oil saturation. The residual oil saturation, Sor, was computed to be 0.34 which at a pore volume of 42.85 mL would suggest 14.50 mL of mineral oil available for recovery. The estimated oil recovery based on the effluent collected was approximately 3.95 mL of mineral oil. This led to a residual oil recovery of about 27%. It is interesting to note this decrease in residual oil recovery with an increase in the flow rate and consequently shear rate. A hypothesis for this might be the decrease in emulsion coalescence and attempted regeneration with an increase in flow rate. With a slower flow rate, there is a greater duration for emulsion coalescence and regeneration as well as miscibility between the continuous and residual oils. This would lead to a greater recovery with lower flow rate as is seen in Core U Experiment 1.

Core U – Experiment 3					
k (mD)	ϕ	Pore Volume (mL)	Sor	Flow Rate (mL/min)	Percentage Recovery (%)
635	0.29	42.85	0.29	0.5	74

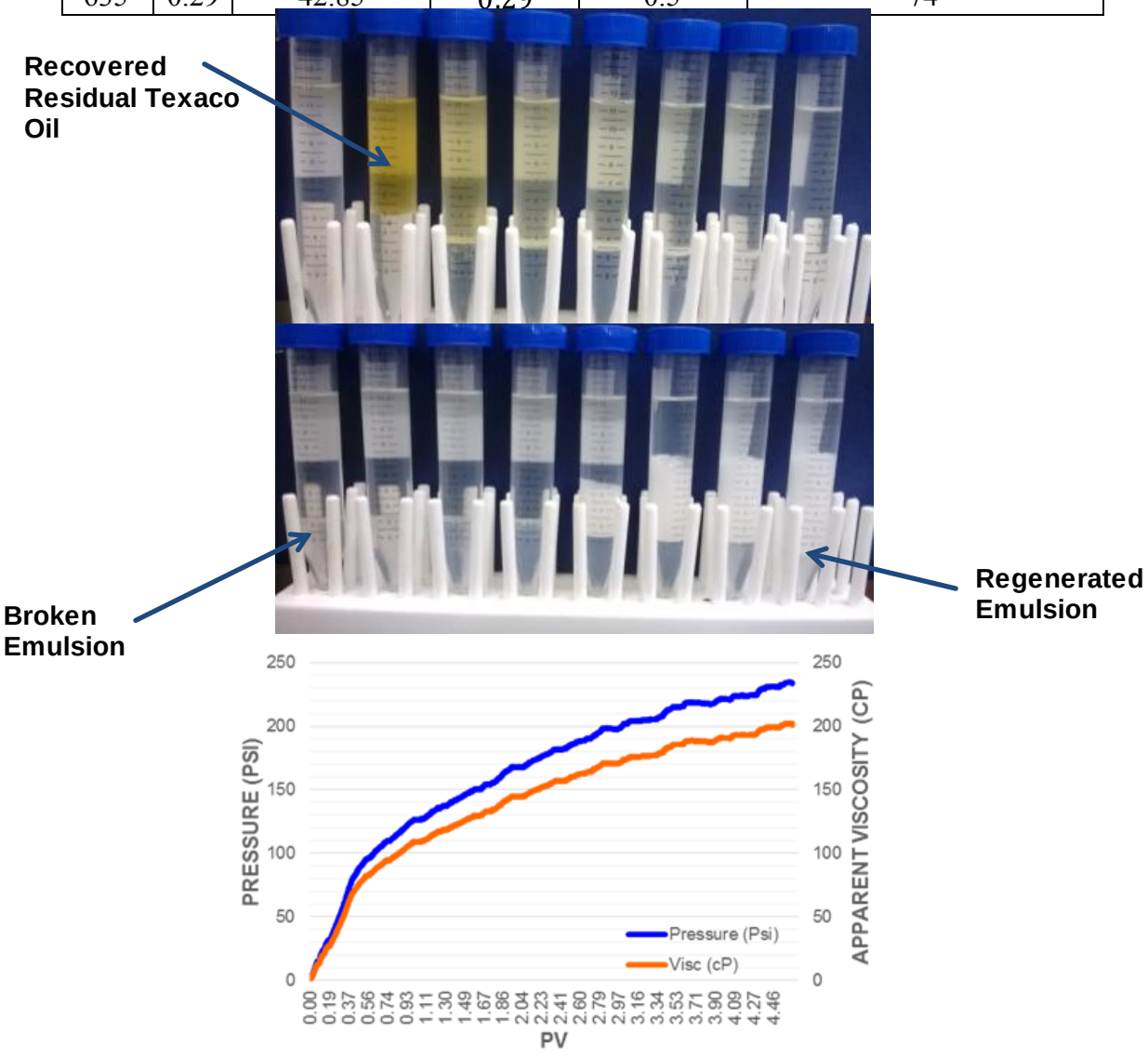

Figure 4.7 Core U Experiment 3: Recovery of Texaco oil (light brown) by mineral oil emulsion stabilized by Nyacol DP9711 nanoparticles. The mineral oil present in the emulsion was colorless. The amount of recovered oil can therefore be assessed by the lightness of the brown shade. Experiment performed at 0.5 mL/min.

In Core U Experiment 3, a mineral oil emulsion was injected into a sandstone core at an initial saturation of brine and residual oil saturation, with the resident oil being Texaco oil. The mineral oil emulsion was stabilized with Nyacol DP-9711 nanoparticles dispersed to a 2 wt% concentration in 3 wt% brine solution. The emulsion generation took place using a beadpack which was filled with glass beads of 180 micron diameter. The flow through the beadpack was performed at a 1:1 phase ratio for a total flow rate of 24 mL/min.

Figure 4.7 shows the experimental conditions, effluent of emulsion injection into Core U, pressure drop and apparent viscosity for Experiment 3. This experiment had a flow rate of 0.5 mL/min and the mineral oil emulsion was continuously injected throughout the duration of the experiment. The pressure drop recorded was seen to increase throughout the duration of the experiment. Stable emulsion was regenerated from the core and was seen to start emerging in the effluent between 3 and 4 pore volumes. The injected mineral oil emulsion was seen to partially coalesce, leading to miscibility with the residual resident Texaco oil present in the core. This can be seen from the shade of the dye in the effluent. Test tube 2 shows the darkest brown, which would suggest the most amount of Texaco oil recovered.

When the mineral oil was injected, the sandstone core was at an initial saturation of brine and residual oil saturation. The residual oil saturation, Sor, was computed to be 0.29 which at a pore volume of 42.85 mL would suggest 12.50 mL of Texaco oil available for recovery. The estimated oil recovery based on the effluent collected was approximately 9.25 mL of Texaco oil. This led to a residual oil recovery of about 74%.

It is interesting to note the significant increase in residual oil recovery between Core U Experiments 2 and 3. One reason as to why there was significantly more Texaco oil recovered in Experiment 3 as compared to Experiment 2 might be due to the viscosity

difference between Texaco oil and light mineral oil. When the mineral oil emulsion coalesces inside the core, the 40.5 cP mineral oil is miscible with the 25 cP Texaco oil. A more viscous, heavier organic phase will likely recover more of the lighter, less viscous organic phase. In Experiment 2, there was no viscosity advantage as mineral oil emulsion was injected to recover resident mineral oil. In Experiment 3, there is a significant viscosity advantage which might be the leading factor attributing to the 74% recovery.

4.5.2 Slug-size Emulsion Injection

Core W – Experiment 4					
k (mD)	ϕ	Pore Volume (mL)	Sor	Flow Rate (mL/min)	Percentage Recovery (%)
855	0.27	41.85	0.25	0.5	19

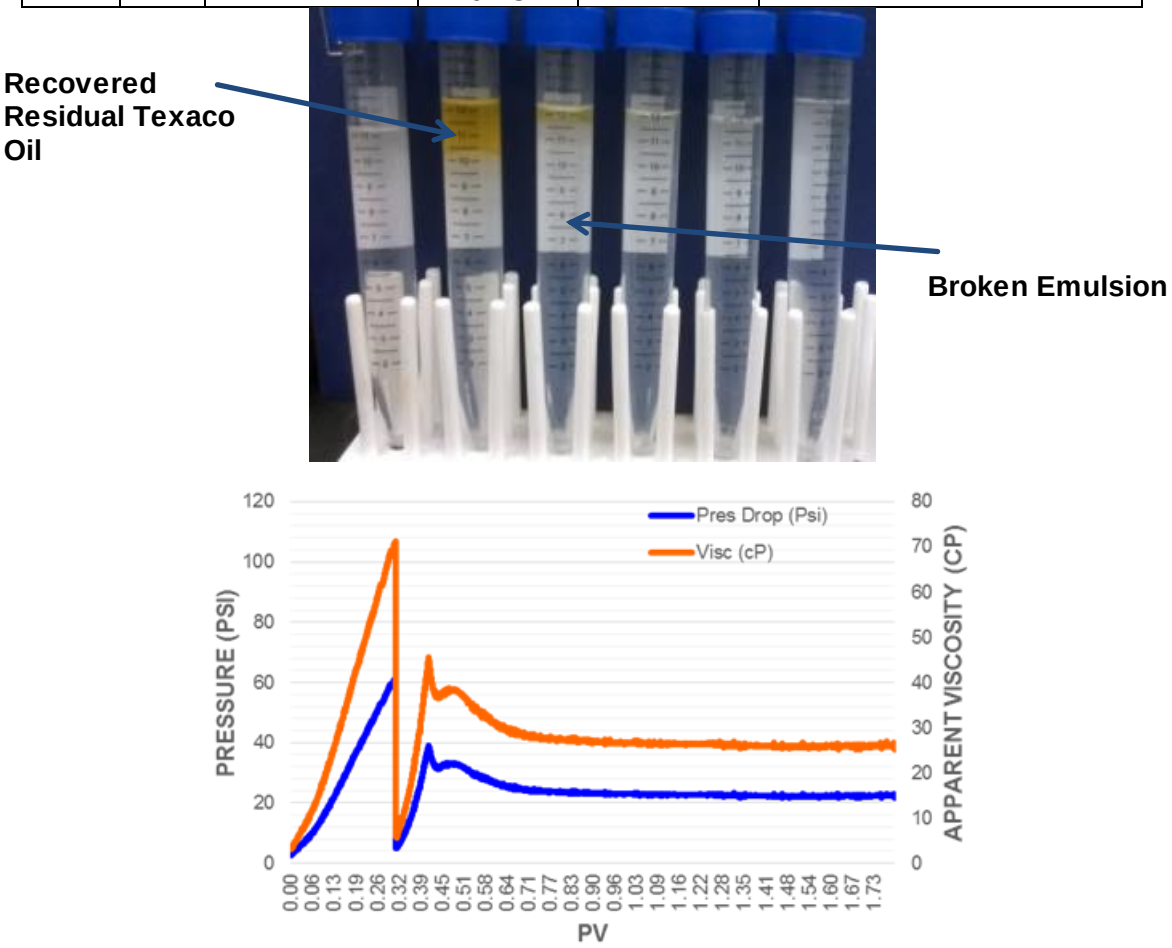

Figure 4.8 Core W Experiment 4: Recovery of Texaco oil (light brown) by 0.33 PV slug of mineral oil emulsion stabilized by Nyacol DP9711 nanoparticles. The mineral oil present in the emulsion was colorless. The amount of recovered oil can be assessed by the lightness of the brown shade. Experiment performed at 0.5 mL/min.

Figure 4.8 shows the experimental conditions, effluent of emulsion injection into Core W, pressure drop and apparent viscosity for Experiment 4. This experiment had a flow rate of 0.5 mL/min. A 0.33 PV slug of mineral oil emulsion was injected into the sandstone core after which a post-brine flush was performed. This configuration was used to assess percentage residual oil recovery given a feasible amount of emulsion injection; for practical purposes it is beneficial to assess the optimal pore volumes of emulsion necessary to obtain the greatest amount of residual oil recovery. The pressure drop recorded was seen to increase throughout the duration of emulsion injection as has been the commonly observed trend thus far. Pressure drop was seen to stabilize when brine was flushed after the emulsion slug was injected. No emulsion was regenerated from the core which would be expected as there is limited amount of emulsion injected. The injected mineral oil emulsion was seen to completely coalesce, leading to miscibility with the residual resident Texaco oil present in the core. This can be seen from the shade of the dye in the effluent. Test tube 2 shows the darkest brown, which would suggest the most amount of Texaco oil recovered.

When the mineral oil was injected, the sandstone core was at an initial saturation of brine and residual oil saturation. The residual oil saturation, Sor, was computed to be 0.25 which at a pore volume of 41.85 mL would suggest 10.50 mL of Texaco oil available for recovery. The estimated oil recovery based on the effluent collected was approximately 2 mL of Texaco oil. This led to a residual oil recovery of about 19%.

One reason as to why there was significantly less Texaco oil recovered in Core W Experiment 4 as compared to Core U Experiment 3 might be due to the lack of continuous emulsion injection. If emulsion is continuously injected, the process of coalescence and regeneration is ongoing, which would assist in miscibility between the organic phase from the emulsion and the resident oil present in the core therefore leading

to a higher residual oil recovery. As we have only a 0.33 PV slug of emulsion, there is a limit to the amount of miscibility and consequently the residual oil that can be recovered.

Core W – Experiment 5					
k (mD)	ϕ	Pore Volume (mL)	Sor	Flow Rate (mL/min)	Percentage Recovery (%)
855	0.27	41.85	0.31	0.5	44

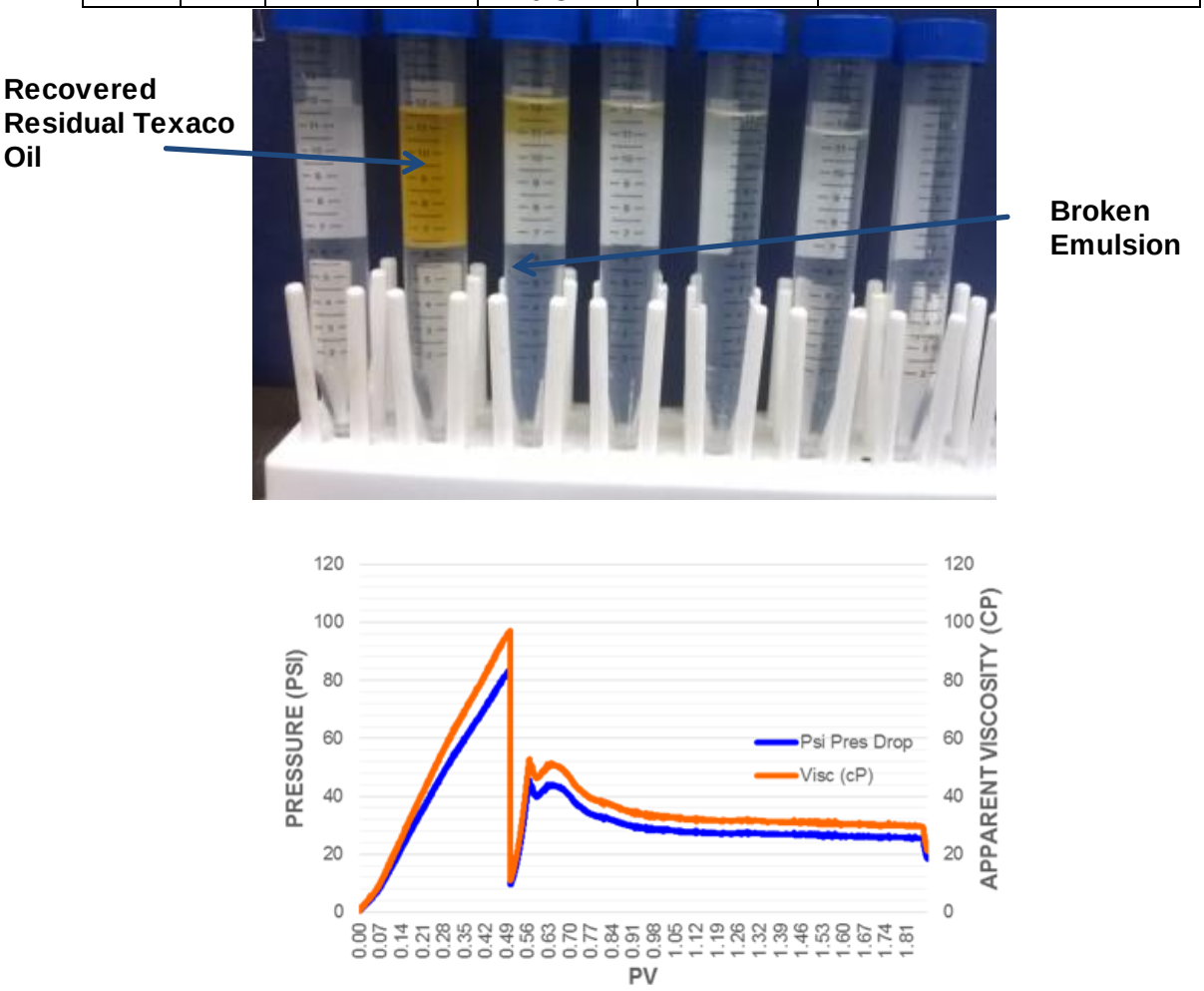

Figure 4.9 Core W Experiment 5: Recovery of Texaco oil (light brown) by 0.50 PV slug of mineral oil emulsion stabilized by Nyacol DP9711 nanoparticles. The mineral oil present in the emulsion was colorless. The amount of recovered oil can be assessed by the lightness of the brown shade. Experiment performed at 0.5 mL/min.

Figure 4.9 shows the experimental conditions, effluent of emulsion injection into Core W, pressure drop and apparent viscosity for Experiment 5. This experiment had a flow rate of 0.5 mL/min. A 0.50 PV slug of mineral oil emulsion was injected into the sandstone core after which a post-brine flush was performed. The pressure drop recorded was seen to increase throughout the duration of emulsion injection. Pressure drop was seen to stabilize when brine was flushed after the emulsion slug was injected. No emulsion was regenerated from the core which would be expected as there is limited amount of emulsion injected. The injected mineral oil emulsion was seen to completely coalesce, leading to miscibility with the residual resident Texaco oil present in the core. This can be seen from the shade of the dye in the effluent.

When the mineral oil was injected, the sandstone core was at an initial saturation of brine and residual oil saturation. The residual oil saturation, Sor, was computed to be 0.31 which at a pore volume of 41.85 mL would suggest 13.0 mL of Texaco oil available for recovery. The estimated oil recovery based on the effluent collected was approximately 5.70 mL of Texaco oil. This led to a residual oil recovery of about 44%. A higher recovery is expected with an increase in the size of the slug of mineral oil emulsion injected.

Core W – Experiment 6					
k (mD)	ϕ	Pore Volume (mL)	Sor	Flow Rate (mL/min)	Percentage Recovery (%)
855	0.27	41.85	0.29	0.5	55

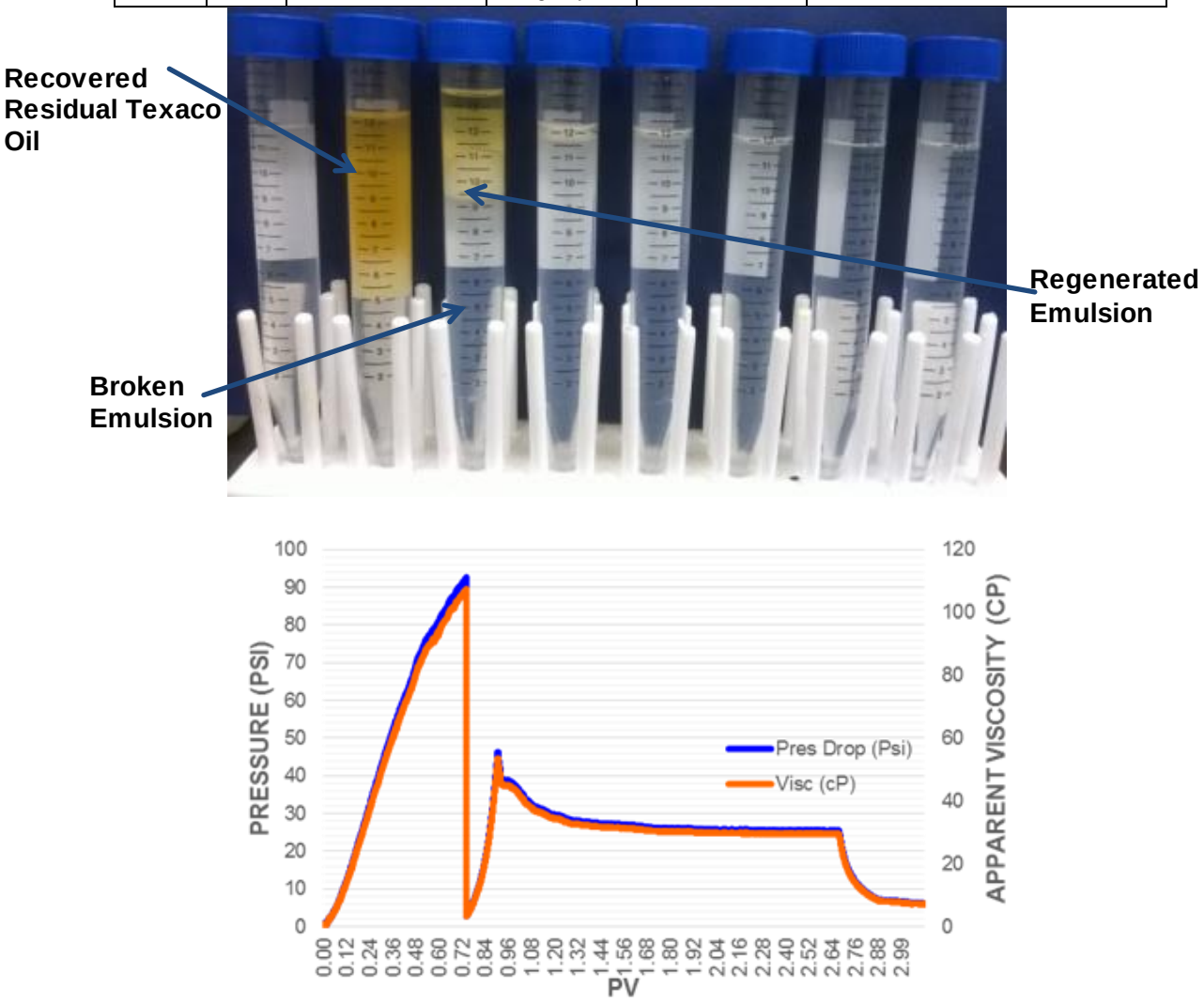

Figure 4.10 Core W Experiment 6: Recovery of Texaco oil (light brown) by 0.75 PV slug of mineral oil emulsion stabilized by Nyacol DP9711 nanoparticles. The mineral oil present in the emulsion was colorless. The amount of recovered oil can be assessed by the lightness of the brown shade. Experiment performed at 0.5 mL/min.

Figure 4.10 shows the experimental conditions, effluent of emulsion injection into Core W, pressure drop and apparent viscosity for Experiment 6. This experiment had a flow rate of 0.5 mL/min. A 0.75 PV slug of mineral oil emulsion was injected into the sandstone core after which a-post brine flush was performed. The pressure drop recorded was seen to increase throughout the duration of emulsion injection. Pressure drop was seen to stabilize when brine was flushed after the emulsion slug was injected. Small amounts of emulsion were seen to be regenerated from the core which would be expected as there is a slightly higher amount of emulsion injected. The injected mineral oil emulsion was seen to partially coalesce, leading to miscibility with the residual resident Texaco oil present in the core. This can be seen from the shade of the dye in the effluent.

When the mineral oil was injected, the sandstone core was at an initial saturation of brine and residual oil saturation. The residual oil saturation, Sor, was computed to be 0.29 which at a pore volume of 41.85 mL would suggest 12 mL of Texaco oil available for recovery. The estimated oil recovery based on the effluent collected was approximately 6.65 mL of Texaco oil. This led to a residual oil recovery of about 55%. A higher recovery is expected with an increase in the size of the slug of mineral oil emulsion injected.

With increase in slug size from 0.33 PV to 0.50 PV to 0.75 PV the residual oil recovery increased from 19% to 44% to 55%. As the continuous emulsion injected lead to 74% recovery, it can be noted that approximately 1-2 PV of emulsion injection would lead to the same necessary effect as would continuous emulsion injection. This is believed as there appears to be a plateau in the amount of recovery that can be obtained with continuous emulsion injection.

Core X – Experiment 7					
k (mD)	ϕ	Pore Volume (mL)	Sor	Flow Rate (mL/min)	Percentage Recovery (%)
1055	0.26	40.84	0.47	0.1	30

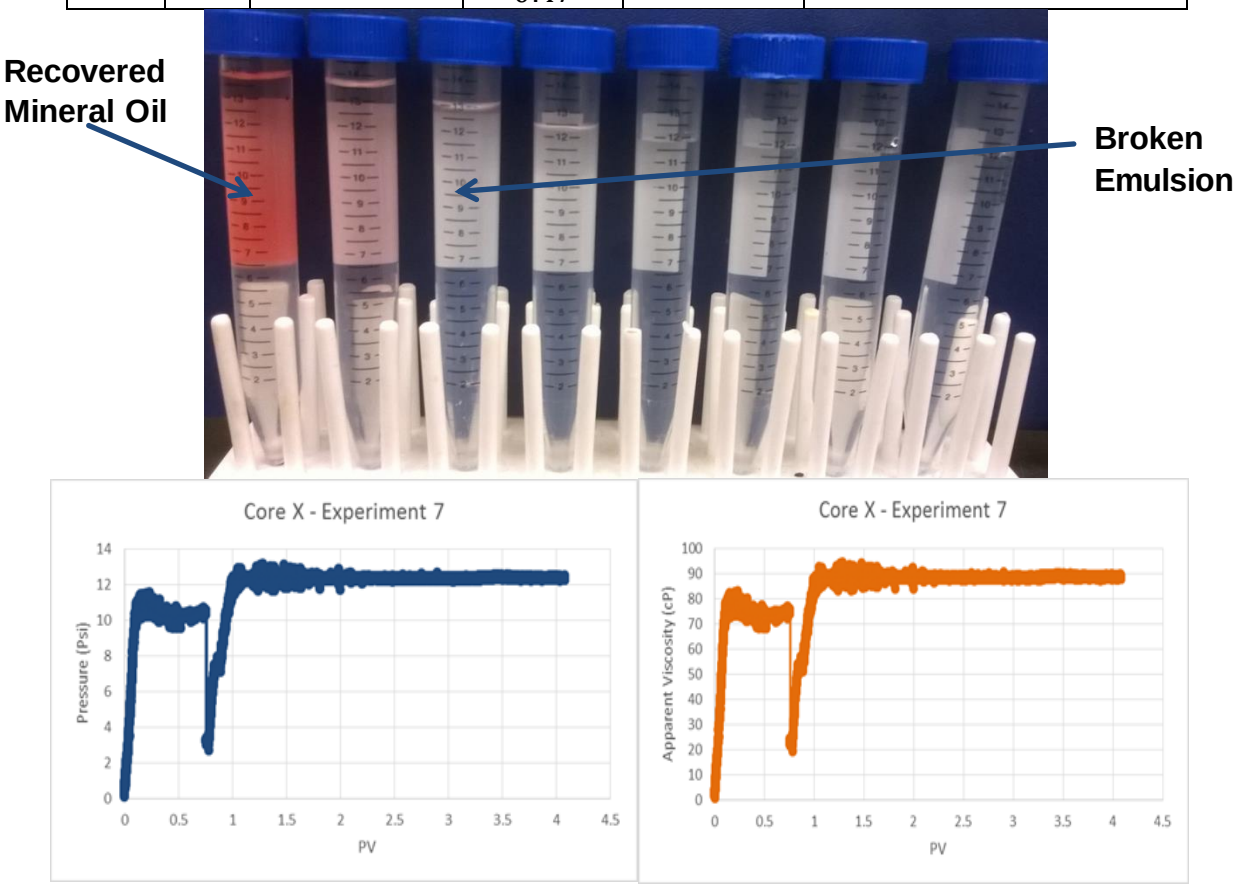

Figure 4.11 Core X Experiment 7: Recovery of light mineral oil (dyed reddish pink) by 0.75 PV slug of octane emulsion stabilized by Nyacol DP9711 nanoparticles. The octane present in the emulsion was colorless. The amount of recovered oil can be assessed by the lightness of the red shade. Experiment performed at 0.1 mL/min.

We have currently looked at recovery of residual lighter oil by more viscous continuous oil in emulsion. Although this has shown promising recovery potential, this approach might not be the most feasible. In order to significantly reduce field costs, it is essential to be able to incorporate lower viscosity oils to recover high viscosity resident

oils. For this purpose, we will assess the recovery potential of light mineral oil by using an octane in water emulsion stabilized using nanoparticles.

In Core X Experiment 7, an octane emulsion was injected into a sandstone core at an initial saturation of brine and residual oil saturation, with the resident oil being light mineral oil. The octane emulsion was stabilized with Nyacol DP-9711 nanoparticles dispersed to 2 wt% concentration in brine solution. The emulsion generation took place using a beadpack which was filled with glass beads of 180 micron diameter. The flow through the beadpack was performed at a 1:1 phase ratio for a total flow rate of 24 mL/min.

Figure 4.11 shows the experimental conditions, effluent of emulsion injection into Core X, pressure drop and apparent viscosity for Experiment 7. This experiment had a flow rate of 0.1 mL/min. A 0.75 PV slug of octane emulsion was injected into the sandstone core after which a post-brine flush was performed. The pressure drop recorded was seen to increase until about 0.25 PV after which a slight decrease is seen followed by what seems to be another increase after 0.50 PV. The pressure decrease might be occurring as mineral oil is being recovered. The increase that follows might be a result of coalescence and attempted regeneration of the octane emulsion. Pressure drop was seen to stabilize when brine was flushed after the emulsion slug was injected. No emulsion was regenerated from the core which would be expected as there is a limited amount of emulsion injected. The injected octane emulsion was seen to completely coalesce, leading to miscibility with the residual resident mineral oil present in the core. This can be seen from the shade of the dye in the effluent. Test tube 1 shows the darkest red, which would suggest the most amount of mineral oil recovered.

When the mineral oil was injected, the sandstone core was at an initial saturation of brine and residual oil saturation. The residual oil saturation, Sor, was computed to be

0.47 which at a pore volume of 40.84 mL would suggest 19.0 mL of light mineral oil available for recovery. The estimated oil recovery based on the effluent collected was approximately 5.62 mL of mineral oil. This led to a residual oil recovery of about 30%. Although the lower flow rate provided the opportunity for coalescence and regeneration as well as miscibility between the continuous and residual oils, there was a significant viscosity difference between octane and mineral oil. The increased viscosity difference, when combined with a limited amount of emulsion injected (0.75 PV slug) might be the reason behind the low residual oil recovery.

The most accurate calculation of mineral oil recovery, gas chromatography-mass spectroscopy (GCMS) techniques were performed on the two effluent test tubes (samples 2 and 3). Sample 1 was prepared using a 50:50 relative abundance for octane to mineral oil to provide a calibration peak. The organic phase was separated from effluent test tubes 1 and 2 and was tested for relative abundance of octane compared to mineral oil by comparing octane and mineral oil peaks with sample 1. Sample 2 (effluent test tube 1) showed a relative abundance of 45% octane to 55% mineral oil whereas sample 3 (effluent test tube 2) showed a relative abundance of 80% octane to 20% mineral oil. This yielded the previously mentioned 5.62 mL of mineral oil recovered. The peaks for samples 1-3 are shown below in Figure 4.12:

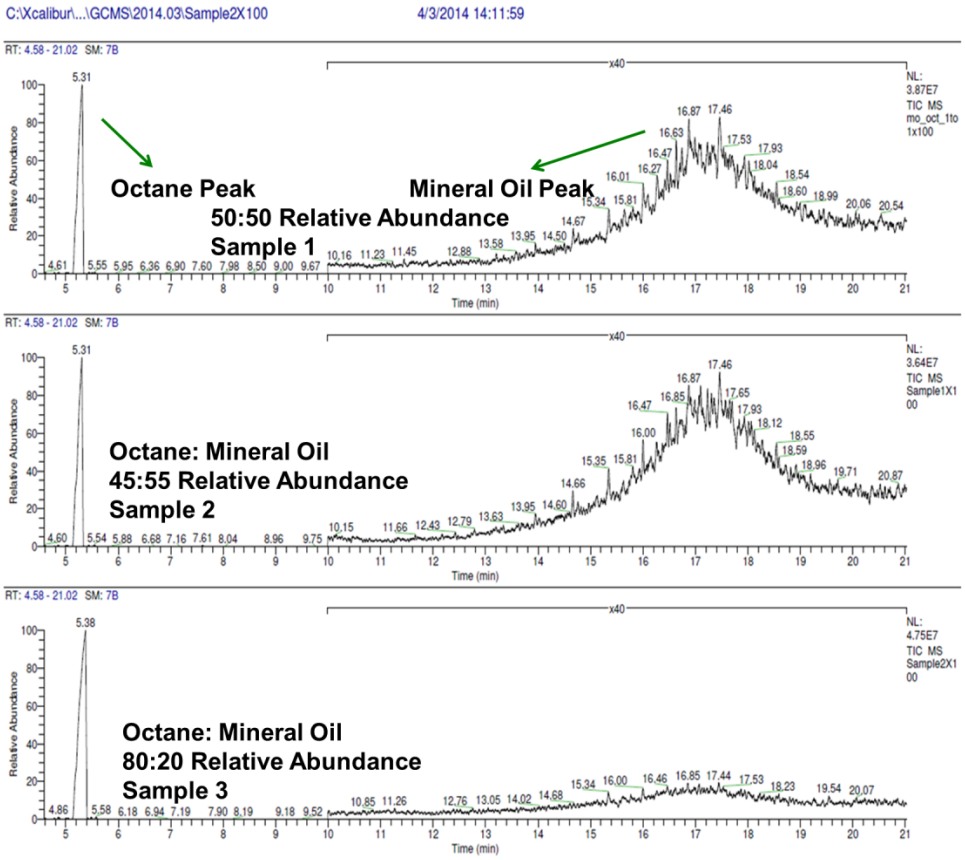

Figure 4.12: GCMS for effluent organic phase for Core X Experiment 7

Core X Experiment 8 showed very similar conditions to Core X Experiment 7. A 0.70 PV slug of octane-in-water emulsion was injected into a sandstone core at an initial saturation of brine and residual oil saturation of 0.37. Given a pore volume of 40.84 mL, this would provide up to 15 mL of mineral oil available for recovery via the octane emulsion injection. Flow rate was increased to 2 mL/min to assess any changes in results. 4.25 mL of mineral oil was recovered leading to a recovery of 28%. It appears that flow rate does not seem to have any positive effects on residual oil recovery. The experimental conditions and pressure and apparent viscosity plots are shown in Figure 4.13:

Core X – Experiment 8					
k (mD)	ϕ	Pore Volume (mL)	Sor	Flow Rate (mL/min)	Percentage Recovery (%)
1055	0.26	40.84	0.37	2	28

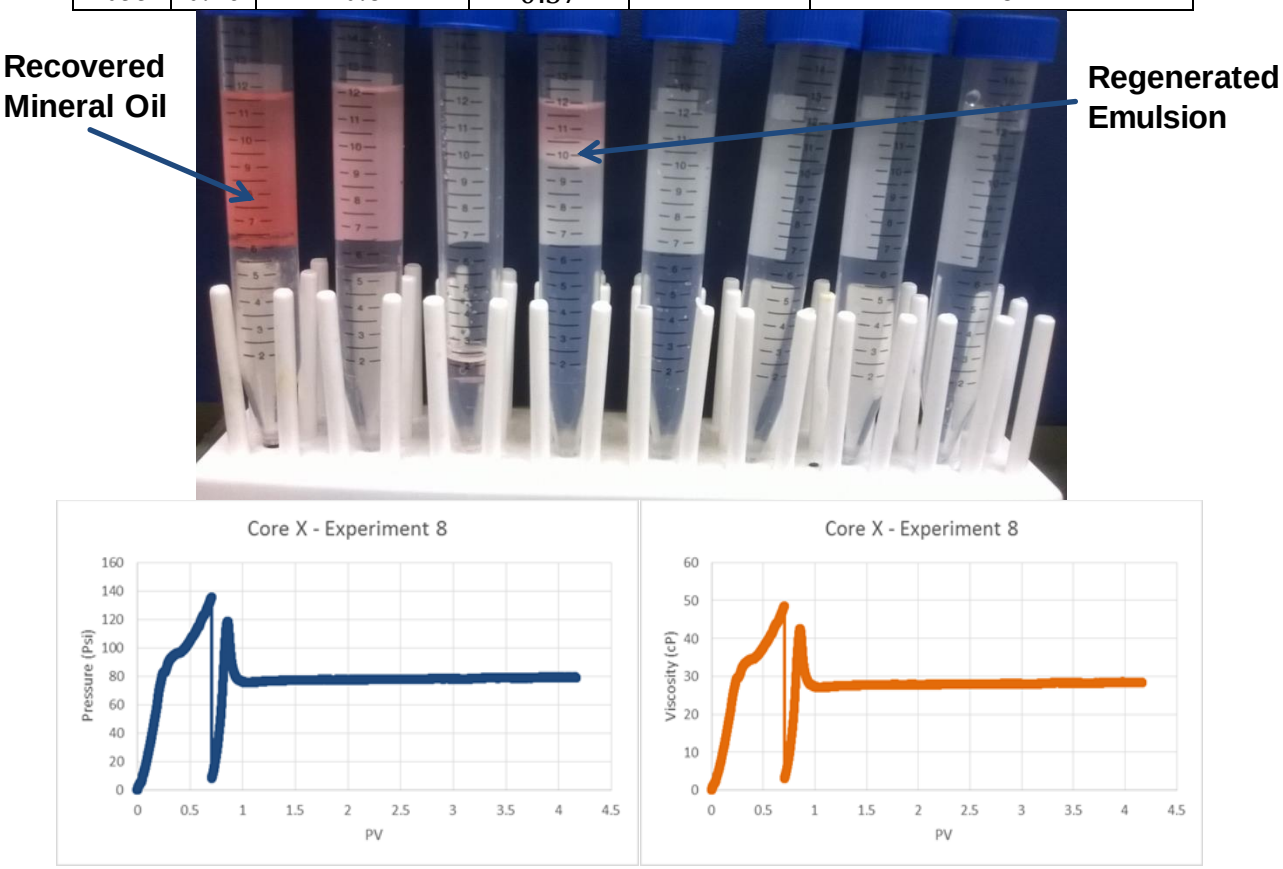

Figure 4.13 Core X Experiment 8: Recovery of light mineral oil (dyed reddish pink) by 0.70 PV slug of octane emulsion stabilized by Nyacol DP9711 nanoparticles. The octane present in the emulsion was colorless. The amount of recovered oil can be assessed by the lightness of the red shade. Experiment performed at 2 mL/min.

4.5.3 Effectiveness of Surfactant-Stabilized Emulsions & Co-Injection Experiments

Core Y – Experiment 9					
k (mD)	ϕ	Pore Volume (mL)	Sor	Flow Rate (mL/min)	Percentage Recovery (%)
3750	0.27	42.27	0.26	0.5	99

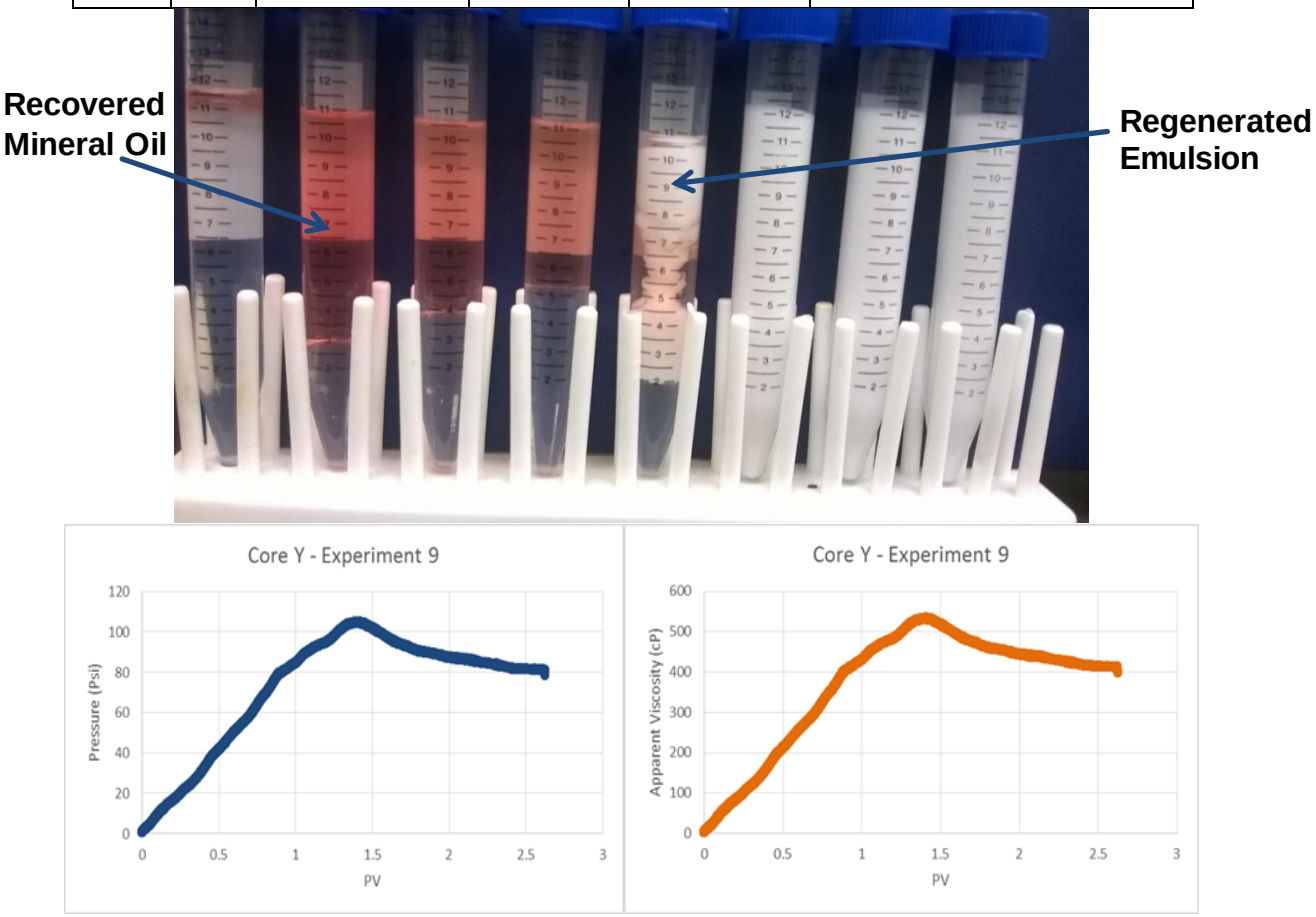

Figure 4.14 Core Y Experiment 9: Recovery of light mineral oil (dyed reddish pink) by octane emulsion stabilized by Igepal Co-70 surfactant. The octane present in the emulsion was colorless. The amount of recovered oil can be assessed by the lightness of the red shade. Experiment performed at 0.5 mL/min.

In Core Y Experiment 9, an octane-in-water emulsion was injected into a sandstone core at an initial saturation of brine and residual oil saturation, with the

resident oil being light mineral oil. The octane emulsion was stabilized with Igepal Co-70 surfactant dispersed to 2 wt% concentration in brine solution. The emulsion generation took place using a beadpack which was filled with glass beads of 180 micron diameter. The flow through the beadpack was performed at a 1:1 phase ratio for a total flow rate of 24 mL/min. This experiment was performed to compare the capability of nanoparticles as emulsifying agents relative to surfactants. The octane-in-water surfactant-stabilized emulsion is shear thinning in its rheology as can be seen below:

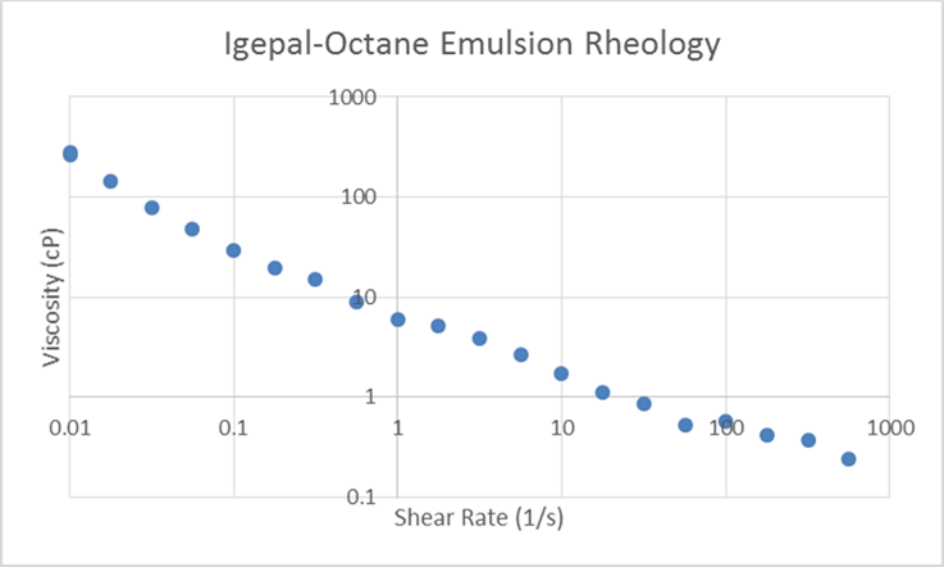

Figure 4.15 Rheology of octane-in-water surfactant stabilized emulsion. Emulsion is seen to be a shear thinning power law fluid.

Figure 4.14 shows the experimental conditions, effluent of emulsion injection into Core Y, pressure drop and apparent viscosity for Experiment 9. This experiment had a flow rate of 0.5 mL/min. The pressure drop recorded was seen to increase up till about 1.40 PV after which a slight decrease was observed. The pressure decrease was seen after all the mineral oil was recovered. From this point onwards, surfactant emulsion

regeneration was seen in the effluent at an increased rate. The injected octane emulsion was seen to partially coalesce, leading to miscibility with the residual resident mineral oil present in the core. This can be seen from the shade of the dye in the effluent. Test tube 2 shows the darkest red, which would suggest the most amount of mineral oil recovered.

When the octane emulsion was injected, the sandstone core was at an initial saturation of brine and residual oil saturation. The residual oil saturation, Sor, was computed to be 0.26 which at a pore volume of 42.27 mL would suggest 11.0 mL of light mineral oil available for recovery. The estimated oil recovery based on the effluent collected was approximately 10.90 mL of mineral oil which would suggest a recovery of 99%.

Next, co-injection experiments were performed to compare their potential in residual oil recovery in comparison to injecting an emulsion that had previously been generated. These experiments were performed at high flow rates (and consequently shear rates) to allow possibility of regeneration of emulsion.

Core Y Experiment 10 was performed where mineral oil and 2 wt % Nyacol DP 9711 nanoparticles dispersed in brine at a 3 wt% salinity were co-injected into a core at initial saturation of brine and residual oil saturation. The resident oil present in the core was also light mineral oil and was dyed red. The mineral oil and nanoparticle dispersion were each injected at 2 mL/min providing a 1:1 phase ratio with a total flow rate of 4 mL/min.

Figure 4.16 shows the experimental conditions, effluent of emulsion injection into Core Y, pressure drop and apparent viscosity for Experiment 10. The pressure drop recorded was seen to increase throughout the duration of the experiment. The injected mineral oil showed miscibility with the resident mineral oil present in the core which helped in its recovery. This can be seen from the shade of the dye in the effluent. Test

tube 2 shows the darkest red, which would suggest the most amount of mineral oil recovered.

The residual oil saturation, Sor, for Core Y Experiment 10 was computed to be 0.34 which at a pore volume of 42.27 mL would suggest 15.2 mL of light mineral oil available for recovery. The estimated oil recovery based on the effluent collected was approximately7.22 mL of mineral oil which would suggest a recovery of 48%. This recovery seemed to be close to the range of recovery seen by injecting mineral oil-in-water emulsion to recover residual mineral oil at a low flow rate, which for Core U Experiment 1 at 0.1 mL/min was assessed to be 45%. On increasing the flow rate of injection to 12 mL/min (1:1 phase ratio of mineral oil to nanoparticle dispersion at 6 mL/min each) the recovery was seen to increase to 58%. This can be seen in Figure 4.17 which shows the co-injection experimental conditions for Core Z Experiment 11.

Core Y – Experiment 10					
k (mD)	ϕ	Pore Volume (mL)	Sor	Flow Rate (mL/min)	Percentage Recovery (%)
3750	0.27	42.27	0.34	4	48

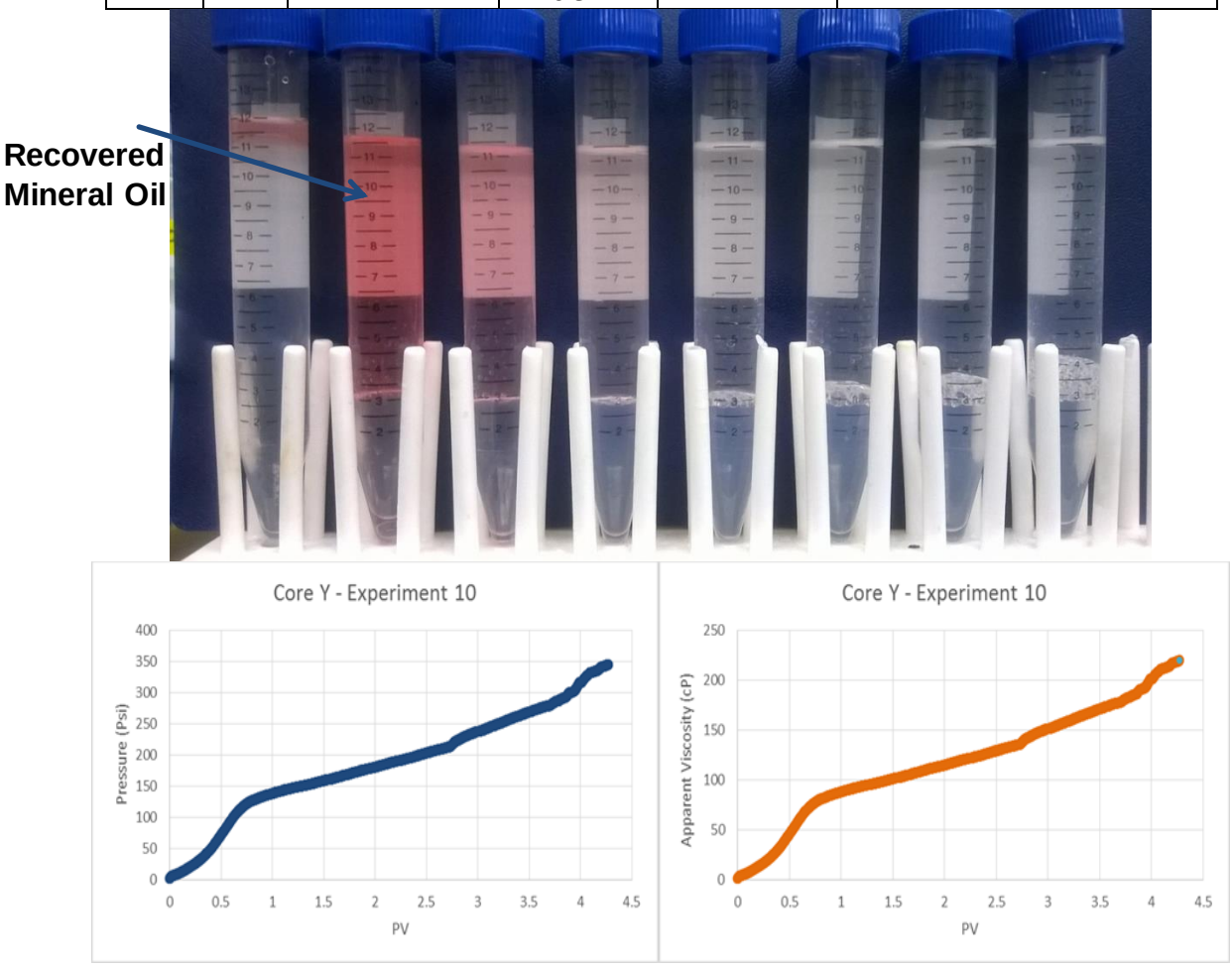

Figure 4.16 Core Y Experiment 10: Recovery of light mineral oil (dyed reddish pink) by co-injection of mineral oil with Nyacol DP9711 nanoparticles dispersed in brine. The injected mineral oil was colorless. The amount of recovered oil can be assessed by the lightness of the red shade. Experiment performed at 4 mL/min.

Core Z – Experiment 11					
k (mD)	ϕ	Pore Volume (mL)	Sor	Flow Rate (mL/min)	Percentage Recovery (%)
3350	0.29	41.29	0.33	12	58

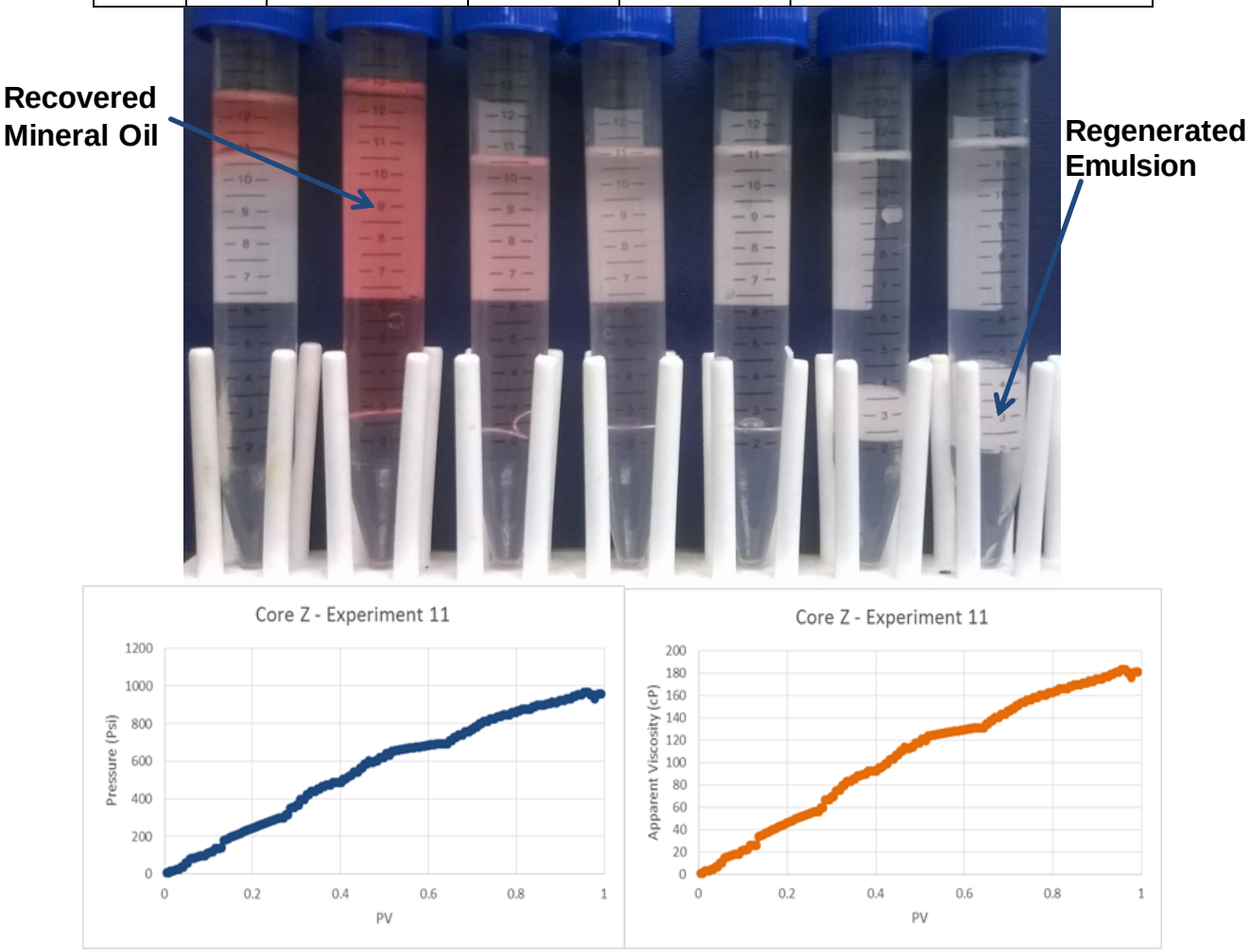

Figure 4.17 Core Z Experiment 11: Recovery of light mineral oil (dyed reddish pink) by co-injection of mineral oil with Nyacol DP9711 nanoparticles dispersed in brine. The injected mineral oil was colorless. The amount of recovered oil can be assessed by the lightness of the red shade. Experiment performed at 12 mL/min.

Core Z – Experiment 12					
k (mD)	ϕ	Pore Volume (mL)	Sor	Flow Rate (mL/min)	Percentage Recovery (%)
3350	0.29	41.29	0	0.5	N/A

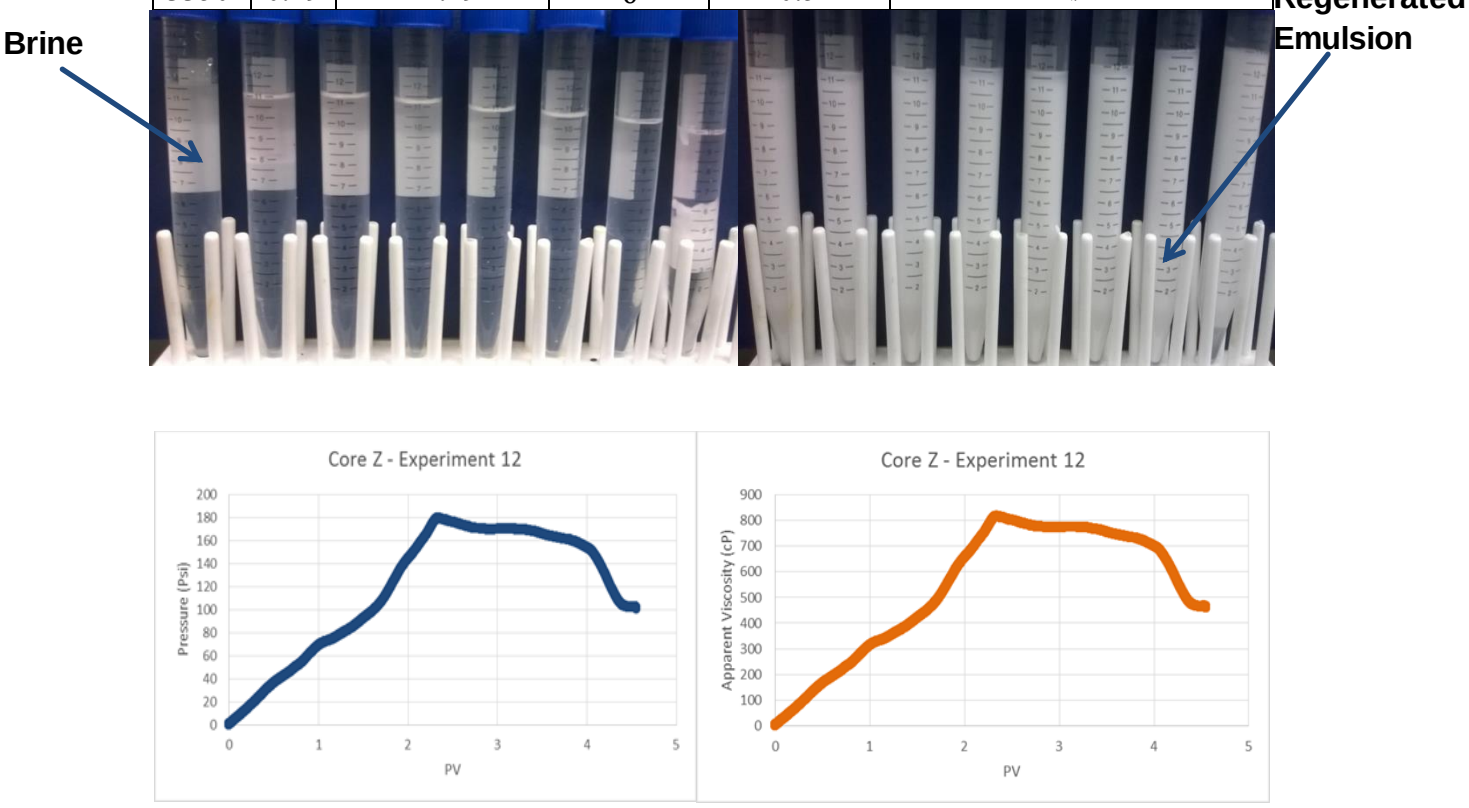

Figure 4.18 Core Z Experiment 12: Assessment of stability of octane-in-water surfactant stabilized emulsion through a brine saturated core. The injected octane was colorless and the octane emulsion was stabilized using Igepal Co-70 surfactant. Experiment performed at 0.5 mL/min.

Figure 4.18 shows the experimental conditions, pressure and apparent viscosity plots for Core Z Experiment 12. This was performed to assess the transport and stability behavior of an octane-in-water surfactant stabilized emulsion. The emulsifying agent was Igepal Co-70 dispersed to a 2wt % concentration in brine. The pressure and apparent viscosity plots were quite similar to those observed in Core Y Experiment 9 where

pressure was seen to increase up till the emulsion is seen to be regenerated again. After the octane-in-water surfactant stabilized emulsion is continuously regenerated, the pressure profile shows what appears to be signs of stabilizing at about 4.2 PV.

Core A Experiment 13 was performed as a control experiment to assess recovery of residual oil by injection of only surfactant. Igepal Co-70 was injected into a core at an initial saturation of brine and residual oil saturation. The residual oil saturation, Sor, was computed to be 0.30 which at a pore volume of 42.87 mL corresponds to about 13 mL of light mineral oil available for recovery. As can be seen from the effluent, no mineral oil was recovered. This is confirmation to how the coalescence and regenration of emulsion combined with miscibility of the continuous and resident oils helps in increased residual oil recovery. Figure 4.19 shows the experimental conditions, pressure and apparent viscosity plots for Core A Experiment 13.

Core A – Experiment 13					
k (mD)	ϕ	Pore Volume (mL)	Sor	Flow Rate (mL/min)	Percentage Recovery (%)
4750	0.28	42.87	0.30	0.5	0

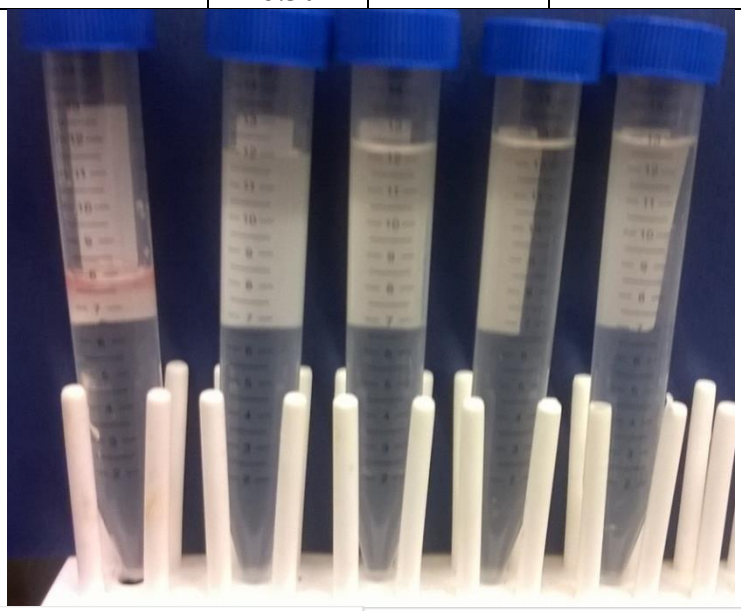

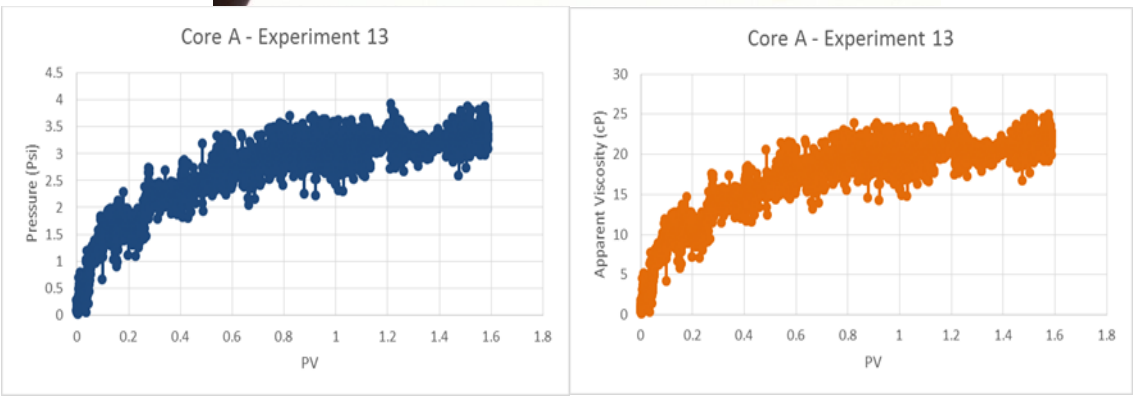

Figure 4.19 Core A Experiment 13: Recovery of light mineral oil by surfactant injection. The Igepal Co-70 surfactant was colorless. No mineral oil was seen to be recovered. Experiment performed at 0.5 mL/min.

4.5.4 Displacement of Heavy Residual Oil with Pentane Emulsion

As previously discussed, natural gas liquids contain a mixture of light hydrocarbons and are considered the "by-products" on the oil and gas industry. As we are

looking to incorporate light organic phases into our nanoparticle stabilized emulsions, experiments were performed using pentane, which is the shortest alkane that is liquid at standard temperature and pressure. In Core E Experiment 14, a pentane emulsion was injected into a sandstone core at an initial saturation of brine and residual oil saturation, with the resident oil being light mineral oil. The pentane emulsion was stabilized with Nyacol DP-9711 nanoparticles dispersed to 2 wt% concentration in brine solution. The emulsion generation took place in a beadpack which was filled with glass beads of 180 micron diameter. The flow through the beadpack was performed at a 1:2 phase ratio of pentane: nanoparticle dispersion for a total flow rate of 24 mL/min. Because pentane has a very low vapor pressure at room temperature and pressure, rapid evaporation prohibited normal rheology techniques to measure the potential shear-thinning behavior of the emulsion. However, a Beckman-Coulter Laser Diffraction Particle Size Analyzer was used to determine the droplet size of the pentane-in-water nanoparticle stabilized emulsion. The emulsion had a particle diameter of 69.5 microns.

Figure 4.20 shows the experimental conditions, effluent of emulsion injection into Core E, pressure drop and apparent viscosity for Experiment 14. This experiment had a flow rate of 4 mL/min. A pentane-in-water emulsion was continuously injected into the sandstone core until no more light mineral oil was seen to be recovered. The pressure drop recorded was seen to increase throughout the duration of the experiment. No emulsion was regenerated from the core which would be expected as the emulsion is not seen to remain stable under room temperature and pressure conditions. The injected pentane emulsion was seen to completely coalesce, leading to miscibility with the residual resident mineral oil present in the core. This can be seen from the shade of the dye in the effluent. Test tube 1 shows the darkest pink, which would suggest the most amount of mineral oil recovered. To assess the amount of recovery of the residual

mineral oil, the effluent test tubes were placed under the fume hood and the pentane was allowed to evaporate from the samples.

When the pentane emulsion was injected, the sandstone core was at an initial saturation of brine and residual oil saturation. The residual oil saturation, Sor, was computed to be 0.33 which at a pore volume of 43.70 mL would suggest 14.5 mL of light mineral oil available for recovery. The estimated oil recovery based on the effluent at steady state after pentane was allowed to evaporate was approximately 10 mL of mineral oil. This led to a residual oil recovery of about 69%. Given the viscosity difference between pentane and mineral oil, this is an encouraging recovery number. It may be that because the pentane-in-water emulsion does not stay quite stable inside the core, it may allow for more miscibility between the continuous and resident oils thereby leading to a larger potential oil bank.

Core E Experiment 15 had similar conditions to that of Core E Experiment 14, with the only change being the reduced flow rate. The residual oil saturation, Sor, was computed to be 0.31 which at a pore volume of 43.70 mL would suggest 13.5 mL of light mineral oil available for recovery. The estimated oil recovery based on the effluent at steady state after pentane was allowed to evaporate was approximately 11 mL of mineral oil. This led to a residual oil recovery of about 81%. This number was not expected to be greater than that of 69% recovery at a higher flow rate but is an interesting observation. We have normally seen higher flow rates to lead to lower recoveries due to smaller durations for coalescence and regeneration and miscibility in the core. The results can be seen in Figure 4.21.

Core E – Experiment 14					
k (mD)	ϕ	Pore Volume (mL)	Sor	Flow Rate (mL/min)	Percentage Recovery (%)
3225	0.28	43.70	0.33	4	69

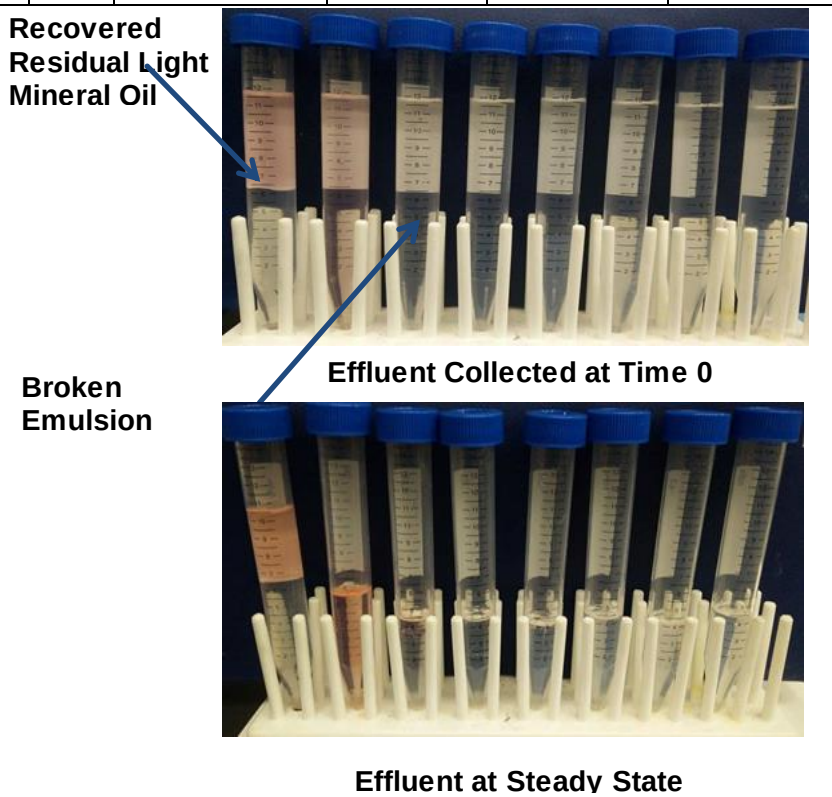

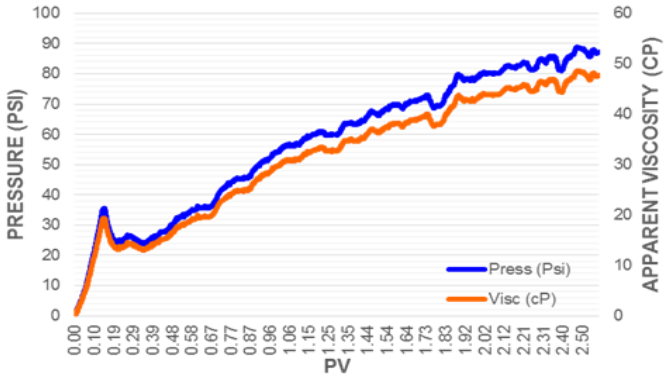

Figure 4.20 Core E Experiment 14: Recovery of light mineral oil (dyed pink) by pentane-in-water emulsion stabilized with Nyacol DP9711 nanoparticles dispersed in brine. The injected pentane was colorless. The amount of recovered oil can be assessed by the lightness of the pink shade as well as when the effluent reaches steady state. Experiment performed at 4 mL/min.

Core E – Experiment 15					
k (mD)	ϕ	Pore Volume (mL)	Sor	Flow Rate (mL/min)	Percentage Recovery (%)
3225	0.28	43.70	0.31	1	81

Figure 4.21 Core E Experiment 15: Recovery of light mineral oil (dyed red) by pentane-in-water emulsion stabilized with Nyacol DP9711 nanoparticles dispersed in brine. The injected pentane was colorless. The amount of recovered oil can be assessed by the lightness of the red shade as well as when the effluent reaches steady state. Experiment performed at 1 mL/min.

Figure 4.22 shows the experimental conditions, effluent of emulsion injection into Core F, pressure drop and apparent viscosity for Experiment 16. This experiment had a flow rate of 4 mL/min. A 0.50 PV slug of pentane-in-water emulsion was injected into the sandstone core after which a post-brine flush was performed until no more light mineral oil was seen to be recovered. The pressure drop was seen to increase throughout the duration of the emulsion injection and was seen to stabilize during the post-brine flush. No emulsion was regenerated from the core which would be expected as there is a limited amount of emulsion injected. The injected pentane emulsion was seen to completely coalesce, leading to miscibility with the residual resident mineral oil present in the core. This can be seen from the shade of the dye in the effluent. Test tube 2 shows the darkest red, which would suggest the most amount of mineral oil recovered. To assess the amount of recovery of the residual mineral oil, the effluent test tubes were placed under the fume hood and the pentane was allowed to evaporate from the samples.

When the pentane emulsion was injected, the sandstone core was at an initial saturation of brine and residual oil saturation. The residual oil saturation, Sor, was computed to be 0.25 which at a pore volume of 44.40 mL would suggest 11.0 mL of light mineral oil available for recovery. The estimated oil recovery based on the effluent at steady state after pentane was allowed to evaporate was approximately 9 mL of mineral oil. This led to a residual oil recovery of about 82%.

Core F Experiment 17 had similar conditions to that of Core F Experiment 16, with the only change being the reduced flow rate. The residual oil saturation, Sor, was computed to be 0.26 which at a pore volume of 44.40 mL would suggest 11.5 mL of light mineral oil available for recovery. The estimated oil recovery based on the effluent at steady state after pentane was allowed to evaporate was approximately 6.5 mL of mineral oil. This led to a residual oil recovery of about 57%. The results are shown below:

Core F – Experiment 16					
k (mD)	ϕ	Pore Volume (mL)	Sor	Flow Rate (mL/min)	Percentage Recovery (%)
1690	0.28	44.40	0.25	4	82

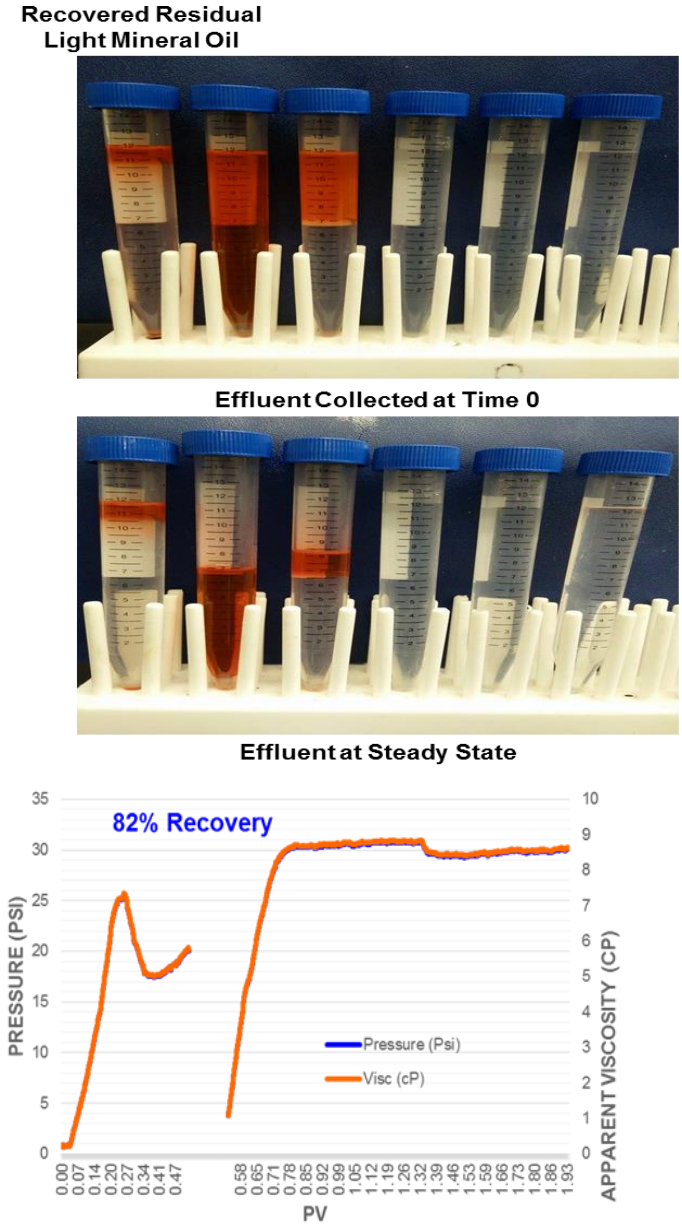

Figure 4.23 Core F Experiment 16: Recovery of light mineral oil (dyed red) by 0.50 PV slug of pentane-in-water emulsion stabilized with Nyacol DP9711 nanoparticles dispersed in brine. The injected pentane was colorless. The amount of recovered oil can be assessed by the lightness of the red shade as well as when the effluent reaches steady state. Experiment performed at 4 mL/min.

Core F – Experiment 17					
k (mD)	ϕ	Pore Volume (mL)	Sor	Flow Rate (mL/min)	Percentage Recovery (%)
1690	0.28	44.40	0.26	1	57

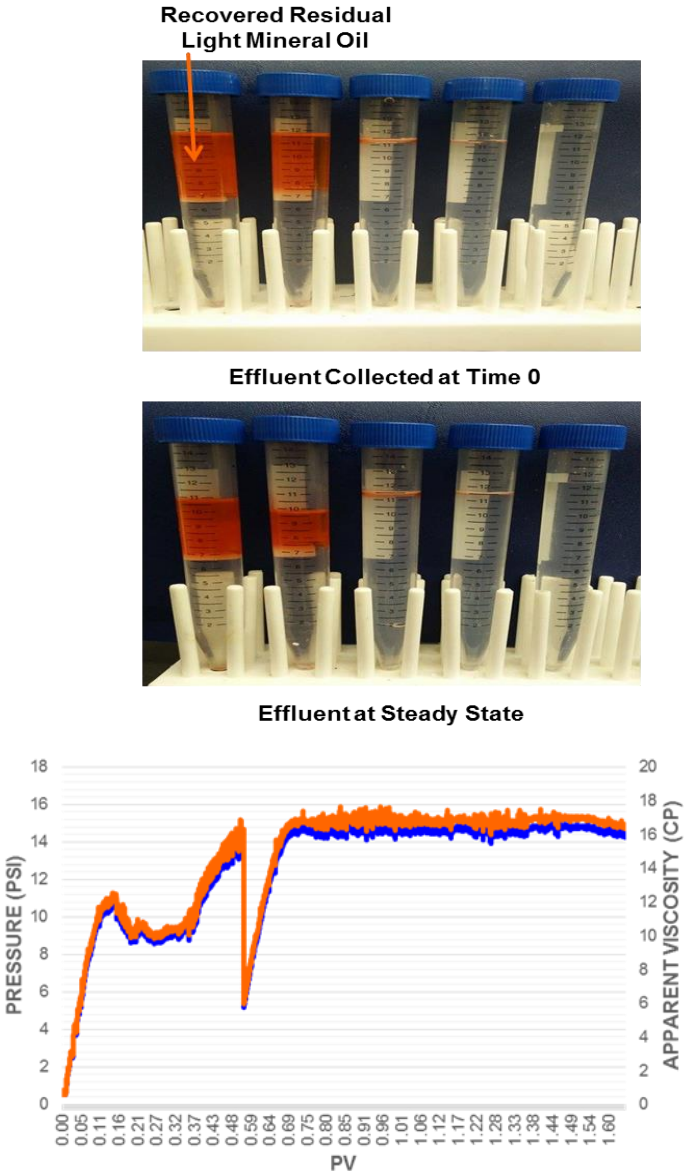

Figure 4.24 Core F Experiment 17: Recovery of light mineral oil (dyed red) by 0.50 PV slug of pentane-in-water emulsion stabilized with Nyacol DP9711 nanoparticles dispersed in brine. The injected pentane was colorless. The amount of recovered oil can be assessed by the lightness of the red shade as well as when the effluent reaches steady state. Experiment performed at 1 mL/min.

4.6 DISCUSSION

Core U Experiments 1 and 2, where a mineral oil emulsion was injected through a Boise sandstone core, were intended to assess recovery potential of residual mineral oil. The experiments were performed at two different flow rates: 0.1 and 0.5 mL/min. The lower flow rate showed a higher percentage of residual oil recovery than the larger flow rate. There was no emulsion seen in the effluent for Core U Experiment 1 whereas small amounts were collected in the effluent in Core U Experiment 2. This indicated that perhaps there is a critical shear rate above which emulsion regeneration is possible. Pressure drop increased for the duration of the two experiments which suggested movement of a possible oil bank followed by continuous coalescence and regeneration of the emulsion droplets.

Core U Experiment 3 and Core W Experiments 4-6 were performed to gain insight on the advantage of viscosity between the continuous oil in the emulsion to the residual oil present in the core. Core U Experiment 3 was performed where mineral oil emulsion was continuously injected into a core containing residual Texaco oil. The added advantage was confirmed as the percentage recovery was computed to be 74%. Furthermore, the effect of slug size of emulsion injected was also assessed and it was confirmed that increasing the slug size of emulsion injected helps increase the amount of residual oil recovered. It is believed that a plateau value exists for each type of residual oil recovery experiment performed above which it would not be possible to recover any additional residual oil. Where enough emulsion was available, emulsion was seen to be regenerated in the effluent and this was consistent with the flow rate of 0.5 mL/min being above the critical shear rate of emulsion regeneration.

Core X Experiments 7 and 8 were performed to assess the capability of lighter continuous organic phases in emulsion in recovering more viscous, heavier resident oils.

A 0.75 PV and 0.70 PV slug of octane-in-water emulsion was injected into a Boise sandstone core at residual mineral oil saturation. Core X Experiment 7 was performed at 0.1 mL/min and showed a higher percentage recovery than Core X Experiment 8 which was performed at 2 mL/min. Recovery for the former experiment was seen to be higher than that of the latter with no emulsion regeneration seen for the former and very little emulsion regeneration seen for the latter. These percentage recoveries were significantly lower than those where high viscosity continuous oil in emulsion was recovering a low viscosity residual oil. Core Y Experiment 9 was performed to compare recovery of an octane-in-water emulsion stabilized using a surfactant and this showed the greatest recovery with the recovery equal to 99%. It is interesting to note that for surfactant-stabilized octane-in-water emulsion a significant amount of emulsion was regenerated in the effluent. This was due to a more stable emulsifying agent which can also be reason for the increased residual oil recovery. It is interesting to note that for the case of the surfactant stabilized octane-in-water emulsion, the pressure drop was seen to decrease after all the mineral oil was recovered and emulsion was consistently regenerated. This might be because not much coalescence is occurring in the core, with mostly regeneration taking place, leading to a more stable condition inside the core.

Core Y Experiment 10 and Core Z Experiment 11 were co-injection experiments that were performed to assess recovery of residual mineral oil by co-injecting mineral oil and brine through a Boise sandstone core. The experiments were performed at 4 mL/min and 12 mL/min respectively. The pressure drop increased throughout the duration of the experiment for both experiments which is consistent with the attempted coalescence and regeneration hypothesis. Core Y Experiment 10 did not show any regeneration of emulsion, which was interesting because the flow rate appeared to be slightly above the critical shear rate. One reason for this might be the large permeability of the core when

combined with the shear rate being close to the critical shear rate. Core Z Experiment 11 was performed well above the critical shear rate and some emulsion was seen to be regenerated in the effluent.

Core Z Experiment 12 and Core A Experiment 13 were performed as control experiments to simply assess the behavior of surfactant stabilized octane-in-water emulsion as well as the surfactant Igepal Co-70 itself. Core Z Experiment 12 was performed with a surfactant-stabilized octane-in-water emulsion injected into a brine saturated core. A similar pressure profile to Core Y Experiment 9 was observed where the pressure profile increased until the emulsion was consistently regenerated. Core A Experiment 13 was performed to assess the recovery potential of simply injecting a surfactant into a core containing residual mineral oil. No mineral oil was recovered for this experiment, which is expected as there does not exist a phenomenon where coalescence and regeneration occurs.

Core E Experiments 14 and 15 were performed using an even less viscous organic phase in emulsion, incorporating a pentane-in-water emulsion to recover residual mineral oil. The experiments were performed at 4 mL/min and 1 mL/min respectively and percentage recoveries were very encouraging. Core F Experiments 16 and 17 had conditions were similar to the previous two stated experiments with the exception being that a 0.50 PV slug of pentane-in-water emulsion was injected rather than a continuous emulsion injection. No emulsion was regenerated in the effluent for either of the 4 experiments which is to be expected due to the volatility of pentane at room temperature and pressure. As this emulsion is not stable, it is possible that increased miscibility may be occurring inside the core which might be leading to a larger oil bank and helping in increased residual oil recovery.

Chapter 5

Conclusions and Future Work

5.1 CONCLUSIONS

5.1.1 Emulsion Flow in Hydrophobic Beadpacks

Hydrophilic nanoparticle-stabilized oil-in-water emulsions of two different droplet sizes were injected into hydrophobic beadpacks of varying bead size diameters. For the majority of the experiments, the smaller sized emulsion appeared to be more stable in its properties, more frequently being regenerated in the effluent in comparison to the larger droplet sized emulsion. In comparison to emulsion flow in hydrophilic beadpacks, however, a much less emulsion was regenerated in the effluent. In a hydrophilic beadpack it was commonly seen that larger droplet sized emulsion were collected in the effluent after many pore volumes, but in hydrophobic beadpacks, the larger droplet sized emulsion was almost never regenerated. With a decrease in bead diameter, it was seen that even the smaller droplet sized emulsion could not survive passage with regeneration. This was in direct contrast to a hydrophilic beadpack where regeneration was seen soon after 10 pore volumes of emulsion were injected. Smaller bead pack sizes also did not allow passage of the less stable larger droplet sized emulsion. The fastest emulsion regeneration was seen for a small droplet sized emulsion through a beadpack of larger sized beads. This seems intuitive as the largest beads provide the most permeable path and therefore least resistance to the emulsion droplets, this would in turn lead to more successful regeneration of the emulsion. Through the largest bead-sized beadpack, small amounts of the less stable emulsion with a larger droplet size were seen to be regenerated but much later in the life of the experiment. Higher flow rates were able to regenerate emulsion for smaller droplet sizes but were unable to do so for the less

stable larger-sized emulsion. Pressure profiles appeared to similar for most runs where approximately the first 0-10 pore volumes show the greatest pressure buildup followed by what appears to be a more stable and slower increase in pressure. In comparison, hydrophilic beadpacks showed much higher pressure profiles for almost all beadpack runs. It is possible that hydrophilic beadpacks tend to accumulate the hydrophilic nanoparticles on the hydrophilic glass beads. Due to this obstruction in flow, pressure in hydrophilic beadpacks would be high when in combination with the droplets of emulsion trying to coalesce and regenerate. For hydrophobic beadpacks, the glass beads would now not be the ideal positioning place for the hydrophilic nanoparticles. Due to a lack of clumping and retention of hydrophilic nanoparticles in hydrophobic beadpacks, as well as lacking the ideal medium wettability for coalescence and regeneration, nanoparticles would now clump to eachother and would flow out of the beadpack mostly in coalesced form. Particle size analyses were used to confirm the lack of retention of hydrophilic nanoparticles in hydrophobic beadpacks although the NMR measurement results remained inconclusive.

5.1.2 Emulsion Flow in Sandstone Cores for Residual Oil Recovery

Coreflood experiments were performed to assess residual oil recovery for various oil-in-water emulsions. Higher recoveries were seen to be dependent on several factors. For more viscous, stable emulsions, it appeared that lower flow rates lead to higher recoveries. At lower flow rates, no emulsion was produced in the effluent for the duration of the experiment. As pressure profiles increased throughout the experiment, attempted coalescence and regeneration were likely taking place. However, as regeneration was less successful, complete coalescence might be the reason for increased miscibility in the core, leading to higher recovery potentials.

Encouraging recoveries were seen when a more viscous, stable emulsion was used to recover residual oil less viscous than that of the continuous oil in the emulsion. The viscosity difference is an advantage which would help push along a larger oil bank of lower viscosity. Increasing the slug size of the emulsion injected helped recover more residual oil. Increasing the slug size however is only advantageous up to a limiting value where the injected emulsion slug would produce the same result as emulsion injected continuously through the sandstone core. Where enough emulsion was injected and therefore available inside the core, emulsion regeneration was seen. Emulsion regeneration was not seen for low pore volumes of emulsion slugs injected.

It is more practical in terms of financial restrictions in the field to incorporate emulsions of lighter, inexpensive oils to recover more viscous, heavier oils. Following this strategy, lighter organic phases in emulsion form were used for oil recovery coreflood experiments. Similar to experiments performed with heavier organic phases in emulsion form i.e. mineral oil-in-water emulsion, octane-in-water emulsion was also not regenerated for low flow rates, completely coalescing inside the sandstone core. For higher flow rates, small amounts of octane emulsion were regenerated. In this case, similar to that of the mineral oil emulsion, increasing the flow rate seemed to have a negative effect on the percentage oil recovery.

Surfactant-stabilized octane-in-water emulsions showed the highest oil recovery. The pressure plot of these emulsions was different from those of nanoparticle-stabilized emulsions where, although the initial pressure increase matched up with the movement of the oil bank through the core, the later part of the pressure profile appeared to decrease. It is possible that this decrease may be attributed to the increased regeneration of the emulsion. If the majority of the droplets are only regenerating back into emulsion form rather than coalescing and regenerating, this would likely cause stability in the porous

medium and would therefore cause a decrease in the pressure. This pressure profile was seen in both cases where the octane emulsion was injected into a fully brine saturated core as well as a core at residual oil saturation. It is interesting to note, however, that surfactants by themselves are not capable of recovering any residual oil. It is only in emulsion form that this recovery is possible.

Taking the strategy of incorporating light hydrocarbons in emulsion form further, experiments were performed using pentane, the shortest alkane which is a liquid at standard conditions. Pentane-in-water emulsions were not seen to be stable for days, unlike the other emulsions stated above. This was due to partial and continuous evaporation of pentane from the emulsion form at room temperature and pressure. When pressurized to 100 psi, however, the emulsion was seen to be stable for a number of days. Pentane-in-water emulsions showed very encouraging results in terms of residual oil recovery. All experiments were performed at high flow rates however emulsion was not seen to be regenerated in the effluent. This would suggest a lack of stability of the emulsion. Due to complete coalescence of the emulsion inside the core, miscibility would increase and this might be a reason for the higher percentage recoveries. Pressure profiles seemed to mimic all other oil-in-water emulsion injection experiments to sandstone cores at residual oil saturation.

5.2 FUTURE WORK

Work is currently in progress to set up a pressurized system for production of natural gas liquids-in-water emulsions. As natural gas liquid components are gases at room temperature and pressure, they must first be liquefied before they can be incorporated as the organic phase in emulsion form. For this purpose the following set up is currently being built:

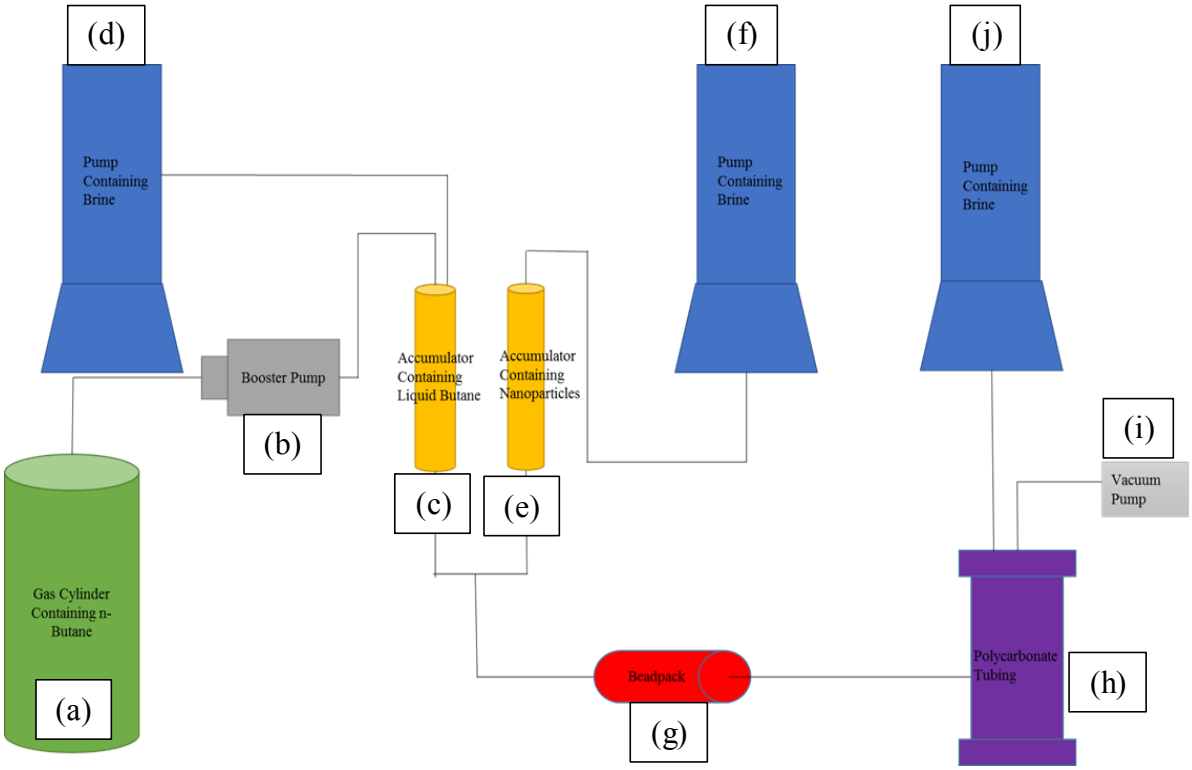

Figure 5.1: Experimental set up proposed for production of natural gas liquids-in-water emulsions: (a) gas cylinder containing butane, (b) booster pump, (c, e) accumulator, (d, f, j) ISCO syringe pumps, (g) beadpack, (h) polycarbonate tubing, (i) vacuum pump

Figure 5.1 shows the proposed experimental set up for the production of natural gas liquids-in-water emulsions. A gas cylinder containing butane (a) will be flowed into the booster pump (b) where it will be liquefied and contained in (c) the accumulator. Pressure will be provided to the accumulator by a syringe pump (d) which will help flow into the beadpack (g). An accumulator containing nanoparticles (e) will be co-injected into the beadpack at the same time as the butane, where flow will be provided through syringe pump (f). Effluent emulsion will be contained in the polycarbonate tubing (h) which will be vacuum pumped beforehand (i). The effluent will be pressurized using either a third syringe pump (j) or a back pressure regulator so that the gas may stay in liquid form in emulsion.

Other potential research objectives are proposed below:

- Residual oil recovery experiments should be performed on oils that are a lot more viscous, ranging from 100 to 1000 cP. Various light hydrocarbons should be used in emulsion form, stabilized using nanoparticles to assess the range of possible residual oil recovery.
- Hydrophobic nanoparticles should be used to form water-in-oil emulsions. Coreflood experiments could then be performed to assess their behaviour in comparison to hydrophilic nanoparticles used to generate oil-in-water emulsions.
- Oil-in-water as well as water-in-oil emulsions can be emulsified by a mixture of nanoparticles as well as surfactants. The concentration of both emulsifying agents should be varied to assess the properties of the generated emulsion in terms of rheology and stability.
- Experiments can be performed at high salinity and high temperature conditions to assess residual oil recoveries at harsh conditions.

References

Aveyard, R., Binks, B., Clint, J. Emulsions Stabilized Solely by Colloidal Particles. Advances in Colloid and Interface Science, 100-102, 503-546, (2003).

Binks, B., Rodrigues, J. Enhanced Stabilization of Emulsions Due to Surfactant-Induced Nanoparticle Flocculation. Langmuir, 23, 7436-7439, (2007).

Binks, B.P. Particles as Surfactants - Similarities and Differences. Current Opinion in Colloid and Interface Science, 7, 21-41, (2002).

Caldelas, F.M. Experimental Parameter Analysis of Nanoparticle Retention in Porous Media, M.S.E. Thesis, The University of Texas at Austin, (2010).

Chung, D.H., Transport of Nanoparticles during Drainage and Imbibition Displacements in Porous Media, M.S.E. Thesis, The University of Texas at Austin, (2013).

Fingas, M.F., Water-in-Oil Emulsions: Formation and Prediction, Journal of Petroleum Science Research (JPSR), Vol. 3 Issue 1, 38-49, (2014).

Gabel, S.T., Generation, Stability, and Transport of Nanoparticle-Stabilized Oil-in-Water Emulsion in Porous Media, M.S.E. Thesis, The University of Texas at Austin, (2014).

Goharrizi, B.A., Experimental Measurement of Sweep Efficiency during Multi-Phase Displacement in the Presence of Nanoparticles, Ph.D. Dissertation, The University of Texas at Austin, (2013).

Lake, L.W. Enhanced Oil Recovery. Englewood Cliffs, NJ: Prentice Hall, (1989).

McAuliffe, C. D. Oil-in-Water Emulsions and Their Flow Properties in Porous Media. Society of Petroleum Engineers, SPE 4369, (1973).

Pickering, S.U. Emulsions, CXCVI, J. Chem. Soc., 91, 2001, (1907).

Roberts, M.R. Shear-Induced Emulsions Stabilized with Surface-Modified Silica Nanoparticles, M.S.E. Thesis, The University of Texas at Austin, (2011).

Tcholakova, S., Denkov, N.D., Lips, A., Comparison of Solid Particles, Globular Proteins and Surfactants as Emulsifiers, Physical Chemistry Chemical Physics, Vol. 10 Number 12, 1597-1712, (2008).

Tellez, G.T., Nirmalakhandan, N., Gardea-Torresdey, J.L., Comparison of Purge and Trap GC/MS and Spectrophotometry for Monitoring Petroleum Hydrocarbon Degradation in Oilfield Produced Waters, Microchemical Journal 81, 12-18, (2005).

Thompson, K.E., Fogler, H.S., Modeling Flow in Disordered Packed Beds from Pore-Scale Fluid Mechanics, AIChE Journal, Vol. 43, No. 6, 1377-1389, (1997).

Yan, Y., Thompson, K.E., Valsaraj, K.T., A Numerical Study on the Coalescence of Emulsion Droplets in a Constricted Capillary Tube, Journal of Colloid and Interface Science, 298, 832-844, (2006)

Zhang, T., Emulsions Stabilized with Nanoparticles for Potential Conformance Control Applications, M.S.E. Thesis, The University of Texas at Austin, (2009).

Zhang, T., Davidson, D., Bryant, S., Huh, C., Nanoparticle-Stabilized Emulsions for Applications in Enhanced Oil Recovery, Society of Petroleum Engineers, SPE-129885-MS, (2010)

Zhang, T., Modeling of Nanoparticle Transport in Porous Media, Ph.D. Dissertation, The University of Texas at Austin, (2012).

Zhang, T., M.R. Roberts, S.L. Bryant, and C. Huh, C. Foams and Emulsions Stabilized with Nanoparticles for Potential Conformance Control Applications, Presented at the SPE International Symposium on Oilfield Chemistry, Woodlands, TX, SPE 121744, (2009).

Zhang, W., Thompson, K.E., Reed, A.H., and Beenken, L. Relationship between packing structure and porosity in fixed beds of equilateral cylindrical particles. Chemical Engineering Science, 238, 24, 8060-8074, (2006).

Zhu, C., Daigle, H., Bryant, S., Nuclear Magnetic Resonance Investigation of Surface Relaxivity Modification by Paramagnetic Nanoparticles, Society of Petroleum Engineers, SPE-175087-MS, (2015)